Traditional glass and porcelain cap-and-pin transmission line insulators are slowly being replaced by new insulating materials which have better electrical and mechanical properties such as silicon rubber and polymeric. The non-ceramic materials are currently gaining popularity in transmission line applications. For any new type of insulator to be used on transmission line, it has to be tested so that it complies with the requirements of International Electrotechnical Commission Standard on insulators. This book provides comprehensive information concerning the design and development of Artificial Contamination Chamber which encompasses the aspects of electronic instrumentation, video recording, artificial contamination generation system, high voltage source data acquisition system and virtual instrument development. The chamber has all the basic features to conduct type-tests on insulators of ceramic and non-ceramic types.

Muhammad Abu Bakar Sidik, Hussein Ahmad
Muhammad Abu Bakar Sidik, PhD: Staff of Department of Electrical Engineering, Faculty of Engineering, Sriwijaya University and Senior Lecturer at Institute of High Voltage and High Current, Universiti Teknologi Malaysia.
Hussein Ahmad, PhD: Professor and Director of Institute of High Voltage and High Current, Universiti Teknologi Malaysia.

9 783639 349689
978-3-639-34968-9

Muhammad Abu Bakar Sidik
Hussein Ahmad

rtificial Contamination Chamber for Solid lation Material Testing

Design and Development

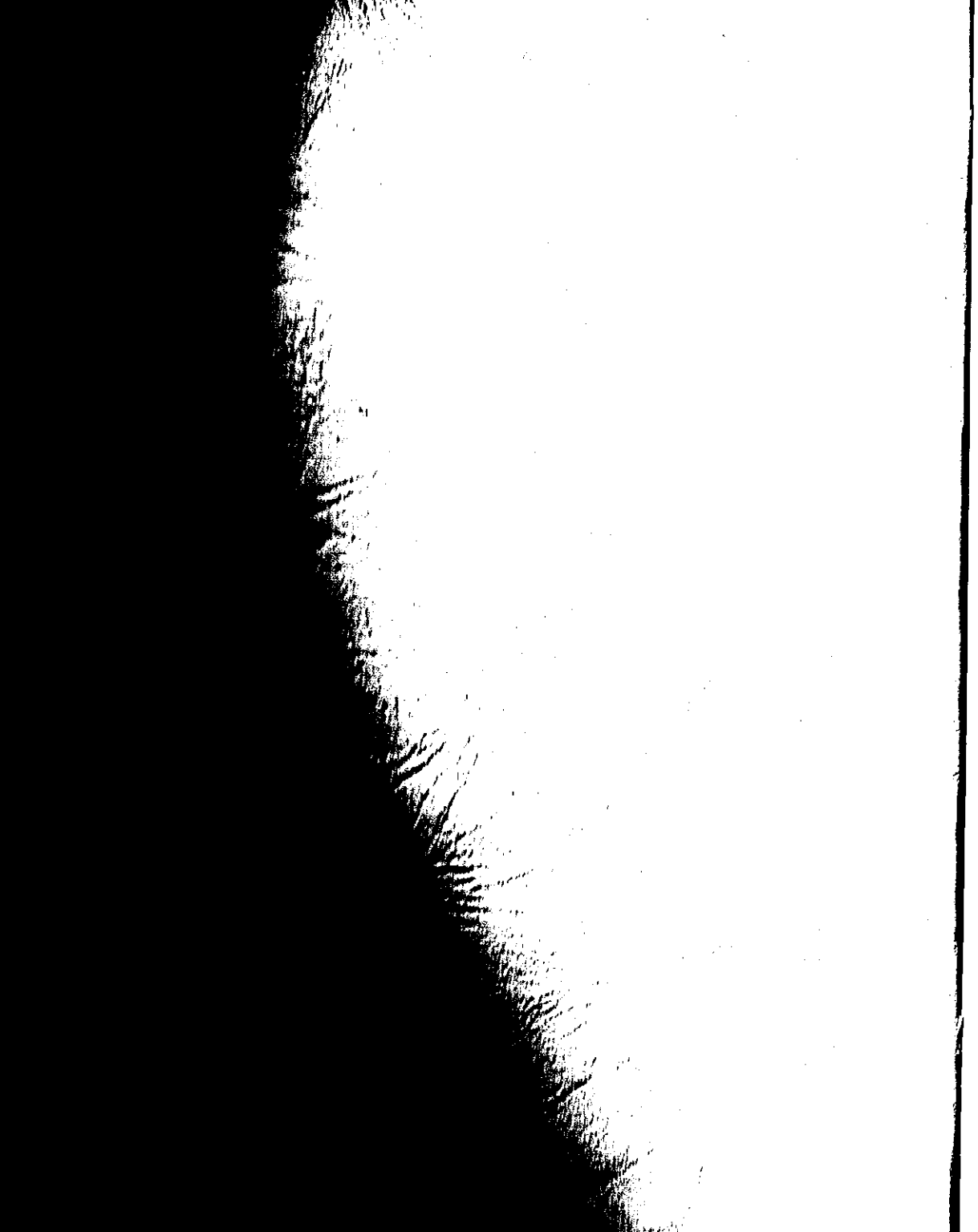

Muhammad Abu Bakar Sidik
Hussein Ahmad

Artificial Contamination Chamber for Solid Insulation Material Testing

Muhammad Abu Bakar Sidik
Hussein Ahmad

Artificial Contamination Chamber for Solid Insulation Material Testing

Design and Development

VDM Verlag Dr. Müller

Impressum/Imprint (nur für Deutschland/ only for Germany)
Bibliografische Information der Deutschen Nationalbibliothek: Die Deutsche Nationalbibliothek verzeichnet diese Publikation in der Deutschen Nationalbibliografie; detaillierte bibliografische Daten sind im Internet über http://dnb.d-nb.de abrufbar.

Coverbild: www.ingimage.com

Verlag: VDM Verlag Dr. Müller GmbH & Co. KG
Dudweiler Landstr. 99, 66123 Saarbrücken, Deutschland
Telefon +49 681 9100-698, Telefax +49 681 9100-988
Email: info@vdm-verlag.de

Herstellung in Deutschland:
Schaltungsdienst Lange o.H.G., Berlin
Books on Demand GmbH, Norderstedt
Reha GmbH, Saarbrücken
Amazon Distribution GmbH, Leipzig
ISBN: 978-3-639-34968-9

Imprint (only for USA, GB)
Bibliographic information published by the Deutsche Nationalbibliothek: The Deutsche Nationalbibliothek lists this publication in the Deutsche Nationalbibliografie; detailed bibliographic data are available in the Internet at http://dnb.d-nb.de.

Cover image: www.ingimage.com

Publisher: VDM Verlag Dr. Müller GmbH & Co. KG
Dudweiler Landstr. 99, 66123 Saarbrücken, Germany
Phone +49 681 9100-698, Fax +49 681 9100-988
Email: info@vdm-publishing.com

Printed in the U.S.A.
Printed in the U.K. by (see last page)
ISBN: 978-3-639-34968-9

CONTENTS

LIST OF FIGURES

LIST OF TABLES

CHAPTER 1
INTRODUCTION

1.1 Background of Work

The rapidly growing industrial, commercial, and residential sectors activities have their impact; the world faces an increased the demand of electrical energy. To connect the generating centre with the loads, the transmissions of the electrical energy from remote power stations to the load centres are accomplished by overhead lines. Due to the need to transmit greater amount of power for longer distances, transmission lines with higher operating voltage have been built.

Numerous high voltage (HV) transmission lines were being constructed in the coastal areas. The reason is that these areas are already developed and making lines construction much easier. In upgrading and construction of transmission lines, tower design and insulator selection are crucial to be measured. An insulator would ideally be a solid dielectric which is functionally nonconductive to the flow of electricity. However, no material is a perfect insulator. For practical purposes, an insulator is a material that for a particular application limits the flow of current through it to a value small enough to be ignored [1]. The insulator can be of indoor or outdoor type. The outdoor type is easily affected by the atmospheric contamination and pollution. Therefore, it is imperative that power system network components are affected by environmental conditions.

The build-up of contamination can sometimes be very rapid on HV insulator installed near marine environment. Sudden storms cause excessive build-up of conducting contaminant on the insulator surface in just a few hours. Other hydrometeorology parameters are also responsible in the case of service insulators near coastal areas. Outdoor insulators are contaminated by salt depositing on the surface of the insulators. This obviously can adversely affect the performance of the insulators when

ergized with Alternating Current (AC) or Direct Current (DC) voltages. The Basic ghtning Impulse Insulation Level (BIL) and Basic Switching Impulse Insulation Level SIL) of the insulator are greatly reduced in a contaminated environment.

A contaminated environment can cause the insulation level of outdoor insulators to deteriorated. The degree of contamination on the insulator surface can be correlated th the magnitude of the surface leakage current flowing on these surfaces. In the case the insulators near littoral regions, salt deposition on insulator surface deteriorates its rformance.

Dry salt deposit on the insulator surface is not usually conductive enough by itself to ost electrical flow. But with the presence of dew or light rain, the dissolved salt that olsten the insulator surface produces an electrolytic layer on the surface itself and ntually trigger the flashover which starts from the high voltage point to the grounded rt of the insulator.

The flashover of a contaminated insulator can cause failure of the power system for long period of time [2]. During the flashover period, the total resistance of the insulator creases abruptly. This flashover is seen by the system protection as an AC power ilure and can trip the complete line. It becomes worst when no automatic mean of losure to restore the supply installed to avoid possibility of flashover reaching a ngerous level. The performance of the HV equipment in the contaminated condition is most important and decisive factor for determining the external insulator design of the rhead electric power lines and also substations in the coastal area. The environmental act on the performance of the insulator entails the use of right and suitable insulator terials. Two options are available i.e. inorganic and organic materials.

Though inorganic material like porcelain and glass have been widely used for door HV insulator application because of their reliability and cost shaving, still this type insulators cannot work effectively under adverse environmental conditions that cause ntaminant deposition on their surface. To overcome this, polymers were introduced t 40 years ago and presently they are being used extensively for a variety of outdoor insulator application [3]. Polymeric materials are now gaining popularity for outdoor lation application. Their unique integration of mechanical properties along with their

customized fabrication and coupled with electrical dielectric properties make polymer materials as the materials for the future especially for HV applications [4].

The polymeric insulators used as outdoor HV insulation show excellent electrica characteristic when new [5]. Observations showed that polymeric insulators after a long term exposure to operational service stresses proved that these polymeric insulators ma experience some forms of dielectric degradation such as chalking phenomena or eve deteriorations depending on the selected housing material and specific design criteri [6,7].

There is of great interest to obtain information regarding the performance o polymeric insulator on HV lines in term of their service reliability. This information can b obtained first by on-line diagnostic method [8]. Secondly by laboratory tests carried out o insulators which had been removed from the lines [9,10]. Thirdly is by simulating th environmental condition in the laboratory. The first two methods can contribute toward the knowledge regarding the extension and degree of aging occurring in the polymer insulators while they are in service that are stressed by external and internal factors.

Therefore, it is incumbent and of great significance to organize a study on insulator that are exposed to different levels of environmental contamination since these insulator are for HV insulation application to the electrical power networks. The obtained result can be used to produce more reliable and efficient HV network systems which can wor under adverse environmental impact. Insulator performance study is best studied in actua and original service conditions where they are practically installed on the system. Thi method is not easily available and again the ambient conditions are beyon experimentalists' control. So the best option is to use artificial climatic or contaminatio chamber for insulation studies.

1.2 Objective of Work

The objective of this work is to construct an artificial contamination chamber fo testing of ceramic and polymeric insulators. The chamber is a mean to develop amon other techniques to select and use reusable aged glass insulators and to conduc

nments such as flashover accident, leakage current pattern recognition and polymeric lators contamination in order to validate usefulness of the chamber.

Scope of Work

The scope of this work includes the following: (i) design of the mobile artificial ntamination chamber that can simulate naturally occurring fog, and salt-fog spray; (ii) velopment of the mobile artificial contamination chamber which encompasses the ds of development and construction; electronic instrumentation, video recording, ital contamination generation system, HV source, data acquisition system and ware development; (iii) development of an empirical mathematical model for the ation of reusable aged glass insulators; (iv) laboratory assessment to determine the ation between the conductivity and the salinity of solution dissolved with deposits of dant polluting the insulator; (v) development of an empirical model to predict the al Equivalent Salt Deposit Density deposited on the polymeric insulator surfaces based the time of exposure and concentration level.

Outline of Bock

The book is organized in five chapters. Chapter 2 describes the literature review ted to the test chamber, insulators, leakage current measurement and detection and Chapter 3 describes the development of the test chamber that encompasses the ign aspect of the chamber, apparatus fabrication, software development and mental set-up. Chapter 4 presents the experimental results and discussions on minary applications. Chapter 5 presents the summaries of current work.

Main Contributions

They are two main contributions of this work i.e. (i) Fabrication of a unique ium scale mobile artificial contamination chamber designed and developed from

scratch for artificial contamination testing of insulators; (ii) Development a techniqu
select and use reusable aged glass insulators.

CHAPTER
LITERATURE STU

2.1 High Voltage Insulator Materials

After the invention of electricity and transformer the need for insulators increased rapidly [11]. The skirt of conventional insulators made from either porcelai glass is considered resistant against adverse weather condition and electrical discharg In case of polymeric insulators, the surfaces of the polymeric housing materials are abl interact with the pollution under the influence of surrounding weather conditions. A consequence, the insulation capability might vary with time.

2.1.1 Ceramic Insulators

Porcelain and glass are categorized as ceramic insulators and they have a l service history. They were first introduced as components in telegraph networks in late 1800s [12]. Ceramics are inorganic material in which their chemical or phys properties would not change with time [13].

Specific tests have been developed to evaluate their performance under vari service conditions. These insulators should perform satisfactorily under both clean wet condition. A particular interest is paid on the insulators' performance under wet a contaminated conditions, since it is possible for flashover at the nominal operating volt of an insulator to occur.

1.1 Porcelain Insulator

Porcelain insulator, as shown in Figure 2.1, is made from china clay. This material poses of kaolin, feldspar and quarts. A good porcelain insulator has a dielectric ngth of about 60 kV/cm, pressure strength 70.000 kg/cm^2 and tension strength 500 m^2 [14].

Some of advantages of porcelain insulator are [14,15,16]

I. Stable, their strong ionic bond among the atoms compose the porcelain creating a stable structure and usually is not degraded by environment, such as uitraviolet (UV), humidity, electrical activities, etc.;
II Having good mechanical strength;
III. Low cost, due to the materials of porcelain are inexpensive; and
Iv. Durable, fabrication process which consists of several processes, i.e. moulding and burning causes water content to decrease. Therefore porcelain insulator has long-lasting service.

However the porcelain insulator has some weakness [14,15,16,17], namely

I. Easily broken, especially during of transportation or installation. Vandalism is the main factor causing the insulator damage;
II. Heavy weight is one of characteristic of the porcelain. Therefore normally for large insulator the price is very expensive due to transportation and installation cost:
III. Cavity, due to imperfection in manufacturing process could cause internal dielectric breakdown;
Iv. Complex geometry, relatively to increase the creepage distance of porcelain insulator is by increasing the quantity of sheds. This causes the shape of the insulator to be more complex;
V. Easy to be polluted, due to their hydrophilic surface; and
VI. Low strength-to-weight.

Figure 2.1Porcelain insulator [89]

In 1960s an insulator having porcelain sheds supported by an epoxy r fibreglass rod was developed. It was not widely used because of development in ligh weight polymeric insulating materials [18].

2.1.1.2 Glass Insulator

Glass is recognized as the oldest insulator material (see Figure 2.2). General glass insulator has dielectric strength of 10-50 kV/mm, pressure strength of 30-120 N/r and tension strength of 50-100 N/mm^2.

Numerous advantages of the glass insulator are presented below [14,15],

i. High dielectric strength;
ii. Low expansion coefficient;
iii. Easy to design, due to the high dielectric strength;
iv. Transparent, therefore easy investigation for cracking, cavity, or b fracture; and
v. Homogeneous.

On the other hand glass insulator has some disadvantages as follow [14,15],

i. Water vapour is easily to condensate on the surface. Therefore, contaminant particles are easily deposited on its surface;

ii. For HV applications, glass insulators cannot be found in non-uniform shape, due to the non-uniform cooling off arising pressure from inside; and
iii. Can be easy to be broken, vandalism is the main to cause the insulator broken down after installation.

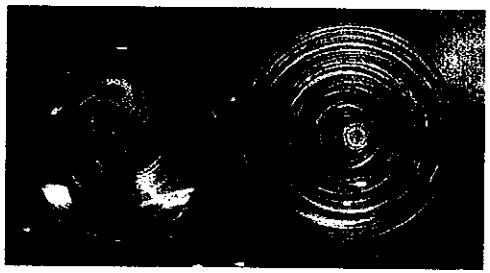

Figure 2.2 Glass insulator

Polymeric Insulator/ Composite Insulator/ Non-ceramic Insulator (NCI)

Researches have been carried out for alternative materials that could provide vement in performance over conventional insulators—porcelain and glass. It had d the development of polymeric insulators which took place globally and have d in several different insulator designs which are now widely used by electric power [19]. Different materials were used for the housing and shed of the polymeric ers [20].

Polymeric outdoor insulators for transmission lines were developed as early as n Germany, and by other manufacturers in England, France, Italy and the USA. .1 shows a list of manufacturers that had introduced the first generation of rolal polymer for transmission line insulators [18].

Table 2.1 : First generation commercial polymeric transmission line insulators

Company	Housing Material	Year	Country
Ceraver	EPR*	1975	France
Ohio Brass	EPR	1976	USA
Rosenthal	SIR**	1976	Germany
Sediver	EPR	1977	USA
TDL	CE***	1977	England
Lapp	EPR	1980	USA
Reliable	SIR	1983	USA

*EPR : Ethylene Propylene Rubber
**SIR : Silicone Rubber
***CE : CycloaliphaticEpoxys

There are four materials that are used widely as the elastomeric covering. The materials are suitable for HV applications. These are [17]

i. Epoxy;
ii. Ethylene Propylene Rubber (EPR), i.e., Ethylene Propylene Monomer (EP and Ethylone Propylene Diene Monomer (EPDM); and
iii. Silicone Rubber (SIR).

Polymeric insulators have a number of advantages i.e. lighter weight, explos proof, high contamination resistance, low cost, easy to install, not prone to vandalis economical, high electrical strength, compactness, earthquake-resistance, and low ra noise [13,21].

But the most important criterion for its choice is the excellent contaminati performance makes them easy to maintain [22]. It was proved that polymeric insulat especially the SIR insulators are better than the traditional porcelain or glass types many aspects. A survey conducted by Electric Power Research Institute (EPRI) indicat that polymeric insulator performed better than the porcelain insulator under contaminat environment [23].

yan, H.M. [24] reported that Polysuphide rubber was the earlier polymeric material Later, EPDM and other monomers were used. Most of these materials suffer damage by attack from ultraviolet. The attack caused the surface to lose the shiny produced during manufacture and become rough, which allowed pollution materials up. The rough surface result in the increase in the magnitude of leakage currents hen sufficient energy is available in the leakage current, the surface melts. The materials are generally organic compounds therefore the surface becomes rapidly ized as a result of the leakage currents. Later on, the use of SIR has improved the hobic property of the weather sheds. It was found that the particles of pollution led on the weather shed also became impregnated with the silicone exuded by the compound. Hence the pollution itself becomes hydrophobic together with the of the weather shed.

The main difference between EPDM and SIR was that the SIR remains hydrophobic after long-term service compared with EPDM. This is due to SIR containing low ular weight (LMW) silicone oil, which migrates to the surface and forms a thin film. If discharge presents then this film will destroy and the surface becomes hydrophilic rarily but migration of the silicone oil restores the surface hydrophobicity [25]. The of EPDM weather shed becomes hydrophilic after a short period of exposure to ather. Due to the hydrophilic surface the flashover mechanism of EPDM insulators ilar to porcelain insulators [26]. Generally SIR insulators show superior insulating illy when compared to conventional insulators or other polymeric insulators [27].

There are two types of SIR, i.e. room temperature vulcanized (RTV) and high ture vulcanized (HTV). RTV was preliminary used by Rosenthal, later called CeramTec, in 1967. The RTV housing did not contain any ATH-filler (only silica) cast directly onto the core in a seamless manner. Since 1979 the most important in manufacturing technology was done when the housing material was replaced H-filled HTV.

The polymeric insulator usually consists of a Fibre Reinforced Plastic (FRP) rod al end-fittings, and is covered by polymeric housing/ weather sheds [24], see .3. The FRP rod carries the mechanical load while the housing protects the FRP inst environmental impact, provides the required creepage distance, and high l strength. A 50 mm diameter core will have a minimum failing load of about 500

kN. The design of the polymeric insulator should be done properly to ensure that FRP polymeric housing assembly do not deteriorate with time. Attention has to be paid to fact that FRP rods perform both elongation and lateral contraction when mechanical is applied. The housing has to follow these movements without forming any gaps in interface between rod and housing. Therefore housings are made from highly ela material.

Under outdoor conditions all polymeric materials show changes on their sur with time, i.e. with ageing. Changes may be caused by physical and chemical attack to weathering (e.g. solar radiation, water, chemical) and electrical activities (e.g. co and leakage current). The changes mainly concern the weather shed surface an hydrophobic properties [7]. TuYanming [13] found that usually the failure of polym insulator was due to flashover, puncture, and other electrical or mechanical damage o sheds or the fibreglass rod. The hydrophobicity could be lost by the action of inte surface discharge activity. When the discharge activity stops, the surface and pollu particle recovered their hydrophobic properties over a period of about 24 (twenty f hours. Polymeric insulators were appropriate to be affected by stress for instance cor dry-band arcing, sunlight, moisture, heat and chemicals, etc.

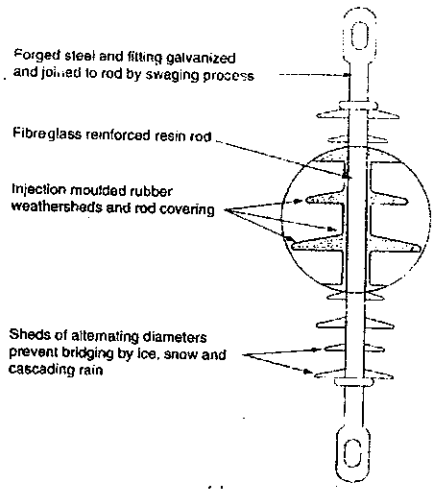

Figure 2.3 Polymeric insulator structure suspension type [24]

Contamination

When insulator are installed and subjected to operating voltage, the environment ave significant impact on its performance. They will be exposed to the natural mination. The various sources of contamination that affect power system insulation e, sea-salt from sea water carried by the wind, industrial product that could contain le salt, road salt, bird excrement, desert sand, etc. Figure 2.4 illustrates the minated insulators.

Insulators normally accumulate contamination in dry weather from dust or pollution. ses are normally initiated as leakage currents flowing over a wet contaminated e. Owing to partial discharges and rapid water evaporation, the currents may self-ulse, continue sporadically, or increase to become destructive high current vers. The arc normally propagates when the field across the film exceeds the field the arc [28,29,30].

(a) (b)

Figure 2.4 Contaminated insulators: (a) cap and pin ceramic insulator [106], (b) suspension type with housing made of SIR [107]

With respect to this environmental phenomenon several research works have been d. In United State the rapid and heavy pollution bring about serious damage in the system as reported by Burnham, J.T,et.al.[31].

A study in Noto Testing Station in Japan and concluded that the salt pollution closely related with the generation of salt particles. The salt deposition on the surface insulators would increase with respect to the magnitude of wind. Salt deposition on insulator is approximately proportional to the cube of wind velocity [32].

These agreed with the mathematical model developed by Ahmad S. Ahmad, [33] in his two papers that described a regression technique method to develop a Equivalent Salt Deposit Density (ESDD) mathematical model to predict the contamin severity. This study was made in Paka Thermal Power Station in the eastern regi Peninsular Malaysia.

From South Korea Nam Ho Choi, et al.[34] reported the distribution characte of salt contaminants with the distance form sea in South Korea in order to evaluat suitability of KEPCO's design standard for contamination. Conventional brush w method was used for about 150 sites, most of which were distributed near the coa measure the ESDD. Gutman, I. [35] developed a test set-up for testing of polyn insulators in the Natal province in South Africa. Some parameters were considere leakage current, insulation, weather, and pollution. All these parameters were continuo or periodically monitored at the Natal test station. In Thailand Sangkasaad, S. [36] r an investigation on the semiconducting glazed insulator under Natural Pollution. From experiment the author obtained that flashover voltage of the semiconducting gl insulators with different kinds of natural pollutions were about 2 - 3 times higher tha normal glazed insulators and a little bit higher than that of SIR insulator.

The influence of natural tropical condition in Bandung, Indonesia on the sur hydrophobicity of the HTV and RTV silicone rubber with different filler contents reported by Sirait, K.T., et al. [37]. The result measurements during 72 weeks on samples indicated that combination of UV radiation and temperature strongly contribu to the transfer speed and recovery of hydrophobicity due to migration of LMW to pollution layer. Heavy rain may lessen the ability to the transfer and recovery of hydrophobicity due to the removal of some LMW in the pollution layer. The pollu played an important role on change of contact angle of SIR. Increasing of pollu accumulated on the surface resulted in higher roughness of the surface and increased contact angle.

Contamination Measurement on the Surface of Insulator

The ESDD is the most commonly used method to characterize the quantity of the contamination severity on the surface of insulators. The method determines the salt pollution density by washing down the insulator surface with known amount of water and measuring the conductivity of the water [38].

The ESDD is defined in mg of NaCl/cm^2 of surface area of insulator, which will have identical conductivity equal to the actual deposit dissolved in the same amount of water used to clean the insulator [39].

ESDD measurement technique is a simple method to verify pollution severity and is only used in laboratory for artificial pollution test. However, this technique does not take account the dynamics involved in the electrical behaviour, since only the pollution layer is evaluated. Besides, it considers that the pollutions are uniformly distributed on insulator surface [40]. The methods have been standardized for porcelain and glass insulators in the IEC 60-1, 1989 and IEC 507, 1991[41,42].

NGK Company developed a method based on measuring the surface layer conductivity. A pair of spherical electrodes is pressed to the contaminated surface and the surface conductivity is measured between the electrodes. The conductivity of the surface will be increased by wetting. This equipment is sensitive to the electrode polarization and the resistance depends on the amount of water that could not be controlled accurately [39]. CIGRE WG 33-04 [38] reported that measurement of the insulator flashover stress, continuous recording of the leakage current and environmental pollution monitoring were used to measure pollution severity.

Effective Contamination Deposit Density (ECDD) method was reported by Liang Jing, et al. [22]. Figure 2.5 illustrates the equipment for ECDD measurement. The adjusted point of two small cylindrical iron tubes is placed vertically against the horizontally placed sample with a slight pressure by virtue of its own weight. Distilled water is injected into the tube. The test probe which was fixed together with the tube cover inserted into the tube internally and immersed in the distilled water but partially above the sample pollution layer. The conductivity measurement is conducted within 1 ~ 3

minutes. The ECDD of pollution layer is calculated by dividing the measured depo
dissolved salt with the area under the tube.

GyulaBesztercey and George G. Karady [43] developed a method and
instrument for measuring the pollution severity on outdoor electric insulators. The m
is called Spot Contamination Measurement (SCM). Meanwhile, Md. Abdus Salam,
[44] proposed a mathematical relation between ESDD, wind velocity and leakage dis
of the insulator by using Dimension Analysis technique [44].

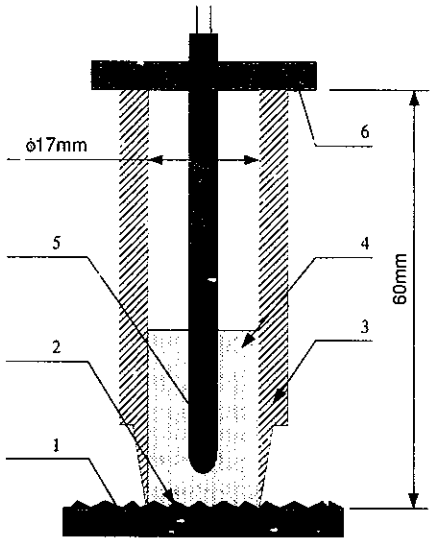

Figure 2.5 Illustration of ECDD Measurement [22]

1. plate sample
2. pollution layer
3. iron tube
4. distilled water (5ml)
5. test probe
6. tube cover

2.4 Artificial Contamination

Artificial contamination tests are conducted in the laboratory to simulate actu
contamination. There are two laboratory testing procedures that are commonly us
Salt fog test method and Clean fog test method. Both of these methods have

standard testing methods that can be conducted in the laboratory. The salt-
method is intended to simulate the contamination mechanism prevalent along
gions that can affect insulator's critical flashover (CFO) voltage. The salt fog is
by means of standardized nozzles. This method is applicable to polymeric and
meric Insulator contamination studies.

th respect to the development of polymeric insulator, several researchers [43,45]
stioned the application of the standard method for polymeric testing. The
s, whether the method could provide true reflection of the actual performance of
Insulators that is typically occurring at site. Since polymeric insulators have
haracteristic known as hydrophobicity the standard method may not be quite
Abrasive method was reported by Cheney, et al. [46] and the use of a chemical
was presented by De Tourreil, C. and Lambeth, P.J. [47]. However, both of these
have little resemblance with the natural pollution pattern on polymeric insulator.

La O, A. et al. [48] introduced a technique for applying contamination uniformly:

Applying dry kaolin powder directly over the sample surface by using dry cotton swabs. Light dabbing is needed to make the kaolin stick to the surface;

Wetting the sample gently with water by using a hose for larger samples and smaller samples were held under a water faucet;

Dipping the samples in the kaolin/ salt slurry and rotate them along their axis to obtain uniform contamination. For larger samples, flow coating produced the same uniformity;

The samples dried by hanging it vertically.

e use of this method did not change the original hydrophobicity behaviour of the
surface. This involved cleaning the sample surface after drying; as a result the
urface of the test sample was as hydrophobic as the virgin sample.

edish Transmission Research Institute (STRI) [49] developed a test method
st Cycle Method (DCM). It used a chamber which was able to apply dust
rtificial rain, fog and test voltage in order to simulate the air-born pollution build-
Insulator surfaces. One of the major advantages of this test was that pollution

was applied by the same way than it occurred in nature. DCM is a complete ins performance test and not merely a pre-contamination method.

George G. Karady, et al. [50] developed a pollution apparatus that employe spraying method. Where, a mixture of salt and kaolin powder was sprayed on the ceramic insulator by mean of a ceramic spraying nozzle. Later on with GyulaBeszter George G. Karady have introduced the Dry-mixing Contamination Method [43]. authors proposed a set of new type of nozzles types to obtain uniform contaminati the surface of polymeric insulator. Afterward GyulaBesztercey and George G. Karad presented the statistical model for ESDD and NSDD with regard to the Dry-m Contamination Method.

Takeshi Goto, et al. [21] introduced a contamination method applied to sil rubber cylindrical model by using a contaminating liquid that consists of NaCl, Tonok water. The contamination liquid, which was applied on the sample surfaces, was dri means of a warm air heater after spraying has been completed. The ESDD level obtained by varying the number of time the contaminating liquid sprayed. This me needs more time and skill personnel to get a uniform contamination and the drying me will be more and less affected the originality of insulator surface.

Another method was also introduced by Liang Xidong, et al. [22] in which authors proposed a new method to obtain uniform pollution layer on the hydroph surface by conducting pre-treating. Initially the polymeric surface was applied uniform dry kieselguhr, and then any surplus kieselguhr was blown off. A very thin laye kieselguhr formed on the surface of object. Then, the test object was contaminated the conventional pollution applying method. An interface will be formed between wettable surface and wet slurry.

2.5 Fog Chamber for Insulator Evaluation

In service insulator may be subject to degradation or aging due to ha environmental conditions, for instance fog. One of the most important laboratory test evaluate the performance of the insulator is to employ fog chambers. Factors parameters for the aging tests are the voltage stress, water conductivity, air and water f

droplet size, temperature, ventilation, geometry, arrangement and orientation of specimen, electrode shapes, surface condition, conductivity of the contamination, composition, duration and daily schedule of the aging tests, and the protection of the fog chamber.

The true purpose of the salt-fog test (underlying its invention in 1963) was to rapidly the relative performances of insulators having different shapes and attitudes in given severities of pollution. In addition, the subsidiary aims were: to the functional relationships between flashover voltage and severity of pollution for insulators; to establish laws, such as the extent of linearity of flashover voltage th, for insulators generally; to predict the performances of new types and shapes ulator.

tephen A. Sebo and Tiebin Zhao [52] in their paper have reported on the various s for non-ceramic outdoor insulator evaluation. Design specification and al feature of various fog chambers were presented in their report, including the main lay out of the fog chambers and their HV sources, data acquisition systems, for simultaneous visual observations, electrical measurements, and test cycles niques.

salt fog chamber and data acquisition system was developed in Ultra High (UHV) research laboratory, Central Power Research Institute (CPRI) by nath, D., et al. [53]. The size of the chamber is 2.0m x 2.0m x 2.5m. It was m stainless steels plate, with 33 kV/ 66 kVA, two phase, 50 Hz transformer, with two IEC nozzles on each side of the chamber.

fog chamber developed at the Ohio State University for polymeric insulator n [54]. The chamber size was 1.72x 2.44x 1.83m^3, and it was fitted with a gable high voltage source was a 240V/ 69000V, 50kVA, 60Hz single phase er. A data acquisition system and its component which was designed for testing insulator using the fog chamber [55]. The DASYLab software was used as a develop software application.

saka, et al. [56] developed a real-time system for simultaneous observation of charge arcs and leakage current on insulator surface under wet-contaminated

condition. Video recording system and a personal computer were used to p simultaneous recording of discharge and leakage current. The program applicatio written in BASIC and in machine language. The BASIC program was used for savin controlling the outputs of data obtained whereas the program written in machine lang was used for the routine leakage current measurements.

A simultaneous electrical and visual measurement of leakage current along po insulators in artificial pollution tests was introduced by Wibawa Tjokrodiponto, et al. in two papers [57,58]. The main component that allows a simultaneous observation wa mirror positioned in front of the test sample. This mirror was attached to a picture f mounted at an angel to a post structure. The mirror covered only half of the picture fr The other half of the frame was left empty to permit the image of the insulator viewab a video camera positioned in front of the chamber. A digital oscilloscope was loc underneath the frame structure. The oscilloscope screen was faced upward in such a that the screen reflection on the mirror could also be seen by the video camera. adjusting the angle of the frame/mirror unit with respect to the post structure, the imag the oscilloscope could be adjusted to cover most of the mirror surface.

Tiebin Zhao and John Sakich [59] developed a data acquisition system for sal aging test on non-ceramic insulators. The data acquisition system consisted of protec circuit, measuring circuit, analog to digital converter (ADC), personal computer, software for data processing. The software was developed using C language LabWindows. The salt fog chamber was constructed of stainless steel sheets wi dimension of 5.0ft x 3.0ft x 4.0ft (60 ft3 or 1.7m3). Test samples was energized by a voltage transformer (19.92 kV/480 V, 15 kVA, 2.05% impedance) fed by a 480/0-480, kVA powerstat.

2.6 Leakage Current Measurement

When a contaminated insulator becomes wet, leakage currents begin to flow on surface. If the leakage current reaches a certain threshold level the insulator experience an external flashover. It is believed that the difference leakage current leve parameters may be functionally related to the different amount of contamination a ageing parameter. For example, highest peak current is normally related to pollu

r.m.s. current may be an indication of power loss on the surface, and therefore n, accumulated charge of different polarity may indicate charge movement over the e, and therefore corrosion [35,60].

The duration of the wetting, in order to reach the maximum layer conductivity, was onstant. It depended on the temperature difference between pollution layers and fogs minant composition and the humidity in the test chamber [61].

Leakage current on the surface of insulators would come up power losses. The e leakage current was resistive; therefore the power losses can be written as, $P = V$ minimize the power losses silicone compound was used to cover the surface of nlo insulator. Silicone compound was effective to increase the hydrophobicity of the nlo insulator and decrease the leakage current and also increase the flashover e of the insulator [62]

Fernando, M.A.R.M. and Gubanski, S.M. [63] presented measurements of low-level e current pattern on naturally aged insulators and artificially contaminated material les as well as insulators. A nonlinear behaviour of leakage current relating to surface phobicity and electric stress was described. Neural network with the learning vector ization (LVQ) technique was used for evaluating the surface state of polluted tor from the leakage current waveforms and their harmonic content.

Butler, K.L., et al. [30] discussed the characteristic of individual and multiple ors leakage current from field experiment recordings. The leakage current for single ors showed an erratic behaviour ranging from half a cycle to many seconds in n. Voltage-current plots showed that the insulator surface discharge was very lo and non-linear. The characteristics for multiple insulators followed from that of insulators. Multiple insulators showed a small period of leakage before one of the ors flashed over.

Fernando, M.A.R.M. and Gubanski, S.M. [64] presented results and analysis of t leakage current waveform on porcelain, RTV coated and polymeric insulators the clean fog pollution testing under laboratory conditions. The resulting leakage rms recorded with different time lapses, after contamination were compared both in nd frequency domain. The waveforms became deformed from sinusoidal shape as

the voltage level increased. A neural network was trained to recognize the patterns and to evaluate their third harmonic content. The results were compared with the Fast Fourier Transform (FFT) analysis of the pattern.

Isaias R.V [65] made a study to investigate the flashover occurred on a 400kV line located in a semidesertic area in Monterrey, Mexico. Five different profiles of glass and porcelain insulators and several online leakage current monitors were installed on the line to determine the leakage current pattern during critical conditions. The obtained values were used to compare the performance of the insulators installed in the field with the purpose of providing preventive maintenance indicators. The maximum leakage current levels have been defined for the different profiles and a tighten relation between the ESDD and the leakage current has been obtained. The current level has been used as a sign of alarm for the maintenance of this line during several years.

Bologna, F.F. et al. [66] worked on online monitoring system installed on Eskom's 275kV line. An online leakage current recorder/analyzer (OLCA) was used to monitor leakage currents flowing along the insulator string, as well as the environmental data. The OLCA had nine leakage current monitoring channels. The test insulators used were standard U 120 cap and pin glass discs with a nominal creepage distance of 280.0 mm and a connection length of 146.0 mm.

H. Matsuo, et al. [67] used a long rod insulator to observe the degree of pollution under a saltwater spray by measurement of leakage current, which flow between electrodes fixed on the surface of insulator under 30 Vac voltage. The followings were found: (1) the effect of the wind velocity on the insulator was small, and was especially small when the distance between the electrodes was short; (2) the effect of the distribution of the saltwater drops on the insulator was small; and (3) the leakage impedance did not depend on initial dryness of the insulator surface before the saltwater spray.

Masashi Sato, et al. [68] reported a laboratory test to study flashover phenomena of insulators under rapid pollution conditions. The leakage current was measured using a personal computer. Time variation of the leakage current and the discharge behaviour on the insulator were investigated with a trial observation system. It is found that the type of time variations and the phase transition current according to discharge growth were responsible for flashover probability.

Devendranath, D., et al. [69] reported a study cor
current and the charge on the flow rate, conductiv
the fog. The test was conducted on RTV coated
current integrator has been developed u
sion.

George G. Karady and Felix Amarh [70] presented a signature analysis to
waveforms of polluted insulator. This study was intended to investigate th
ity of modern high resolution digital spectral analysis method. The leakage current
ntinuously acquired and stored during flashover tests. It was observed that the
magnitude of the odd harmonic in the leakage current increased with the increase
g intensity.

George G. Karady and Felix Amarh [71] presented an application of Extreme Value
to the statistical analysis of the large excursions of the leakage current peak
ude (envelope). The measurement and analysis of leakage current for condition-
monitoring of polluted insulators was well documented. Extreme Value Theory
was used to discriminate and characterize the largest and rarest peaks; namely the
teristics largest value and extreme value risk function. The aim was to analyze the
e continuously until flashover, in order to establish trends which might indicate the
nce of flashover. The risk of flashover increased with increase in the levels and
ncy of large excursions of the leakage current envelope.

M. Sato, et al. [72] presented the results of spectral analysis of leakage current
ms on contaminated insulator under fog conditions. The spectral analysis of the
current waveforms was conducted by the auto regression (AR) method with high
on and without limitation in number of sampling data. The results indicated that the
analysis by the AR method was available for the monitoring of contamination
ne of outdoor insulators.

Sierro-Chavez, J. L., et al. [73] developed a system for the measurement of leakage
and surface resistance of insulators located in the northeast part of Mexico. The
was installed in several towers along with the line as a diagnostic tool to monitor
face condition of the polluted insulator. The leakage current sensor consisted of a

the voltage level increased. A neural network was trained to recognize the patterns and to evaluate their third harmonic content. The results were compared with the Fast Fourier Transform (FFT) analysis of the pattern.

Isaias R.V [65] made a study to investigate the flashover occurred on a 400kV line located in a semidesertic area in Monterrey, Mexico. Five different profiles of glass and porcelain insulators and several online leakage current monitors were installed on the line to determine the leakage current pattern during critical conditions. The obtained values were used to compare the performance of the insulators installed in the field with the purpose of providing preventive maintenance indicators. The maximum leakage current levels have been defined for the different profiles and a tighten relation between the ESDD and the leakage current has been obtained. The current level has been used as a sign of alarm for the maintenance of this line during several years.

Bologna, F.F. et al. [66] worked on online monitoring system installed on Eskom's 275kV line. An online leakage current recorder/analyzer (OLCA) was used to monitor leakage currents flowing along the insulator string, as well as the environmental data. The OLCA had nine leakage current monitoring channels. The test insulators used were standard U 120 cap and pin glass discs with a nominal creepage distance of 280.0 mm and a connection length of 146.0 mm.

H. Matsuo, et al. [67] used a long rod insulator to observe the degree of pollution under a saltwater spray by measurement of leakage current, which flow between electrodes fixed on the surface of insulator under 30 Vac voltage. The followings were found: (1) the effect of the wind velocity on the insulator was small, and was especially small when the distance between the electrodes was short; (2) the effect of the distribution of the saltwater drops on the insulator was small; and (3) the leakage impedance did not depend on initial dryness of the insulator surface before the saltwater spray.

Masashi Sato, et al. [68] reported a laboratory test to study flashover phenomena of insulators under rapid pollution conditions. The leakage current was measured using a personal computer. Time variation of the leakage current and the discharge behaviour of the insulator were investigated with a trial observation system. It is found that the type of time variations and the phase transition current according to discharge growth were responsible for flashover probability.

Govendranath, D., et al. [69] reported a study concerning dependence of the current and the charge on the flow rate, conductivity and pressure of the solution in the fog. The test was conducted on RTV coated porcelain samples. A PC-based-current integrator has been developed using digital capacitive current integration.

George G. Karady and Felix Amarh [70] presented a signature analysis for leakage waveforms of polluted insulator. This study was intended to investigate the ility of modern high resolution digital spectral analysis method. The leakage current ntinuously acquired and stored during flashover tests. It was observed that the magnitude of the odd harmonic in the leakage current increased with the increase g intensity.

George G. Karady and Felix Amarh [71] presented an application of Extreme Value to the statistical analysis of the large excursions of the leakage current peak ude (envelope). The measurement and analysis of leakage current for condition-monitoring of polluted insulators was well documented. Extreme Value Theory was used to discriminate and characterize the largest and rarest peaks; namely the teristics largest value and extreme value risk function. The aim was to analyze the be continuously until flashover, in order to establish trends which might indicate the nce of flashover. The risk of flashover increased with increase in the levels and ncy of large excursions of the leakage current envelope.

M. Sato, et al. [72] presented the results of spectral analysis of leakage current rms on contaminated insulator under fog conditions. The spectral analysis of the current waveforms was conducted by the auto regression (AR) method with high on and without limitation in number of sampling data. The results indicated that the analysis by the AR method was available for the monitoring of contamination ns of outdoor insulators.

Llerro-Chavez, J. L., et al. [73] developed a system for the measurement of leakage and surface resistance of insulators located in the northeast part of Mexico. The was installed in several towers along with the line as a diagnostic tool to monitor face condition of the polluted insulator. The leakage current sensor consisted of a

current transformer (CT) with special magnetic characteristic (high permeability). Both waveform and magnitude of the leakage current signal were monitored and compared to results from a resistive measurement system. Solar cell supply of a 12 V, 18 W and a 105 Ah battery as back-up was used for electronic system.

Felix Amarth, et al. [74] presented a level crossing analysis (LCA) of probabilistic dynamic of the leakage current envelope of polluted insulators. This problem was formulated in terms of the mean crossing rate at specified thresholds and mean time spent above these thresholds. The notion of LCA of the envelope was introduced and a measure of LCA was proposed.

Wibawa T., et al. [58] presented a test series developed at the Ohio State University to observe the progress of the leakage currents along pre-contaminated insulators. It was found that there was no difference in the leakage current waveshapes between SIR and EPDM insulators. The frequency contents of the waveshapes were mainly determined by the magnitude of the leakage current. The higher the magnitude of the leakage current, the higher the content of the third harmonic was.

2.7 Flashover Accident

The development of leakage current and arcing on the insulator exterior whose surface resistance has been reduced due to the contamination and moisture is responsible for flashover. Insulator breakdown is a leading cause of failure/ outage in transmission line for a long time commonly occurred in heavy industry area and coastal [75]. Figure 2.6 illustrates a full flashover on the insulator.

Looms, J.S.T [11] described common precursors of pollution flashover on insulator in actual services:

(i) Arrival of nearly pure water, as dew, rain or mist, at an insulator which carries a burden of pollution comprising soluble ionic components like common salt. This is the most common. Especially in desert areas, pollution flashover occurrences are closely correlated with times of dew and morning mist, while in marine-polluted regions the dangerous times are in still-air fog.

Deposition of droplets from marine or industrial fogs, or of other combinations of water and electrolyte. Simultaneous deposit of water and solute occurs in on-shore storms and, rarely when insulators are immersed in chimney plumes.

Build-up of hoar frost, freezing fog or ice on the fouled surface of an insulator, the ionic components of the fouling then proceeding to depress the freezing pint of the water and allow solution at the interface.

Switching in of a circuit containing insulators which are wet and fouled.

Arrival of a temporary over voltage, or of a switching surge, at an insulator which is wet, fouled and possibly already energized.

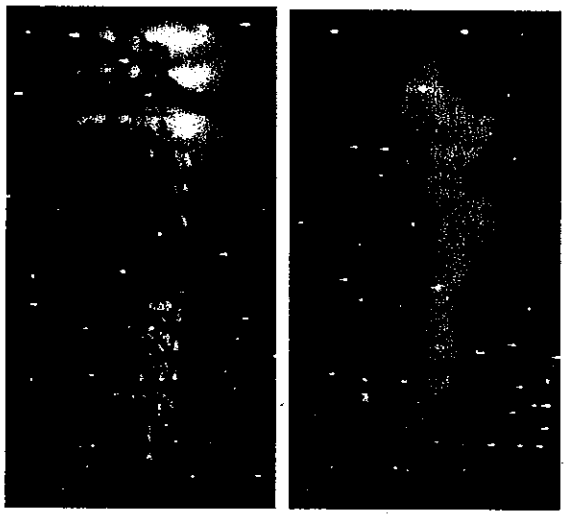

Figure 2.6 Flashover on insulators [108].

following broad stages of the flashover process: initial behaviour of electrolytic r local electric stress; stability of discharges between different parts of the layer; on of discharges along the surface and evolution of an arc which short-circuits e.

Rizk, F.A.M. [76] presented some reviews on the proposed of the flashove mechanism in the form of empirical models. Table 2.2 is important review and analysis o flashover models.

Topalis, F.V., et al. [61] introduced a mathematical model to conclude flashove mechanism qualitatively and quantitatively. The critical voltage of any insulator under an pollution severity can be evaluated. Hence, the electrical behaviour of insulators unde pollution conditions can be predicted to minimize the expensive and time-consumin experimental tests.

Table 2.2: Stability of surface arcs: Principal results

Author	Model	Results
Obenaus	Arc of length x in series with resistance R_p of wet pollution layer. Source voltage U; current i; n and N constants	$V_{arc} = xN / i^n$ $x = (i^n / N)(U - IR_p)$
Neumaerker, Rizk	Uniform pollution resistance $\bar{r}_p$per unit leakage path, L; arc bridges x/L; minimum sustaining voltage U_{cx}; critical stress E_c; critical current i_c	$R_p = \bar{r}_p(L-x)$ $(nN/\bar{r}_p)[U_{cx}/(1+n)NL]^{(n+1)/n}$ $=\left(\frac{x}{L}\right)^{1/n} - \left(\frac{x}{L}\right)^{(n+1)/n}$ $E_c = N^{1/n+1}\bar{r}_p^{n/(n+1)} : i_c = (N/\bar{r}_p)^{1/(n+1)}$
Woodson and McEloy	Disc of pollution resistance between inner and outer ring electrodes, r_i, r_o; arc spans outwards to r_a; surface conductivity K_s	$R_p = \frac{1.6\times10^{-2}}{K_s}(r_o - r_a)^{1.4}$
Hurley and Limbourn	Empirical relationship between minimum AC arc voltage for rod gap x, in series with R_p; strike distance L_a	$U_c = \text{const.}\bar{r}_p^{1/3}L_a^{2/3}L^{1/3}$
Claverie and Porcheron	Minimum arc reignition voltage for given current and distance, $i$and x	$U_{cx} = \frac{800x}{\sqrt{i}}$

Abdul Salam, et al. [44] developed a mathematical model to present ip between flashover voltage and ESDD for DC system. The proposed model Dimensional Analysis technique.

Jiangliu, et al. [45] classified the cause of surface flashover and damages of Insulator that installed in China. Flashover accident occurred due to lightning occupy, bird dropping, contamination flashover, unidentified flashover, damages out-side force.

roure, H.P. [77] described the relationship between the critical flashover voltage d Insulators and the air pressure is normally expressed by the following equation

$$\left(\frac{P}{P_0}\right)^m \qquad (2.1)$$

the reference pressure
the pressure at high altitude
the critical flashover voltage of insulators corresponding to air pressure P_0
the critical flashover voltage of insulators corresponding to air pressure P
constant

value of m characterizes the influence of air pressure on the critical flashover Insulator, and depends on several factors and parameters including insulator age and pollution severity, this was described by Farouk A., et al. [78].

hu et al. [79] conducted a laboratory investigation for determining the AC erformance of two types of insulators, post and suspension insulator, covered l Ice at low pressure. It was found that the atmospheric pressure has an ect on the AC minimum flashover voltage, VMF, of insulators under icing The lower the air pressure corresponding reducing VMF.

Izzularab, M.A., et al. [80] conducted a study for estimating the lightning insulati strength of a distribution line designs. An empirical factor to estimate the flashover volta due to lightning of polymeric insulators used on distribution overhead lines was presente The test was conducted materials used on distribution system that are porcelain, FRP a polymers and their composite combinations. Investigation was made base on t configuration of the polymeric insulators and the point of incident of the lightning impul that may cause flashover and location of grounding wires. In addition, the physical and t active length of polymeric insulators were also determined to evaluate the most effecti configuration and material to be used. Factors that may affect the CFO of polyme insulators was investigated and defined to evaluate different insulator types and polyme material used.

Gonos, I.F., et al. [81]presented a complex optimization method based on t genetic algorithm (GA) for the determination of the arc constants, using experiment results derived from the artificially polluted insulators tests. In addition, the autho proposed a mathematical model to validate the experimental result obtained.

S. Gopal, M.E. and Prof. Y.N. Raom, Dr-Ing[82] proposed a new mathematic model which was based on the dynamic arc voltage-gradient equation. It was found to b in good agreement for calculating the critical pollution withstands voltage of the standa insulators. However, in the case of long-rod insulators the calculated values differ slight from the experimental values.

Sudararajan, R. [83] conducted a flashover voltage study of polymeric insulati material by using a dynamic model for porcelain test. The author managed to show t good correlation between the model and the experimental data.

However, George G. Karady [26] reported laboratory studies indicate that t flashover mechanism of polymeric was different compared to porcelain insulator.

Ghosh, P. S. and Chakravorti, S. [84] applied method of Artificial Neural Netwo (ANN) in pollution flashover studies for function estimation. The arc over a pollut surface was not a constant parameter and depended on several factors that are resistan per unit length R_p, I and applied AC voltage V. A modelling of the complex non-line function $t = f(V, L, R_p)$ was accomplished accurately.

ulator Aging

utdoor insulators are subjected to simultaneous electrical, thermal, mechanical nd natural contamination. All these components influence to the aging of Several studies have been published regarding to the ceramic and polymeric aging observation.

rmendy, I. and Fogarasi, I.[85] made a study on several of porcelain cap and long ators In order to detect the insulators ageing. The effect of the electric strength sured. For the purpose of the standard electric tests, i.e. the determination of ulse voltage flashover level, measurement of power frequency voltage under wet checking of radio interference voltage were applied. The electromechanical d was determined by application of 50 kV continuously on each cap insulator of string. At the same time the mechanical load was increased until flashover The results shown age cap insulators mainly lose their mechanical and echanical characteristics. These parameters may be reduced to half the original ter long operational period. The standard deviation of these values became too

ellman, C. A. et al. [86] published a literature review survey that identified aging nd their effect on polymeric insulators. According to their nature, these factors ssified as electrical, mechanical, ultra-violet radiation, chemical, thermal, and rces. The effects were manifested as external or internal damage with loss of and mechanical viability. Ageing caused surface roughening and tracking, of the housing, expulsion of filler particles onto the surface and a loss of bility. Therefore for testing and development purpose, artificial and accelerated d an important part to play. Identification of natural ageing process should tificial test to be improved.

ongJianchao, et.al. [87] presented the results of studies on the ageing nce of High Voltage Direct Current (HVDC) line porcelain insulators and related g factors i.e. body current and electric field intensity. The residual dielectric of porcelain materials with difference ageing time was measured and the energy

spectrum examination on aged insulators was also carried out. Analysis was carried o regarding to the influence of space charge on field distribution.

TuYanming [13] described some approaches to aging of polymeric insulators. T problems that polymeric insulators face in service or manufacturers were discussed. addition, some measures to estimate or approach the true aging state of operati polymeric insulator in field were exposed.

2.9 Summary of Literature Review

There are two categories of insulator that are currently applied for out-do application, i.e. ceramic and polymeric insulators [12,18]. The main problem experienc by these insulators that are used for cut door is the effects of environmental conditio These environmental conditions have different characteristic impacts on the performan of insulator.

Several researchers had conducted studies to obtain information concerning, t relationship of contamination severity with any other meteorological factors, a performance of insulators under the naturally contaminated condition. Y, Taniguchi [3 conducted a study in Noto Testing Station in Japan. Burnham, J.T., et al. [31] from Unit Stated reported about serious damage in the power system due to rapid and hea pollution. Gutman, I [35] developed a test set-up in Natal province in South Africa. Fr Bandung, Indonesia, Sirait, K.T., et al. [37] reported the influence of natural tropi condition on the surface of the HTV and RTV silicone rubber with different filler conten Ahmad S. Ahmad, et al. [33] reported a study which was conducted in Paka Therm Power Station situated in the eastern region of Peninsular Malaysia. In the same yea Sangkasaad, S. [36] reported an investigation on the semiconducting glazed insula under natural pollution in Thailand. Nam Ho Choi, et al. [34] from South Korea reporte study, which was made to evaluate the suitability of KEPCO'S design standard contamination. The insulator performance study under the natural environmental conditi could be good alternative to obtain the real information about the environmental conditi that affect the insulators performance. However, this study usually could only conducted after the system has been installed, and normally takes longer time completion and incur high cost to implement the actual evaluations.

ncerning the subject of contamination severity, IEC had standardized a method terize the quantity of contamination severity on surfaces of insulators [42]. there were several methods introduced afterwards such as; the ECDD which was d by Liang Xidong, et al. [88]; the measurement of the insulator flashover stress, e recording of leakage current signatures and environmental pollution monitoring ribed by CIGRE WG 33-04 [38]; and the SCM was described by Gyula y and George G. Karady [43], still the IEC standard is the most commonly used However, currently with the advanced capability of electronic conductivity meter, e automatic temperature compensation, the temperature compensation n as presented in IEC standard could be neglected. Coupled with the recent experimental based empirical model, for predicting the values of salinity only ng the measurement of conductivity of a solution rendered temperature ation, calculation unnecessary.

order to solve several limitations of the on-site evaluation of insulators nce, artificial contamination chamber that could simulate the surface ation process is absolutely necessary. Until present, for ceramic and polymeric performance tests still employ to the salt-fog and clean-for method (that had been ted by IEC). However, researchers have questioned the validation of salt-fog n-fog in relation to polymeric insulators testing, due to they have different ristic if compared with ceramic [45,51]. Regarding to the artificial contamination meric insulator there were numerous technique have been proposed namely, method was described by Chenoy, et al. [46], chemical method was introduced urrell, C. and Lambeth, P.J. [47], dry-spraying method was proposed by George y, et. al. [50], and dry-mixing contamination method was presented by ercey and George G. Karady [43]. Later on, Takeshi Goto, et al. [21] a contamination method applied to test silicone rubber cylindrical model by aminating liquid that consists of NaCl, Tonoko and water. The ESDD level was by varying time of application of the contaminating liquid sprayed on the In the same years Liang Xidong, et al. [22] proposed a new method to obtain lution layer on the hydrophobic surface by conducting pre-treating. At present complete equipment for insulator performance test, available in the Swedish lon Research Institute (STRI) [49]. It is called the Dust Cycle Method (DCM). A tment has been addressed for developing this system. From the several

artificial contamination methods mentioned above with the exception the DCM, the mos
efficient, simple and reliable method is dry-mixing contamination method. This is s
because that method does not physically change the polymeric insulator surface unlike th
abrasive and chemical methods. The contaminating process merely depends on th
nozzle system set-up, therefore special trained labour is not needed. Base on thi
advantage, it is better to adopt the dry-mixing contamination method concept fo
developing an artificial contamination chamber. However, only the concept will be adopte
whereas for the nozzle design as well as the dimensions will refer to the IEC standard
The additional nozzle was specially designed to accommodate the non-soluble particl
spraying. This particular design was solely the outcome of the research's imagination.

Regarding to their size Stephen A. Sebo and Tiebin Zhao, [52] in their paper
divided the chamber into three main categorizes, i.e. large size chamber, if at least one o
the its dimensions was > 5.0 m, medium size chamber, if at least two of its dimension
were between 1.0 m and 5.0 m, and small size chamber, if it main dimension were < 1.0m
Generally the size of the chamber developed is related to the working voltage of th
testing to be used. For the medium size, there are numerous publications on this subject.

Information on one of the earliest medium size chambers ever constructed wa
published by Dakin and Mullen of the Westinghouse Research Laboratories (USA) i
1972. The dimension was 1.20 m side cube, energized by a 15 kVA, 12 kV transformer
The second salt fog chamber of Dow Coring was described in detail by Reynaert, Orbeck
and Seifferly. Their salt fog chamber was a cube with 1.52 m sides, a pyramidal roof, an
supplied with a 60 kVA, 30 kV transformer. A 1.52 x 1.52 x 1.37 m^3 chamber with
pyramidal roof developed at Massachusetts Institute of Technology (MIT, USA) wa
discussed by Jolly. The fist fog chamber built at the Arizona State University (USA) wa
described by Gorur. The chamber size was 3.6 x 3.1 x 2.5 m^3, with a 15 kVA, 50 k
transformer. The second chamber built in Arizona State University was a stainless stee
cube of 4 m sides, with a 40 kVA, 100 kV transformer.

A fog chamber (built in Brazil), 1.6 x 2.0 x 2.5 m^3, with 25 kVA, 150 kV transforme
was reported by Garcia, Santiago and Portela. Both fog chambers built by Public Powe
Corporation in Greece were cubical shaped, reported by Ikonomu et al. One of them ha
a 1.5 m side, the others was 4.6 m side. The fog chamber built at the Indian Institute o
Technology (Madras) was 1.9 x 1.9 x 3.3 m^3, reported by Xavier and Rao. A fog chambe

iversity of Manchester Institute of Science and Technology (United Kingdom),
44 kV transformer, but the size of chamber was not given in the paper.

m Japan Isaka, Yokoi, Naito, Matsuoke et al. built a 2.0 x 2.0 x 3.0 m^3 fog
at The University of Tokushima. IREQ (Canada) reported two medium size
there were, a 1.2 m side cube was described by de Oliveira and de Tourreil, and
a 2.3 x 2.3 x 3.0 m^3 was described by de Tourreil and Lambeth. The fog
built in Mexico, reported by De La O and De La Vega was 2.6 x 2.6 x 2.5 m^3,
tainless steel sheets. In China, from Tsinghua University, Guan et al. reported
4.0 x 4.0 x 6.0 m^3, fog chamber with a source of 250 kVA, 44 kV transformer.
iversity of Wales College of Cardiff (United Kingdom), the fog chamber size is 2.0
0 m^3. Its source was a 7.5 kVa, 100 kV transformer. Benzaoua, Harid, Rowlands
re discussed the used of the chamber for artificial pollution tests on distribution
sulators.

wana, Buganski and Kvarngren at the Royal Institute of Technololgy (Sweden)
m side cube fog chamber. It was used either with a 30 kVA, 60 kV, or with a 700
kV transformer. At Ain Shams University (Egypt), a fog chamber, 1.4x0.9x2.3
18 kVA, 150 kV transformer was used for performance test of polyester material
d by Risk et al. A chamber size 2.0x2.0x2.5 m^3 was reported by Vasudev et al.,
on ageing study under DC voltage at the Indian Central Power Research Institute
re. The fog chamber at the Technical University of Ilmenau (Germany) was 1.5 x
m^3. At the Swedish Transmission Research Institute, there are two medium size
ere with dimensions of 1.2 x 3.0 x 2.5 m^3, and 2.0 x 2.0 x 2.5 m^3, both with a 30
rmer as the voltage source. The climatic chamber of ABB (Calor EMAG) is 2.9 x
m^3 with a three- phase voltage source, to 45 kV line-to-line voltage. The size of
test chamber at the Technical University of Darmstadt was 2.5 x 2.6 x 2.8 m^3,
-phase transformer, 90 kV line-to-line voltage. Their cold fog chamber is 2.0 x
m^3, with a 20 kV transformer as the voltage source.

chamber at the Ohio State University (USA) is 1.7 x 2.5 x 2.65 m^3, with a
was reported by Sebo, Casale, Cedeno, Tjokrodiponto, Akbar, Sakich and
dicated voltage source was a 50 kVA, 69 kV transformer. Zhao, Sakich, and
r reported the fog chamber at the Ohio Brass Company (USA). The size of the
was 1.5 x 0.9 x 1.2 m^3. The voltage source was a 15 kVA, 20 kV single

transformer. The Ohio Brass Company had also constructed a multistress environme test chamber for 5000 h accelerated weather aging test on polymeric insulators arresters. The chamber size was 2.4 x 3.1 x 2.4 m^3. The dedicated source voltage two of 42 kV transformer. This chamber was equipped with UV panels, heat humidification systems, and rain and salt fog systems were installed for the chamber. environmental condition and test cycles were controlled by a computer.

In many literatures the use of computer measuring system and camera record was important part of the testing using artificial contamination chamber. This facilita observation and analysis of leakage current data and flashover scenario. Different ty of software had been used for instance, DASYLab, BASIC, C, LabWindows and OL [55,56,59,66]. Also different ADCs have been utilized. To capture the flashover and recording purpose generally 1 (one) camera is sufficient. It means that 1 (one) side of insulator can be captured [54] but the weakness is there is a possibility flashover activi could be captured.

CHAPTER

DEVELOPMENT OF THE TEST CHAMB

3.1 Introduction

The prime aim of this work is to develop an indigenously designed and fabrica
Artificial Contamination Chamber (ACC) system. The ACC incorporates improved nozz
design for ceramic and polymeric insulator testing. To realize and materialize the A
several stages of activities are involved, i.e. design, development, construction a
commissioning.

The secondary aim is to use the ACC to test glass and polymeric insulators un
contaminated conditions with the intention to establish a useful technique for insula
selection.

3.2 The Artificial Contamination Chamber

In the last decade tremendous amount of efforts have been utilized to understa
the insulators performance especially the polymeric insulator. Many researchers ha
been found to adopt various testing procedures to observe the performance of
insulator exposed to prolonged contaminated condition. Various types of testing w
conducted on the insulator and invariably an artificial contamination chamber was used.

In this work, an ACC is designed, developed and constructed. The chamb
development is intended to simulate the real service condition so that tests can
conducted in the laboratory. For this a mock-up system which is able to simulate
variation in ambient conditions and also contaminant impact commonly affecting insulat
can be used as an alternative testing method enabling the tester to control the vario

ndition prevalence on site. In this way, time-saving tests or accelerated
nducted on insulators.

hing the metrological condition, some parameters have to be considered in
ent of an indigenous ACC system. Particularly in dimensioning of the size of
ratory space availability has to be considered. Every chamber components
reprlately designed and suitably located to ease the chamber installation to
functioning of the system. Consequently, it facilitates the ease in organizing
ivities of testing work, a reduction of development cost, and minimal space

election of materials for the chamber is considered meticulously. The
esen are corrosion-resistant. The structure has to be strong enough to support
t and also operator/ researcher. The chamber wheels should be capable to
weight of structure, test object, and operator when doing work in the chamber.
re, the design of the contamination generation system is an important
n as well.

n of the Artificial Contamination Chamber

y engineering works proper design practice is essential to obtain the best
on implementation. Therefore technical drawings are required to provide an
implementation work. This is also important to obtain some information
mount of materials required, appropriate size of the relevant equipment, the
uitable location of the relevant objects, scope of works, cost estimations
in implementation.

nical drawing is materialized by means of AutoCAD which is currently
powerful software for a technical drawing. The AutoCAD can help to
ion in three dimension and also orthographic presentation [90,91,92]. Fine
awing design, zoom in and zoom out drawing and editing of the drawing
h AutoCAD aided design.

The drawing design was divided into three major parts, i.e. the structure, contamination generation system and the draining or water circulation system.

3.2.1.1 The Chamber Frame Structure

The structure is made of corrosive resistant material i.e. stainless steel. structure joints are jointed perfectly to ensure chamber could withstand maximum loa The chamber is fitted with swinging wheels to give chamber more mobility and portab It is of cubicle in shape with 1.415 x 1.415 x 1.650 m^3, (W x L x H), in dimension. Fi 3.1 shows that the top and bottom frame structure consists four windows formed welding up four-hollow-steel bars at the perimeter of the frame and reinforced at the ce with two-hollow steel bar welded at right angle. Whereas vertical sides of the chamber constructed of the same type of metal-bar pieces, the only different is one side is fitted the prototype door leaf. This opening is used to access the chamber interior par hanging the insulator, adjusting the fog nozzle, connecting HV cable and others. On opposite side of the chamber door is the side through which the HV bushing entered chamber.

3.2.1.2 Prototype Contamination Generation System

The Prototype Contamination Generation System (PCGS) is designed compliance with the IEC Std. 507 but some adaptive approach is taken which involv additional nozzle intended to come up with dry mixing contamination method [51]. combining these two methods the chamber can be used for ceramic insulator polymeric insulator tests. The nozzles are made of a corrosive resistant material. some practical observations the suitable material for the nozzles is stainless steel, due strengthen and polish surface can be obtained. The nozzles units are attached transparent housing. This housing is made from transparent polycarbonate mat Figure 3.2 shows the design of the nozzle units.

The nozzle units are placed at two corners of the chamber, one at each co placed diagonally facing each other in the chamber. The nozzle-units along with

mped to a stainless steel cylindrical hollow pipe. Another part of the hed to the screwing rod. The screwing rod is supported by mean of two e stainless steel bearing units. At the top end of the screwing rods, gear unit, a DC motor is coupled to it. The motor speed is controlled by a gulator unit. In addition a mechanical switch and relay system is installed rity of the motor. If the screwing rod is turned clock-wise then the nozzle downward, and vice versa.

supply to the nozzle is obtained by means of a corrosive resistant pump. pump with plastic body cover is very suitable. An air compressor unit is air supply. The water and air flowed from two different tubes. The tubes al of high pressure resistant, corrosive resistant, and bendable. Figure 3.3 reticulation system of water and air supply of the nozzles.

Draining System

ater produced during the running of the test has to be slugged out in order ing collected at the floor of the chamber. Therefore a water reservoir is chamber floor. At this floor four holes are drilled to allow the water to be reservoir. The water reservoir is furnished with PVC piping system to of the water from the reservoir. Figure 3.4 shows the design of the The complete technical drawings of the chamber are shown in Appendix

nt of the Artificial Contamination Chamber

ment of mobile artificial contamination chamber is divided into four hamber construction, contamination generation system, electronic source unit. Figure 3.5 illustrates the block diagram of the mobile on chamber. Figure 3.6 shows the view of the chamber and Figure 3.7 ing and collecting system unit.

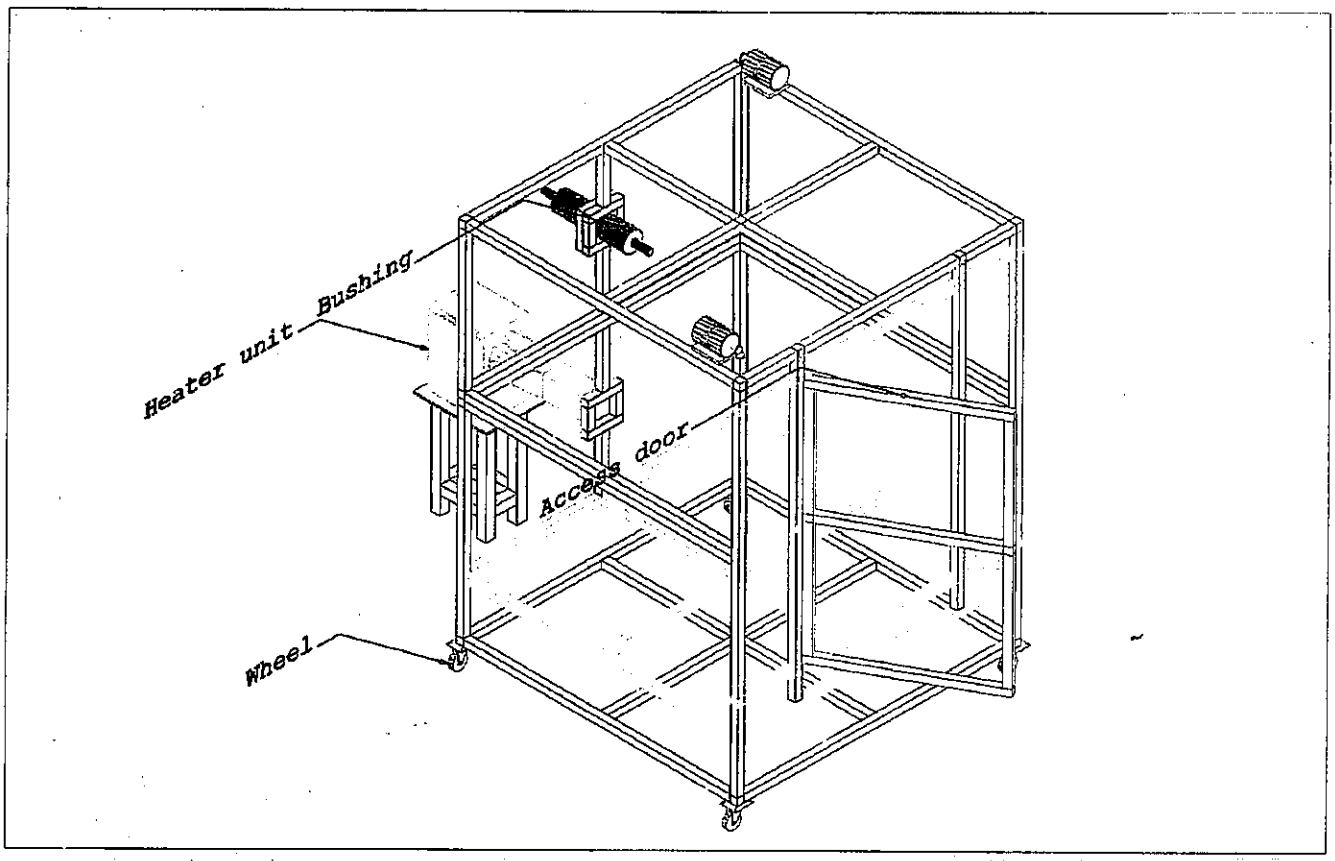

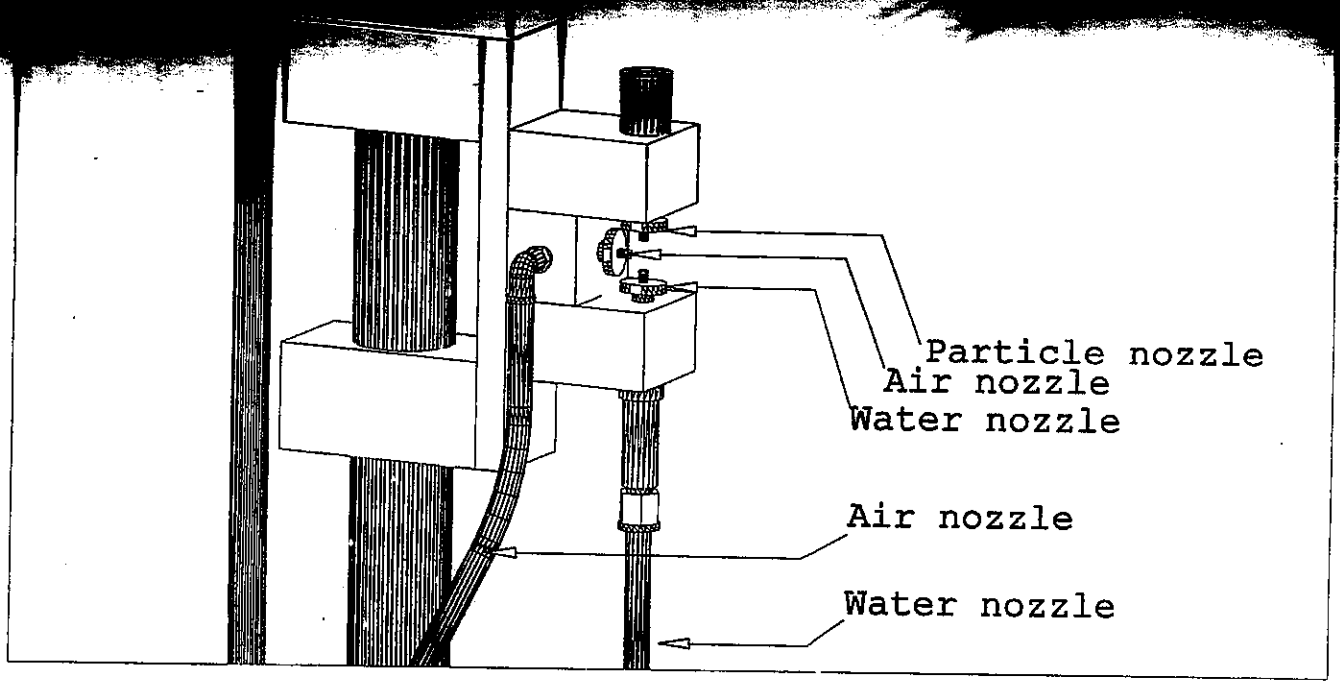

Figure 3.2 The artificial contamination nozzle

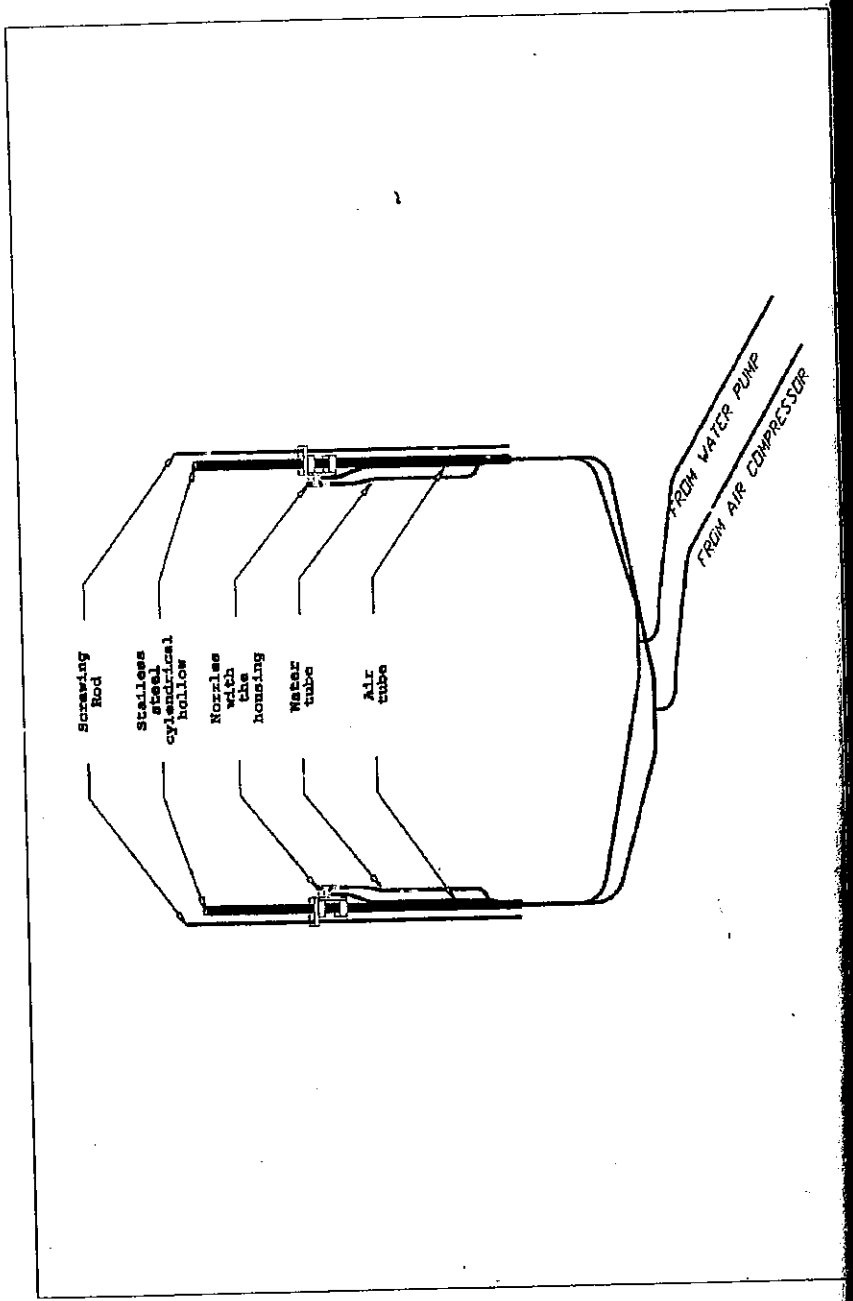

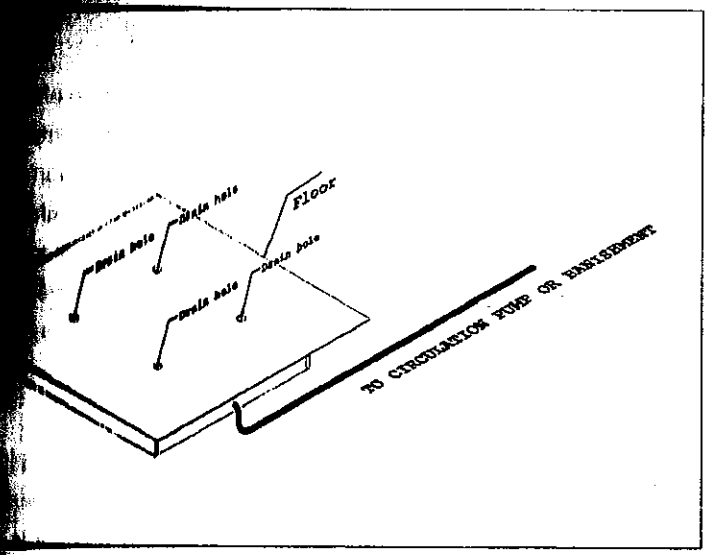

(a)

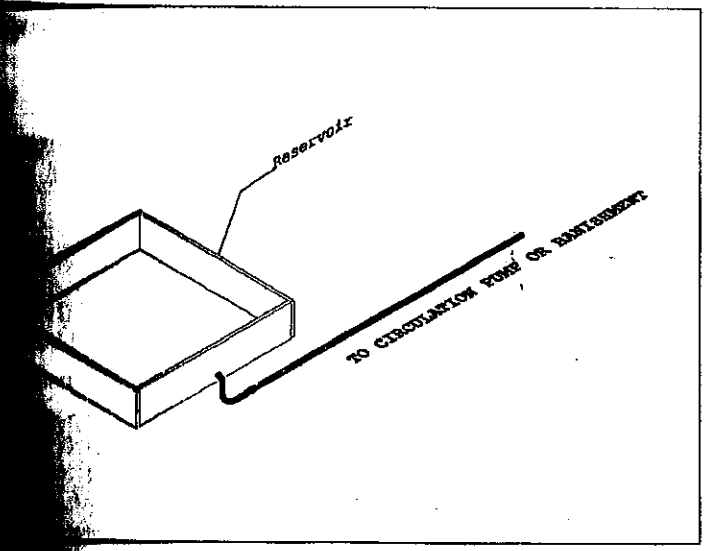

Draining system of mobile artificial contamination chamber
rvoir covered by the chamber floor, (b) construction of the reservoir.

3.2.2.1 Construction of the Chamber

The most important activity in construction work is assembling of the chamb structure. The steel base frame has to be welded perfectly. All components ar elements for their mechanical strength. The mechanical connection of the c structures with the four nylon wheels is executed carefully. This mechanical con has to be done properly and good enough to prevent unaccepted accident connection is unintentionally being released. The wheels itself are provided with and released toggles in order to prevent accidental rolling of the chamber once it ha positioned to the floor.

The chamber walls are made of transparent (see through) plastic m Polycarbonate sheets are selected due to their impact strength, thermal stress resi construction flexibility and chemical inertness. The polycarbonate sheet is more s to that of acrylic materials. Acrylic tends to become brittle with age, whilst polycar does not. The polycarbonate sheet is cut with a special cutting machine, namely a saw. The cutting is done carefully to obtain the best result of cutting surfac ensuring no defective edges.

The walls and roofs are constructed in double layer. The first layer (inner la meant to protect the steel frame structure from direct contact with test contaminan avoid any side flashover voltage, from energized test object to the frame. The layer is intended to reinforce the structural strength of the chamber. The two l system chamber conserved chamber space and regulated conditioning, for instance fog generation, and also provide a support to the test-object-bushing. polycarbonate layers were joined to the steel structure by means of bolt-and-nut s All the gaps in the inner layer are sealed with acetic silicone sealant. This mak chamber leak-proof.

From Figure 3.5, the supply of AC/DC voltage to the test object is via a b which is sticking through the wall of the chamber. Meanwhile the access door is l opposite to the HV bushing. A galvanized steel hanger was fixed at the centre of ch roof, allowing any insulators under test to be suspended vertically.

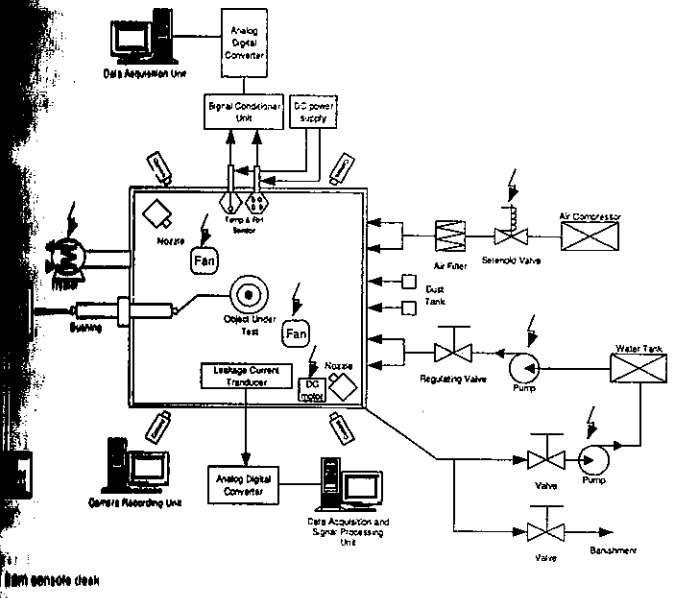

ure 3.5 Block diagram of artificial contamination chamber

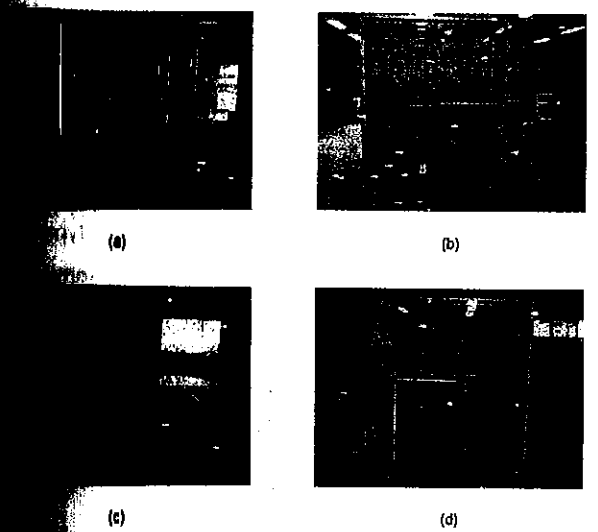

of the artificial contamination chamber (a) Front, (b) Right, (c) Back, (d) Left.

Figure 3.7 Pictorial views of observing and collecting system unit

3.2.2.2. Electronic Equipment

A. Temperature monitoring system

For chamber ambient temperature monitoring, two integrated-circuit tem sensors, namely, the LM35 series are installed. The output voltage of LM35 is proportional to the Celsius (Centigrade) temperature. The LM35 has an advanta linear temperature sensors calibrated in Kelvin, (as the user is not required to su large constant voltage from its output to obtain convenient Centigrade scaling). T does not require any external calibration or trimming to provide typical accuracie °C at room temperature and ± ¾ °C over full -55 to +150 °C temperature rang LM35 has low output impedance 0.1Ω for 1mA, linear output + 10.0 mV/°C scal and precise inherent calibration make interfacing to readout or control circuitry e easy. It can be used with single power supplies, or with plus and minus supplies from 4 up to 30 volts. It is suitable for remote applications [100]. Figure 3.9 illust circuit diagram.

itoring system

r of choice is HU10 (from thermometric). The HU10 is designed for esistance of the sensor decreases with increasing RH. This sensor voltage output, 1.5 – 3.0 Vdc., with humidity variation in order of 25 and ure 3.8 shows the typical output characteristic of the sensor.

The advantages of the sensor, among others are ease to install and d at 5±0.2 Vdc and maximum current 2 mA. It can be applied in respect itoring, humidity controlling, air conditioning, humidifying, dehumidifiers, ntilating [101. The circuit diagram is shown in Figure 3.9.

upplies

en, all the sensors required stable DC power supply. The DC power ed and constructed in the laboratory. It comprises of four basic elements, nsformer, a rectifier, a regulator and filter. For this application one unit ±5 ty output is used. Figure 3.9 shows the schematic diagram of the supply ure and the humidity sensor system. The step-down power transformer wn the main AC supply to the desired DC output voltage. The secondary l. A bridge diode was used to convert the AC voltage into a DC voltage. diodes type are used for the AC rectification. The fixed output voltage s) is used to provide the desired output voltage. The capacitors values nd 0.22μF are used as filtering device to reduce ripple. Figure 3.10 view of the DC power supply.

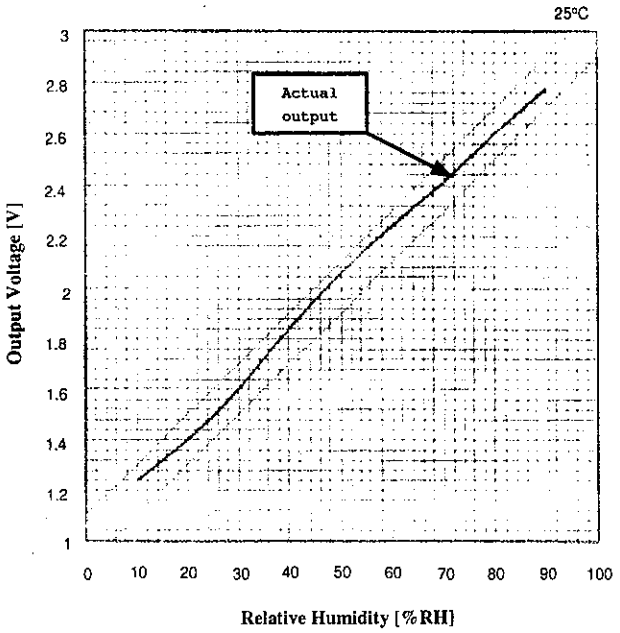

Figure 3.8 Graphic typical output characteristics of the HU10

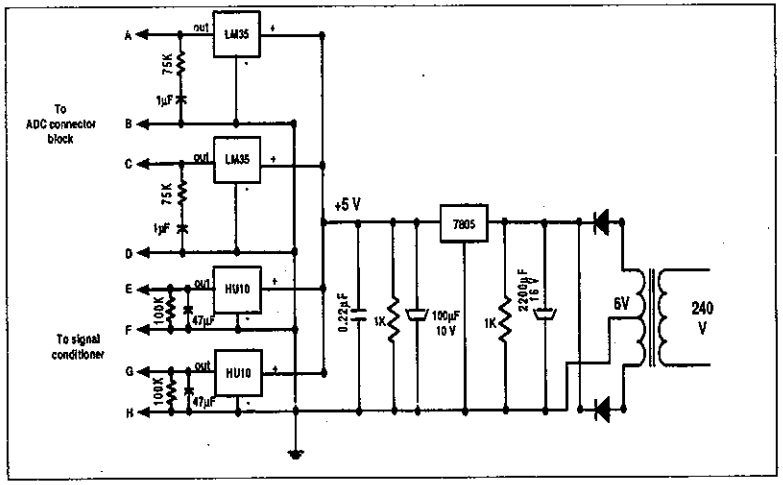

Figure 3.9 Schematic diagram of DC regulated power supply and sensing circuit

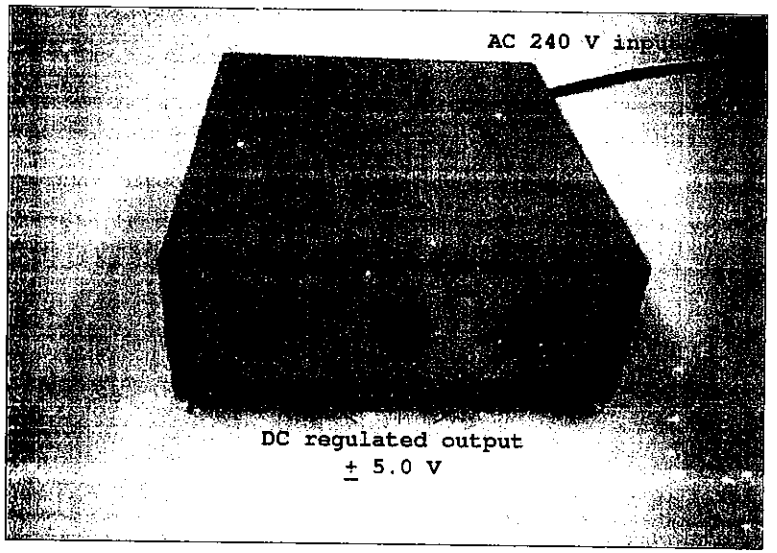

Figure 3.10 Pictorial view of DC power supply

Signal conditioning unit (SCU)

An analogue signal derived from sensors or transducers often has to be conditioned to display, either by amplifying or scaling down its magnitude. This can ensure the racy of the system display. The SCU is designed and constructed in-house. Figure hows the circuit diagram of the SCU. A precision resistor (R_a) with ± 1% tolerance is in place in series with a sealed, multi-turn cermet trimming type 3299 Bourns' ilometer (R_b) [102]. The circuit provided a scaled down magnitude of the sensor l. In this way the input voltage to the ADC will not exceed the voltage limit of the

The highest output voltage limit from the sensor module was 3.0 Vdc, whereas the t value of the ADC input is only 2.5 Vdc. Therefore, 2.0 Vdc is considered the most e voltage level selection with regard to the safety of the ADC unit. The following ons use to determine the operation value of the resistor R_b. The equations are:

$$V_i = V_{R_a} + V_{R_b} \tag{3.1}$$

$$\frac{V_i}{V_{R_b}} = 1 + \frac{R_b}{R_a} \tag{3.2}$$

Therefore,

$$R_b = \left(\frac{V_i}{V_{R_b}} - 1\right) R_a \tag{3.3}$$

where,

R_a is the fixed value resistor 20 kΩ with ±1% tolerance.

R_b is the potentiometer 100 kΩ.

V_i is the input voltage from the humidity sensor.

V_{Rb} is the output voltage from the signal conditioning units.

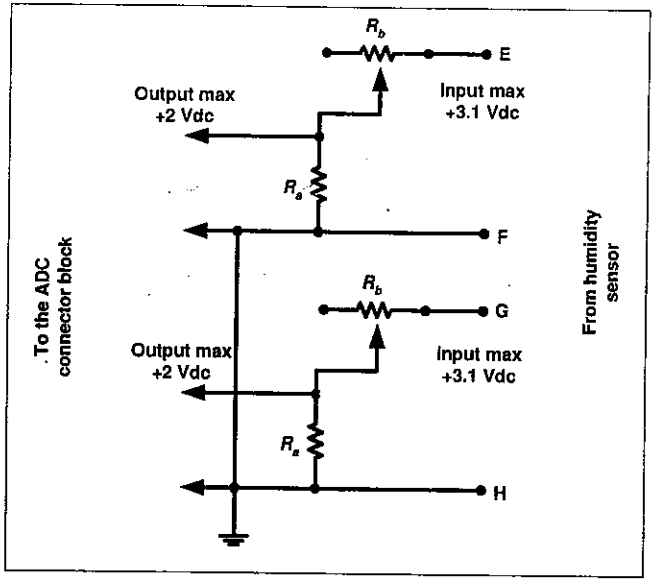

Figure 3.11 Circuit diagram of the signal conditioning unit

Digital Video Recording (DVR)

Flashover scenario on the tested insulator surfaces are observed by means of a Video Recording (DVR) system. It is installed with a Falcon MIG4ch DVR board. It impact-application-equipment for a real-time monitoring system. It grabs images Closed Circuit Television (CCTV). Clear and more vivid images can be monitored corded. The DVR board is installed with a Personal Computer (PC).

Four CCTV cameras are placed on the exterior sides of the chamber as shown in 3.5. They are connected to the MIG4 DVR board using a 75Ω RG 59/U coaxial and powered with a 12 Vdc power supply. By this way the whole surface mene of the insulator test object can be observed. Figure 3.12 shows the pictorial f the boar and Figure 3.13 illustrated the records of flashovers during insulator

Figure 3.12 Pictorial view of MIG4 board

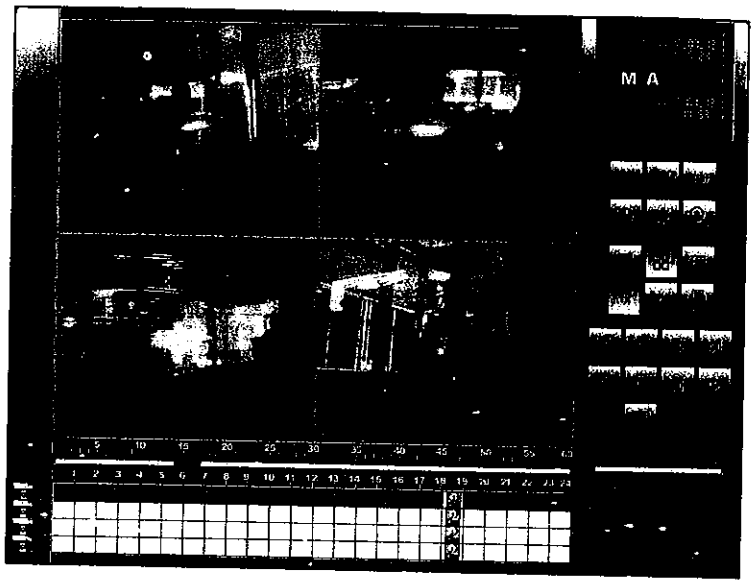

Figure 3.13 Typical snap shots of the insulator flashover on the insulator surface.

3.2.2.4 Contamination Generation System

Among the components installed in the contamination generation system i.e. the installation of two units of nozzles as described in section 3.2.1.2, are the most challenging task to accomplish. The nozzles-unit is place into an adapter securely. A hollow cylindrical stainless steel bar is erected located at the opposite corners of the chamber. This bar supports the adapter. The adapter unit can be moved up and down easily. In addition, lock and release toggle is also provided. One of the adapter units is attached on the screwing rod. These two components, adapter unit support and screwing rod, are perpendicular on the floor. The screwing rod coupled to a DC motor. By changing the polarity of the input voltage the direction of the motor rotation will change. This determines whether the adapter moving up or down. Figure 3.14 illustrates the nozzles units.

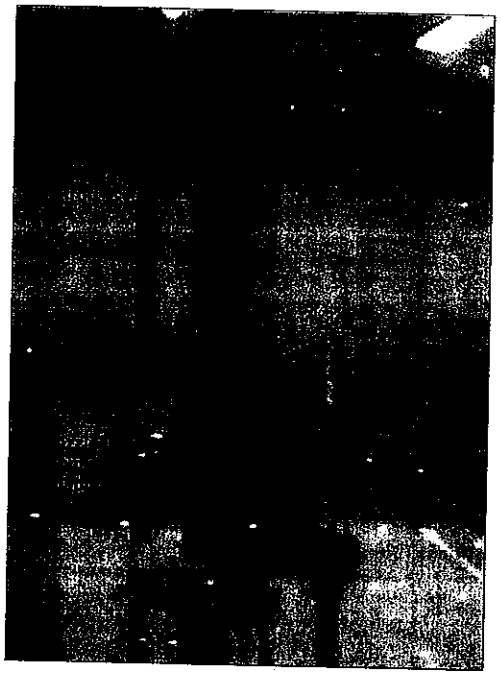

Figure 3.14 The nozzles unit mounted in the chamber.

The nozzle is supplied with salt-water and air. The flow rate of water and air of each nozzle can be adjusted to change the water droplets' size. The air pressure can be set to a value up to 80.0 psi. The water and airflow rates are controlled with a mechanical unit valve (MUV). The compressor supplies the air flow. A solenoid valve is installed and used the means to switch on/off the airflow. The filter functions to filter any foreign particles, such as water or oil that could attach with air. The detail block diagram is shown in Figure 3.15. For the simulation of the artificially non-soluble particle contamination, a container is connected to the nozzle. These particles drop into the compressed air flowing area of the nozzle unit by gravitational force.

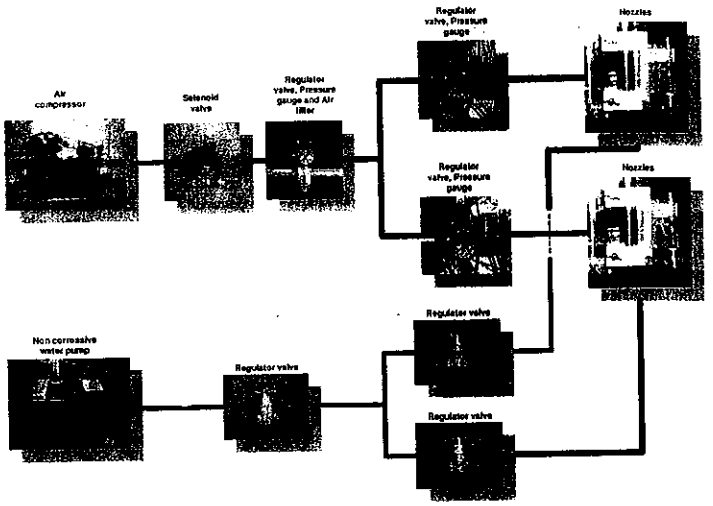

Figure 3.15 Block diagram of contamination generator

3.2.2.5 High Voltage Source

The HV source is a 230V / 100000V, 21.7A/0.05A, 5kVA, 50Hz single testing transformer. The HV transformer output is controlled from a remote control desk setting up of the control desk is quite simple that involve setting the individual comp of the HV construction kit. The desk is constructed from aluminium profile and h slag enamelled sheet strip panels. The table top and front panels are made from s steel which guaranteed low wear and a long-lasting finish.

The control desk is comprised of the following items.

(a) A single-phase regulating transformer for excitation of the HV transformer, controlled by mean of a hand wheel fixed to the front pan

(b) A key-operated switch for switching on/off the control of voltage.

(c) Fuses and automatic breakers for the control and the main circuits.

(d) Illuminated push-buttons for the main contactor which connec regulating transformer to the 220 or 380 V supply.

(e) Illuminated push-buttons for secondary contactor which interconnected the regulating and test transformers.

(f) Push-buttons for pre-warning signal (horn) and switching off the panel lighting.

(g) An emergency push button for immediate switch-off in case of emergency.

(h) A voltmeter for the main voltage register, a two-range voltmeter and ammeter for the regulated voltage and current respectively.

The schematic diagram of the remote control desk is shown in Figure 3.16, Figure 7 shows the pictorial view.

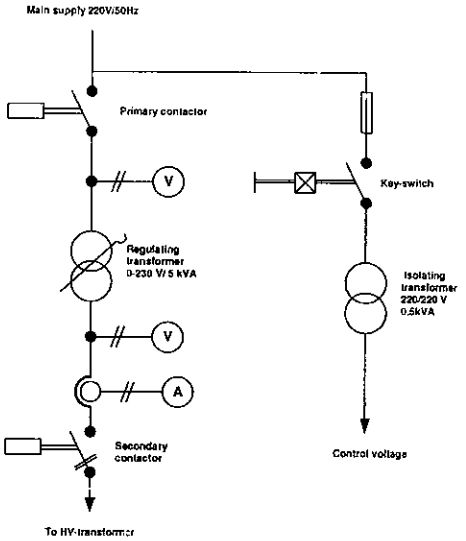

Figure 3.16 Schematic diagram of the control desk.

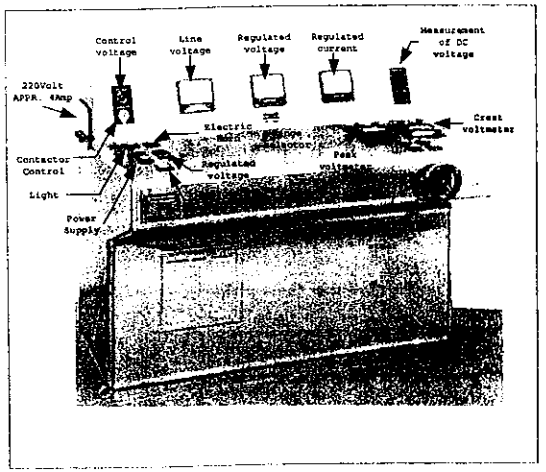

Figure 3.17 Pictorial view of the control desk

A voltage divider is used for measuring the HV that is injected into the test object during testing. There are two types of voltage divider used in the study, i.e. the resistive divider and the capacitive divider. The former is used for HVDC measurement and the latter is used for HVAC measurement. These dividers are calibrated before used to ensure accuracy in reading of the instruments.

Different calibration methods are used for the DC and AC divider calibration. The DC divider is tested by using sphere-gaps technique base on British Standard 358. The diameter of the sphere was 10 cm. Test involved with four different measuring gaps distance are conducted. For each set of gap distance four runs of voltage injection is considered. Figure 3.18 illustrates the typical of set-up for calibration of divider using sphere method.

On the other hand the AC divider is calibrated by using a reference divider, i.e. RCZ500. The reference divider has accuracy ±1%. Two type of precision digital measurement equipments are used, HP34010A and DMI550. The set-up of the AC divider test is shown in Figure 3.19.

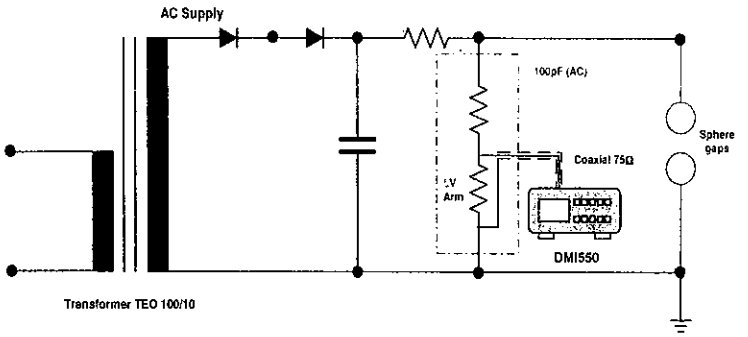

Figure 3.18 Schematic diagram of DC divider calibration

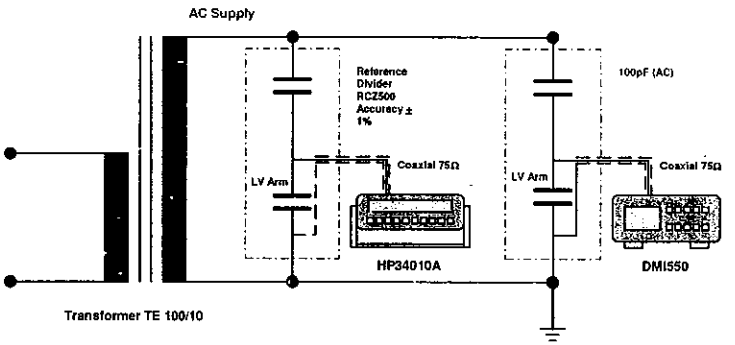

Figure 3.19 Schematic diagram of AC divider calibration

3.2.6 Data Acquisition System

Signals generated from the sensor units are analogue signals. These analogue signals are converted to digital signal prior to sending to PC. The Pico Analogue Digital Converters (ADCs) are used for the purpose of interfacing sensor units with the PC.

A. Pico ADC-11

Pico ADC-11 is used as an interface interconnecting the temperature senso humidity sensors with the PC. As described in section 3.2.2, signals from the h sensors are conditioned before being processed by ADC-11. The Pico ADC-1 eleven analogue inputs. With a ten bits resolution it gave fine digital output [104]. 3.20 shows a block diagram of the temperature and humidity data acquisition system temperature and humidity level inside the chamber are displayed as an average valu

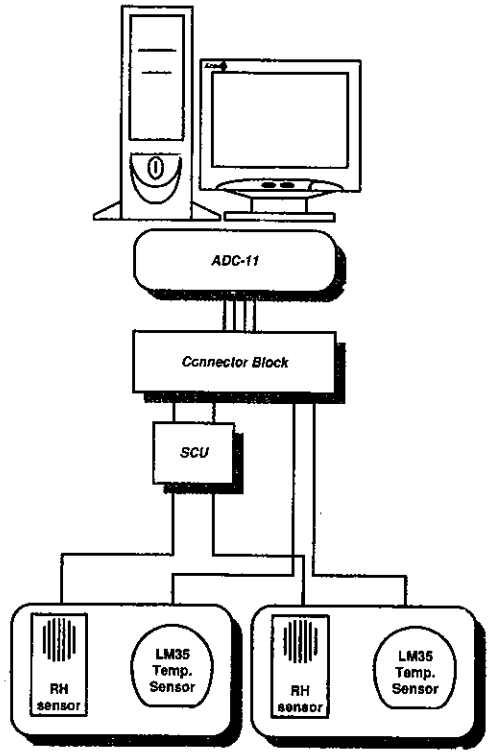

Figure 3.20 Block diagram of the chamber ambient data acquisition system

Screened multicore cables with 7/0.1 mm tinned copper stranded conducto and 0.2mm PVC sheath are used. Since lengthy cables are used, the losses alo

bles are considered. A preliminary observation is conducted to determine whether the lance has significant effect to the output signals of sensors. In this way, displays of mperature and humidity level can be ascertained to be reliable (true value display).

. Pico ADC-200 and leakage current measurement

. Pico ADC-200 is used as an interface for the leakage current signal measurement ia voltage drop across a series resistor outside the chamber) between the resistor and e PC. Depending on the level of the leakage current, different shunt values are used ,5Ω, 470Ω, 1kΩ, 22kΩ tolerance ±5%, 50W, 2500V). The maximum input voltage celved by ADC-200 was ± 20V with 8 bits resolution. Having two BNC connectors for nalogue input channels with 1M Ω input impedance, the ADC-200 is coupled to the PC ing D25 connector [105].

The leakage current that is flowing through the contaminated surface of the ulators under test is monitored, digitized, processed, displayed and finally stored for rther analysis. The voltage drop across the shunt (due the leakage) is monitored. As own in Figure 3.21, a surge protector is put in placed between the shunt and ADC-200. e protective system consists of 2 (two) stages. In this manner if one stage experienced al failure the back-up can protect the ADC and PC. Figure 3.22 shows that an EC90X discharge tube is placed in the first stage protection circuit. For the second stage, ck-to-back zener diodes (BZZ\X55-C15) are used with clamping voltage up to 15 volt. e serial resistor serves as a current limiter. Figure 3.21 illustrates the leakage current asuring circuit and Figure 3.23 shows the hardware used for protection.

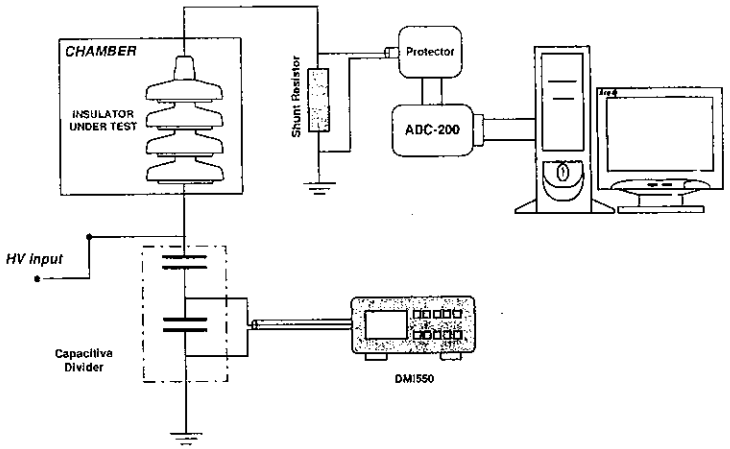

Figure 3.21 Leakage current measuring circuit

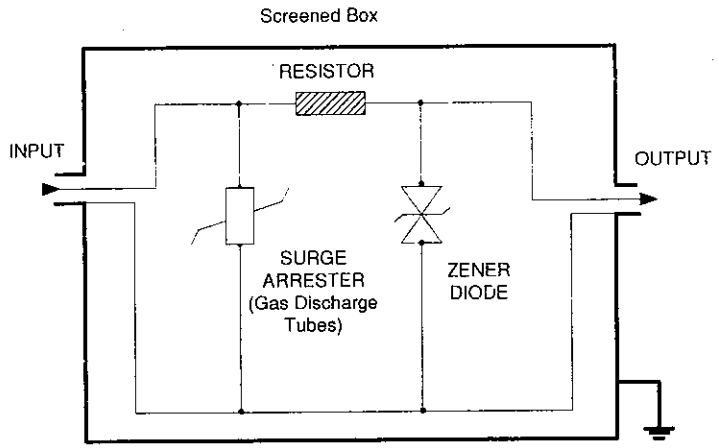

Figure 3.22 Protection system of leakage current measuring system

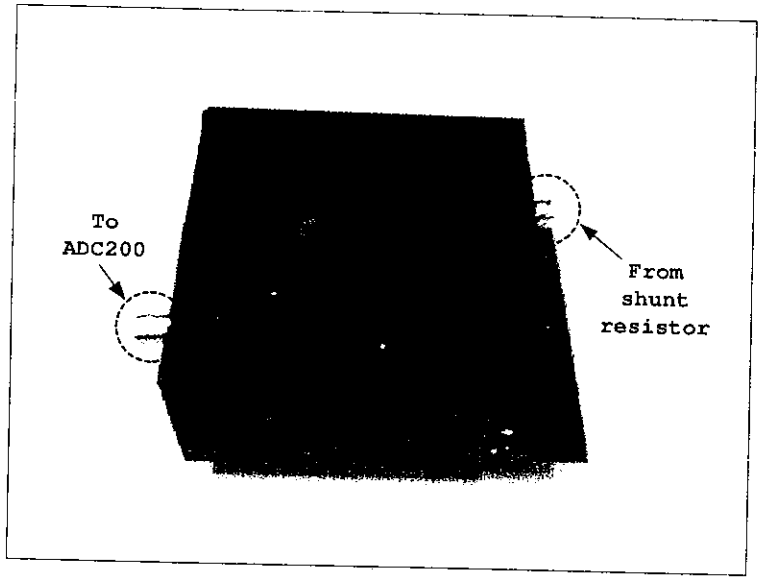

Figure 3.23 Pictorial view of the protection system

3.7 Software Development

LabView 5.11 virtual instrument software is used as the platform for the software lication development for monitoring purpose. The software is an icon based-program. oftware has facilities which include the database result window, graph window, and r function buttons. Using the software, data reading can be visualized [98,99].

Two application programs are developed, i.e. for the leakage current and for the mber ambient condition monitoring. The application programs are facilitated with a phical User Interface (GUI) for easy display of data.

Figure 3.24 illustrates the GUI for the leakage current measurement. Before the is displayed windowing and filtering processes are executed. The GUI display prises of five windows of data display.

a) Output voltage waveform

b) Current waveform
c) RMS voltage
d) Leakage current, and
e) Power spectrum

Figure 3.25 illustrates the GUI for the chamber ambient condition monitoring. The displayed data are average value of the two sensors outputs.

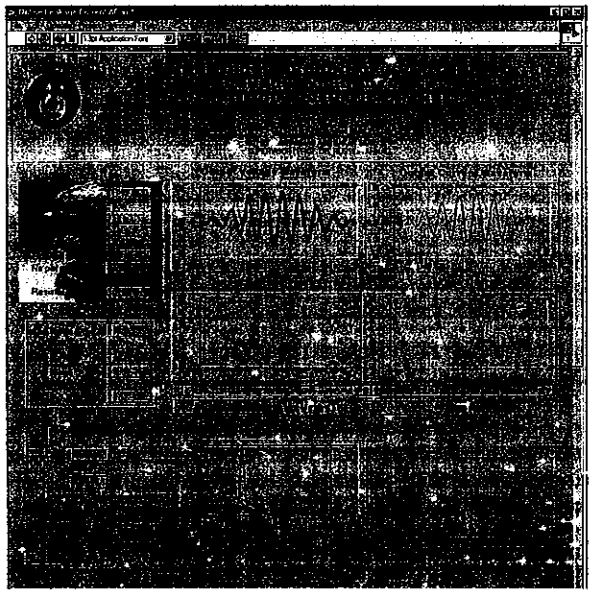

Figure 3.24 GUI for leakage current measurement.

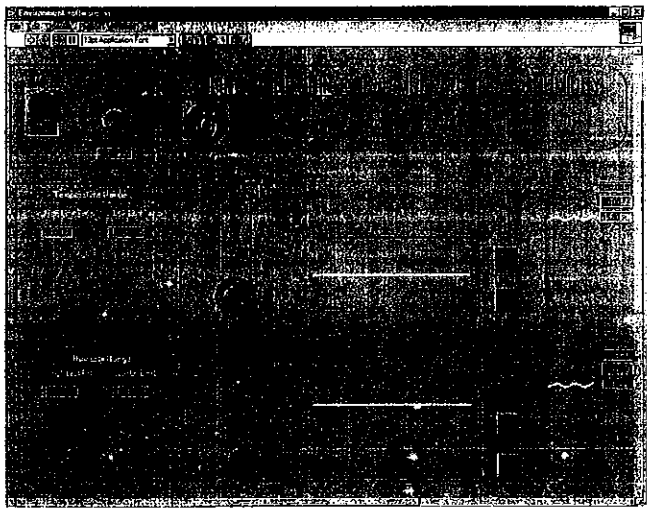

Figure 3.25 GUI for the chamber ambient conditions.

CHAPTE

RESULTS AND DISCUSSIONS ON PRELIMIN
APPLICATI

4.1 Introduction

The design and fabrication of the ACC has been accomplished. Usin chamber, several studies have been conducted to verify that the contamination sys running properly and effectively.

4.2 Selecting Reusable Aged Glass Insulator

Transmission line insulators aging is influenced by several factors su mechanical and electrical defects. The leakage current magnitude on the surface insulator, and tan δ are associated with insulator degradation. The tan δ relates dielectric loss/ power loss [93]. The relationship can be represented by the fo equation.

$$\vartheta = f(i, I, \tan \delta)$$

where,

ϑ ; insulator selective unit
i : ac leakage current
I : dc leakage current
tan δ : dielectric loss

This study conducted involved nine anti fog cap-and-pin glass insulators of the type M92. Its creepage distance is 330 mm (as shown in Figure 4.1). The experimental rig for leakage current measurement was in accordance to the clause 3.2.2.6, B. Initially the insulators were cleaned to remove all traces of dirt and grease according to IEC 507, 1991. The insulators were then left to dry, and carefully kept to avoid additional contamination.

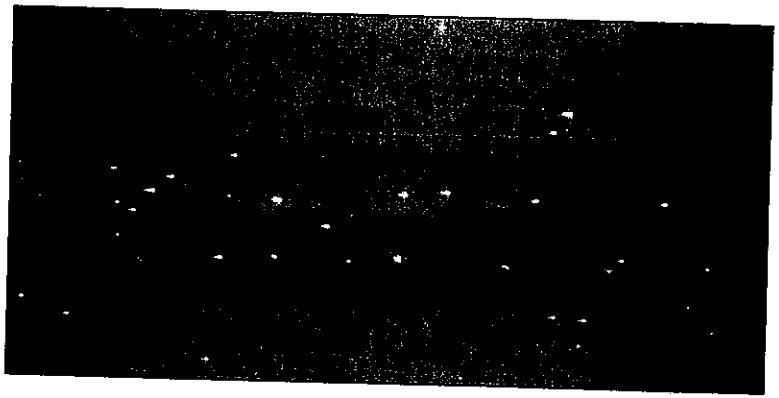

Figure 4.1 Insulator samples

The entire test samples were placed in the mobile artificial contamination chamber in turn and the corresponding leakage current measurement were taken. In this chamber the ambient temperature and humidity could be observed and collected. The leakage current was measured for corresponding variation in voltage from 0 kV up to 10 kV. All the information regarding the leakage current including the flashover incident was observed and recorded. Simultaneously the LeCroy LT344L Digital Storage Oscilloscope (DSO) was used as a counter check. The LeCroy DSO readings validated the reading obtained from the LabView's program.

A study of the corona inception observation was also carried out. The detecting unit employed a simple balanced multi elements UHF antenna connected to the LeCroy LT334L DSO through coaxial cable. The antenna was mounted on to a support and placed securely at a safe distance from the test object. The leakage current and the

corona inception measurement were conducted simultaneously. Fig. 4.2 illustrates th pictorial view of the experimental setup.

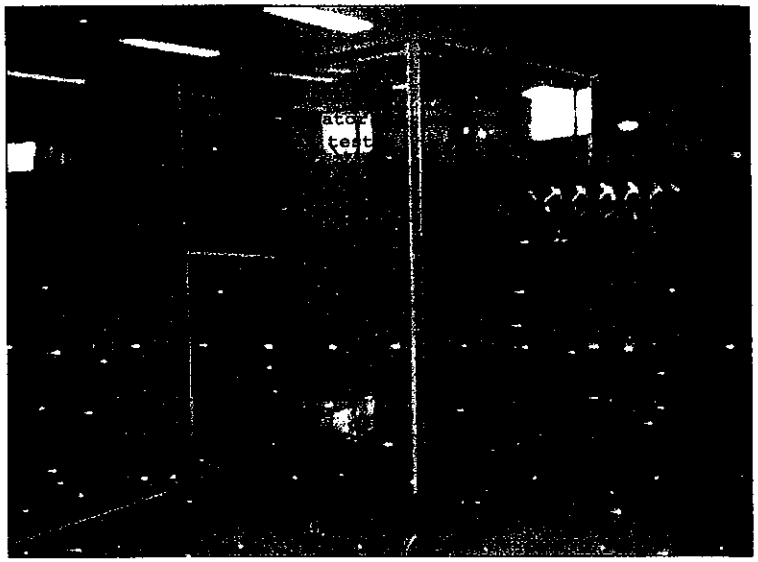

Figure 4.2 Pictorial view of experimental setup

In order to measure power loss in the dielectric a Capacitance and Dissipatio Power Factor Test Set 2816/5284U BR YB together with the High Voltage Supply a Control 2816/5284U CU YB by Tettex Instrument was used. Fig 4.3 shows the circu diagram of a basic test circuit for capacitance and tan δ measurement, while Figure 4 illustrates the pictorial view of the experimental set-up.

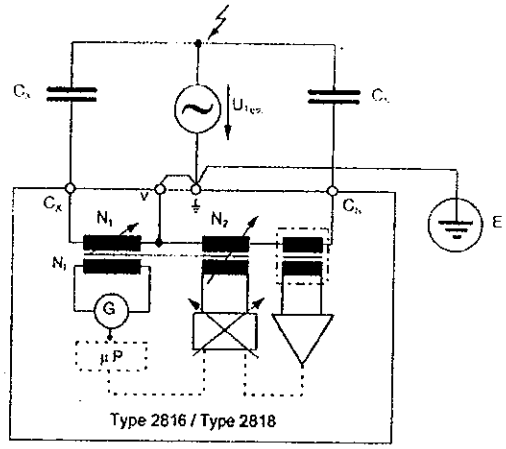

U_{Test} : High Voltage supply (e.g. high voltage transformer)
C_N : Standard Capacitor
C_X : Test object
E : Earth connection
G : Null detector
µP : Microcomputer

Figure 4.3 Basic test circuits for C and tan δ measurement.

Figure 4.4 Pictorial view of tan δ measurement

4.2.1 Mathematical Modelling of Selecting

The measurement results of leakage current, and tan δ were regressed using linea regression method. Afterward equations (4.2), (4.3), and (4.4) were obtained.

$$i_{(j,k)} = m_j V_k + b_j \quad (4.2$$

$$I_{(j,k)} = m_j V_k + b_j \quad (4.3$$

$$\tan \delta_{(j,k)} = m_j V_k + b_j \quad (4.4$$

where,

i : ac leakage current

I : dc leakage current

$\tan \delta$: dielectric loss

m : constant value

j : 1,2, ..., 9 (insulator code)

k : 1,2, ..., 10 (injection voltage)

Table 4.1 shows the tabulation of the magnitudes related to the AC and DC leakage current, and tan δ for 10 kV test voltages.

Table 4.1: The leakage current and tan δ magnitude

J	i (mA)	I (μA)	tan δ
1	0.1720	1.2909	0.0797
2	0.1746	5.8878	0.0699
3	0.1660	2.0834	0.0508
4	0.1685	1.6493	0.0560
5	0.1376	1.3573	0.0564
6	0.1447	0.9370	0.0482
7	0.1438	0.2637	0.0420
8	0.1726	0.5030	0.0536
9	0.1728	0.2456	0.0641

In order to simplify the classification, the actual value of i, I and tan δ were converted to per-unit using the following equations,

$$i_{j\ perunit} = \frac{i_j}{i_{\max}} \quad (4.5)$$

$$I_{j\ perunit} = \frac{I_j}{I_{\max}} \quad (4.6)$$

$$\tan \delta_{j\ perunit} = \frac{\tan \delta_j}{\tan \delta_{\max}} \quad (4.7)$$

where,

j : 1, 2, ..., 9

The per-unit value of i, I and tan δ were converted into selective unit. This was obtained by using the following equations,

$$\phi = \frac{\Delta\Psi}{3} = \frac{\Psi_{max} - \Psi_{min}}{3} \quad (4.8)$$

where,

ϕ : The range of grade

Ψ_{max} : The maximum value of i, I or tan δ

Ψ_{min} : The minimum value of i, I or tan δ

In this study the range of the grade was made as follows,

$$x < A \leq y$$
$$y < B \leq z$$
$$z < C \leq 1$$

where,

$$x = \Psi_{min} \quad (4.9)$$
$$y = \Psi_{min} + \phi \quad (4.10)$$
$$z = \Psi_{min} + 2\phi \quad (4.11)$$

The selective units are $A=3$, $B=2$, and $C=1$.

It should be noted that higher the numerical values in Table 4.2, the selective unit assigned is in descending order.

$$\vartheta = \frac{i + I + \tan\delta}{3} \quad (4.12)$$

Equation 4.11 is now useful for calculating the selective unit.

Table 4.2: Grade of Tested Insulator

j	Grade			ϑ
	i	I	$tan\ \delta$	
1	A	C	C	1.666
2	C	C	C	1.000
3	A	C	A	2.333
4	A	C	B	2.000
5	A	A	B	2.666
6	A	A	A	3.000
7	A	A	A	3.000
8	A	C	A	2.333
9	A	C	B	2.000

Table 4.2 shows the insulator #6, and #7 have the highest magnitude of selective unit, whereas the insulator #2 shows a contrary result. The segregation was made using three performance classifications, i.e.

1. if $1.000 < \vartheta \leq 1.666$ then the insulators are classified as BAD;
2. if $1.667 < \vartheta \leq 2.332$ then the insulators are classified as GOOD; and
3. if $2.333 < \vartheta \leq 3.000$ then the insulators are classified as SATISFACTORY,

4.2.2 Corona Inception

The preliminary study to determine corona inception level was conducted on the test of AC voltage only. The comparison between two measurement results (shunt resistor and by antenna receiver) are illustrated in the Figure 4.5. It is obvious that the profile of the measurement using shunt resistor was similar to the profile of the antenna receiver voltage.

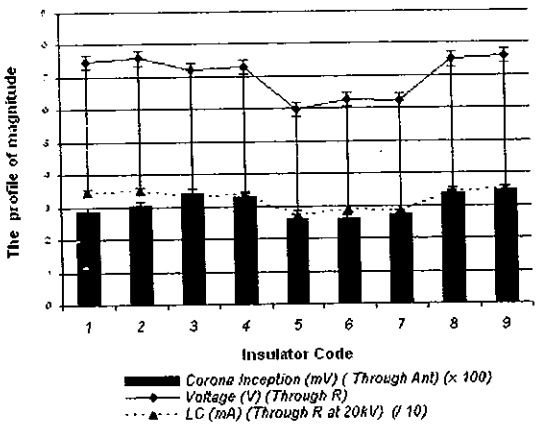

Figure 4.5 Graph of voltage measurement related to corona inception level, and the leakage current magnitude

4.3 Flashover Studies

A preliminary study was conducted in order to simulate the flashover phenomenon in the developed mobile artificial contamination chamber.

The insulator was thoroughly rinsed with tap water [42]. The insulator was covered by appropriate plastic bag to ensure its cleanliness. The insulator was stored for about 24 hours before testing.

To start the test, a suspension consisted of 120 grams kaolin and 510 grams of NaCl were dissolved in a 3 litre tap water to develop contaminant of ESDD level of about 0.12468 mg/cm^2. Once this process was done the insulator was dipped in the suspension. For uniform contamination of the entire surface of the insulator, complete immersion of insulator in the solution must be maintained and at the same time the insulator was regularly rotated and moved horizontally and vertically while it was still in the solution.

The insulator were then removed from the container and placed to dry under the direct sunlight for duration of not less than 6 hours. This ensured that no traces of moisture still remained on the insulator surfaces. After this activity has been completed, the artificially contaminated insulators were stored in an environmentally cleaned room for testing.

To proceed with the testing the contaminated insulator was placed in the chamber. An AC supply of 17 kV, 50 Hz was continuously applied on to the tested sample. Concurrently, artificial fog was introduced in the chamber, by activating the fog generator, with constant spraying capacity of 25.0 ml/second with 80.0 psi air pressure. The fog generated filled up the chamber, not allowing it to be sprayed directly to the test insulator. The process sequence was continuously recorded by means of cameras which were further connected to a PC. Event the leakage current oscillogram was recorded.

In just a few minutes the leakage current signatures were incessantly observed. Once the fog accumulation has reached the threshold after energizing, the flashover occurred. What really happened was that partial discharges appeared at the bottom surface of the insulator in the form of surface tracking and finally a complete flashover took place.

All these flashover events were continuously videoed by means of a four-camera system and stored in a PC. The leakage current signatures were visually displayed in the form of graphic showing leakage current magnitude and time variation. A resistor with value 468 Ω was used and connected to measure leakage current magnitude.

With increased fog density in the chamber the leakage current magnitude tends to increase with the time. For instance in just few seconds after the test started the initial partial flashover could be observed. This followed by other incidents of flashover. At about 6 (six) minutes after the test commenced the leakage current magnitude started to decrease. This so called sudden change over of leakage current magnitude was due to insulator surface condition that was completely moisturized with layer of water. Figure 4.6 illustrates the leakage current oscillogram. In addition, a moving average per three point and five order polynomial fitting function were presented graphically providing more information about the wave-shape of leakage current oscillogram and flashover activities. The flashover events captured from DVR were presented in Figure 4.7.

The sharp spikes running over the leakage current oscillogram shows a drastic change in the insulator surface resistance value. This changeover involved resistance value from high to low ohmic. This could be justified by the occurrence of so-called "Dry Bands" on the wetted insulator surfaces. Under cleaned surface condition, the potential was totally across the glass surfaces i.e. between the cap and pin part of the insulator. However as the wetting process started to creep all over the surfaces, the surface resistance R_{srf} started to decrease because of the leakage current thermal effect begun to dry-up the moisture and formed so-called "dry bands", and if the voltage gradient across these bands exceeded the surface dielectric strength partial flashover took place and this could be translated into a sharp jumped in leakage current values.

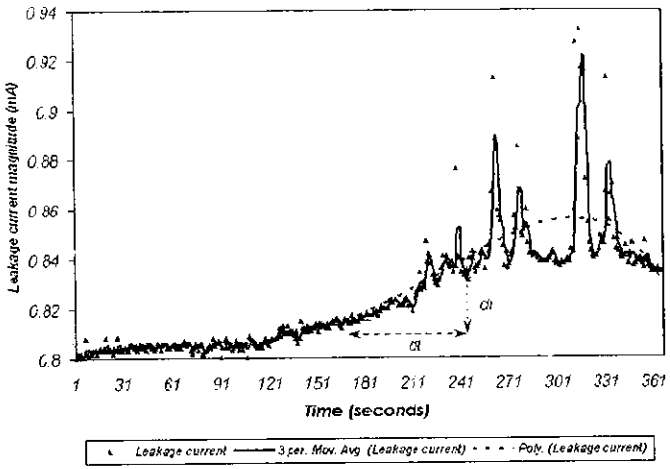

Figure 4.6 RMS leakage current magnitude vs. time.

In the case when contaminated layer on the insulator surfaces was too 'heavy', "Dry Bands" formation could not occur but this did mean that no flashover could occur. On the other hand, if the voltage applied exceeded the insulator critical flashover voltage, a complete flashover occurs and this resulted in a sharp and higher leakage current magnitude formation.

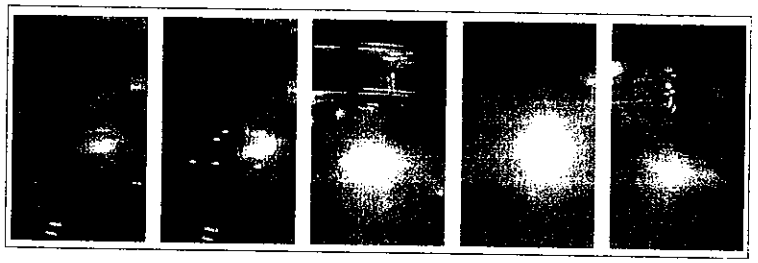

Figure 4.7 A particular event of the flashover scenario.

4.4 Leakage Current Pattern Recognition

This study was conducted to observe the effect of contamination severity to the development of leakage current magnitude. In relation to this the same insulators that were used in the experiment mentioned in section 4.2 were also used for the ESSD modelling development.

Based on the previous researcher findings on the contamination severity in the Paka Power Station, the salt contamination level was in the range of 0.001173 mg/cm^2 to 0.139503 mg/cm^2 [33]. This study was conducted based on these values of contamination due to the sea salts. The intention was to develop an optimum solution which was linked to the desired ESDD level i.e. when the solution would be used for artificial contamination of the insulators. Consequently some form of correlation between solution conductivity and salinity should be determined.

4.4.1 Conductivity and Salinity Determination

There were several activities involved to determine the correlation between the conductivity and the salinity of several different solutions. Firstly a known weight of NaCl was dissolved in a 100 ml of distilled water. A centrifugal machine was used to obtain homogeneous solution. The principle operation is based on the electromagnetic concept. The machine generates electromagnetic field and a magnetic capsule is inserted with the

solution. The electromagnetic generator is turned on, the magnetic capsule could ro
and hence resulted in the solution homogeneity.

After completion of the mixing process a homogenous solution was obtained.
measurement of solution conductivity was conducted by using a Total Dissolved S
(TDS) tester which was able to measure concentrations in the order of 19.99 mS/cm.
tester accuracy is in the range of ± 2% and it also has automatic temper
compensation for 5°C to 50°C. Figure 4.8 shows the experimental rig that was used fo
ESDD determination.

Based on the several tests conducted with different concentration of art
contaminated solution, an empirical model was successfully developed. A simple l
regression model using the least squares method was used for the development o
empirical model. Equation 4.13 provides the empirical model which can be used to pr
the values of salinity (response variable) directly from the values of conductivity
independent variable). [94,95, 96].

The graphical output of the measurement results is shown in Figure 4.9.
coefficient R^2 measures the proportion of variation on predicted value of salinity, wh
explained by the predictor variable. The coefficient R^2 has values range between 0 a
when $R^2 = 1$, that means a perfect explanation of the predicted value derived fro
model. R^2 of the model was 0.9924 which means 99.24% of variance in predicted va
salinity [97,98].

The linear expression is,

$$Sa = 37.241\ \kappa \qquad (4$$

where,

Sa : salinity (mg)

κ : conductivity of the solution (mS/cm)

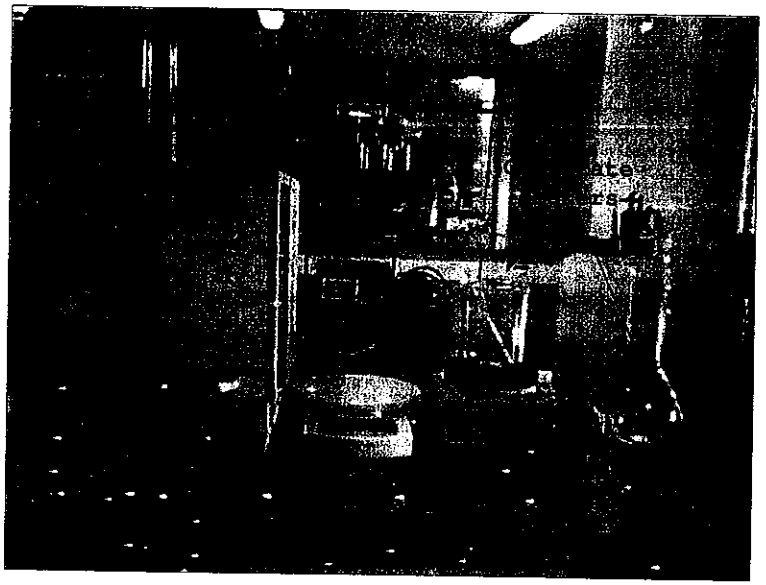

Figure 4.8 Laboratory apparatus for determining ESDD

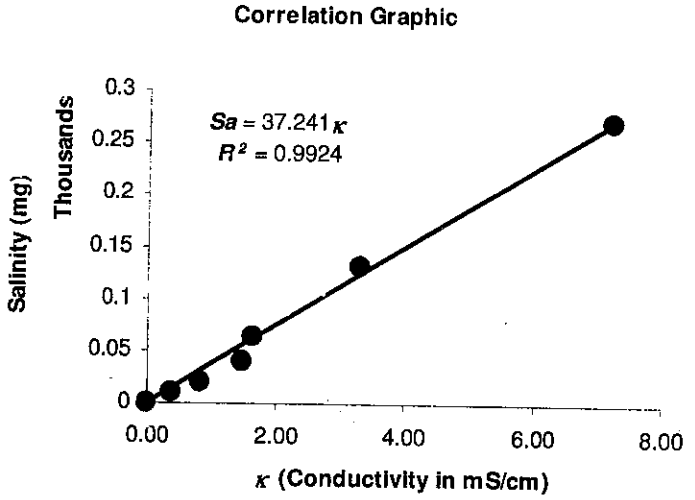

Figure 4.9 Graph of correlation between conductivity with salinity

Six pieces of used insulators type M92 were considered in this test. The total insulator glass area is 1601.4 cm^2. In all the artificial tests carried out, all insulator surfaces were contaminated employing the solid layer method [42].

To produce layers of contaminant that resulted in desired ESDD value, different suspension of mixtures of contaminants consisted of kaolin (g), NaCl (g), and distilled water (ltr) were prepared. These mixtures were prepared and intended to simulate the accumulation of pollutants on insulator [65]. Table 4.3 shows the composition of the pollutant suspension.

Table 4.3: Measured ESDD of insulator for different level of mixtures suspension

Suspension (g/g/ltr)	Conductivity (mS/cm)	ESDD (mg/cm^2)
120/10/3	0.14	0.00326
120/30/3	0.27	0.00628
120/90/3	0.73	0.01698
120/210/3	2.77	0.06443
120/510/3	5.36	0.12468
120/1000/3	8.95	0.20819

4.4.2 Experimental Results

All the experimental procedures adopted in this test were similar with the experimental procedures that were presented in clause 4.2. Nine pieces cap-pin anti-fog insulator type M92 were also tested. The suspension of 120/10/3 and 120/510/3 was selected for the test.

All the tests conducted started with the similar ambient condition i.e. chamber temperature and humidity.

A 12 kVrms source was used in this test. The sample was energized with AC voltage for several minutes without activating the fog generator. Subsequently the fog generator was activated for about 400 seconds. Concurrently the online monitoring system was also turned on.

Table 4.4 illustrates the magnitude of leakage current for two different suspensions. The results show that the two different suspensions have been promoted different level of leakage current. The higher of ESDD promoted higher of leakage current.

However although the test was conducted by the identical setting of fog supply there was different leakage current promoted. This was due to the effect of the uniformity of the contaminant that deposited on the surface of insulator, although this effect have been tried to minimize by recurrent contamination process.

Table 4.4: Magnitude of leakage current for two different suspensions

No.	*Suspension: 120/10/3*	*Suspension: 120/210/3*
1.	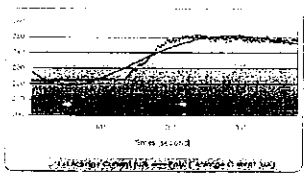	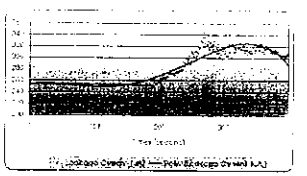
2.	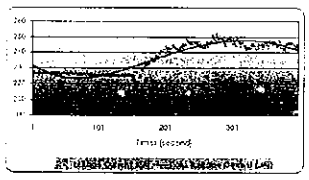	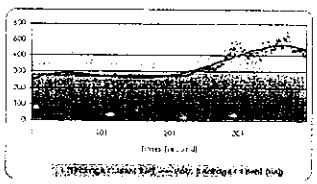

3.	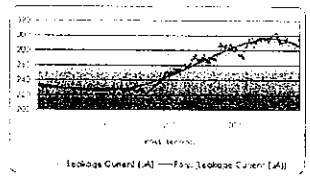	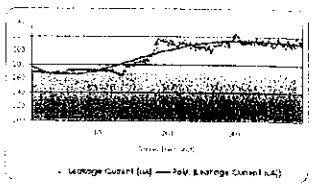
4.	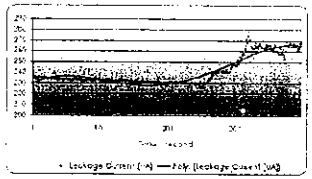	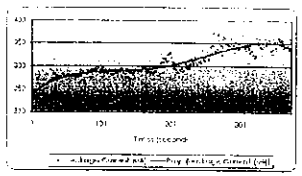

Table 4.4: (Continued)

No.	*Suspension: 120/10/3*	*Suspension: 120/210/3*
5.	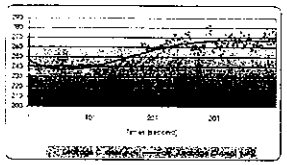	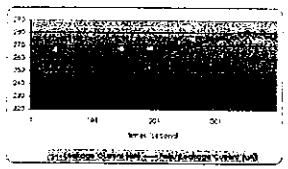
6.	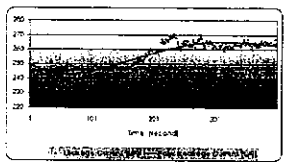	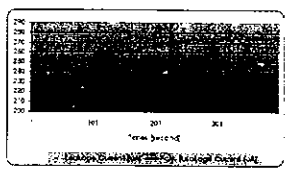

7.	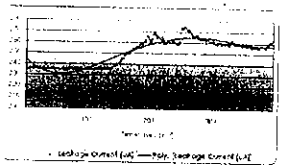	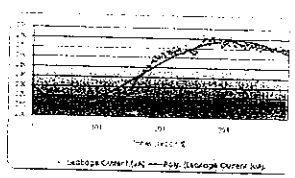
8.	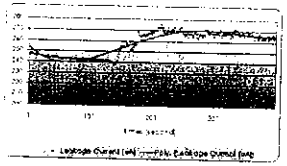	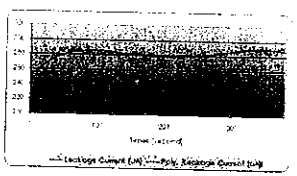
9.	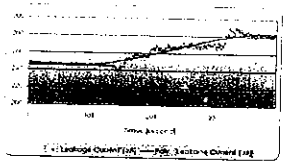	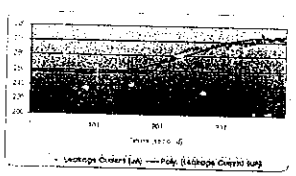

4.5 Polymeric Insulator Contamination

An ACC has been developed satisfactorily and could be used for ceramic and non-ceramic pollution testing. This chamber with a dimension of 1.415m x 1.415m x 1.650m was categorically known as the medium-scale climatic chamber. To check on the chamber performance for polymeric insulator testing, this specific test was conducted.

4.5.1 Test Sample

Test sample of SIR polymeric insulator was used in this experiment, which was a portion of the original size of the insulator. Figure 4.10 illustrates the pictorial view of that part of the polymeric insulator used in the test.

Prior to the test the insulators were washed thoroughly with tap water. After that, these wetted insulators were wiped off with tissue paper and stored properly to ensure they were totally dry and clean.

4.5.2 Contamination Process

The contamination process was initiated by presetting and pre-measured the suitable amount of water sprayed from the nozzle unit. It was found that the suitable flow rate was 1.18 ml/second.

Three types of salt water suspension concentration were used to achieve different levels of ESDD. Both NaCl and tap water were used to develop the suspension concentration which were denoted as kilo grams of NaCl per meter cubic of tap water, i.e. 10 kg/m^3, 30 kg/m^3, and 60 kg/m^3.

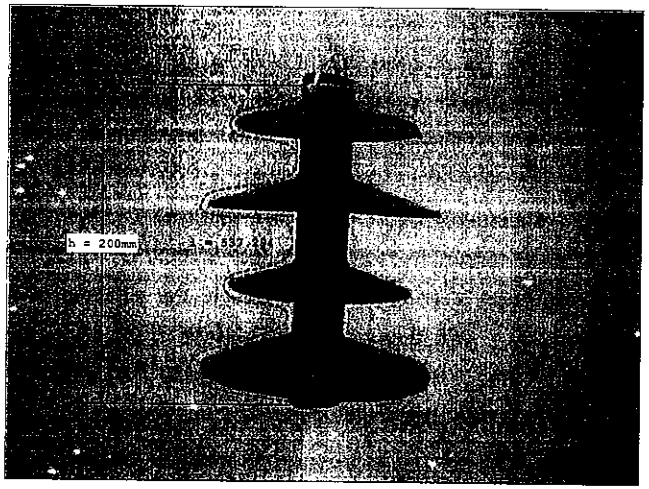

Figure 4.10 Pictorial view of the polymeric insulator.

While for the non-soluble-particle (NSP) typically of silica sand was used. To obtain the correlation between the amount of sand and duration of tests running five measurements were conducted. Table 4.5 shows the result of experimental testing.

Table 4.5: The correlation between amounts of particle with the running duration

No	**Duration** (seconds)	**Amount of Particle** (grams)	x (grams/ second)
1	90	194	2.16
2	87	190	2.18
3	88	190	2.16
4	187	85	2.2
5	193	89	2.17

Finally the average value 2.174 grams/second was obtained from the five measurements.

The task of contamination process was initiated by activating the solenoid switch o the compressor unit. Moist free air from the compressor, with around 80.0 psi was blowin via the nozzle. The non soluble particle container was attached to the nozzle unit too Afterwards the salt solution water pump was turn on. In the mean time the test sampl was hung in the chamber approximately 80.0 cm away from the nozzle-unit. The nozzl action on those non-soluble-particles caused these particles to be air-borned and settle down the test sample surfaces. They were no longer as they were but contaminated wit salt solution. The adhesion of contaminant particle to the surfaces of the test sampl increased as more moisture was absorbed to the surface of the NSP. By extending th contamination exposure time it was possible to pollute the insulator without wetting th surfaces. Figure 4.11 shows the pictorial view of operational principle of contaminatio nozzles.

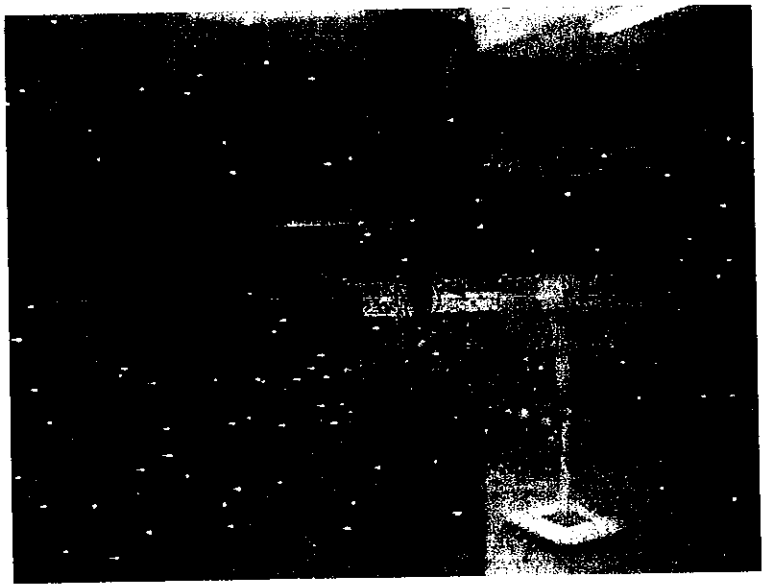

Figure 4.11 Pictorial view of operational principle of nozzles.

4.5.3 Experimental Results

This section is dedicated to produce certain empirical model to predict the other values of ESDD based on ESDD measurement results. An empirical model is addressed by using the Multiple-Regression Method. Figure 4.12 shows pictorial views of the contaminated polymeric insulator. The experimental results are presented in Table 4.6 and the analysis of ESDD level that depends on duration of spray and solution concentration is given in Figure 4.13.

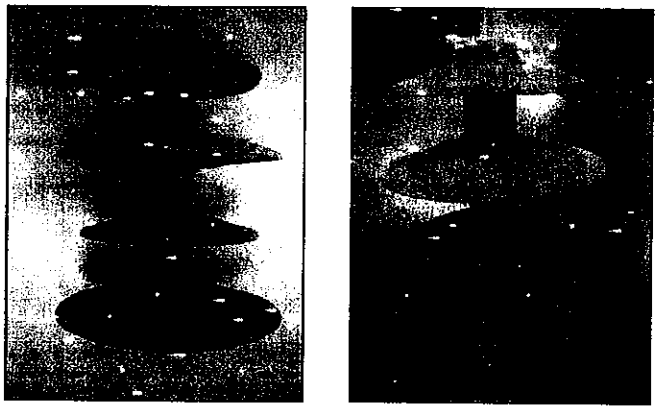

Figure 4.12 Pictorial view of the contaminated polymeric insulator

Table 4.6: Level of ESDD depends on spray duration and concentrations

ESDD (mg/cm^2)	*Duration* (seconds)	*Concentrations* (%)
0.047	30	1
0.097	60	3
0.0989	70	3
0.0919	45	3
0.1065	120	3
0.141	30	6
0.25	60	6
0.186	42	6
0.43	125	6

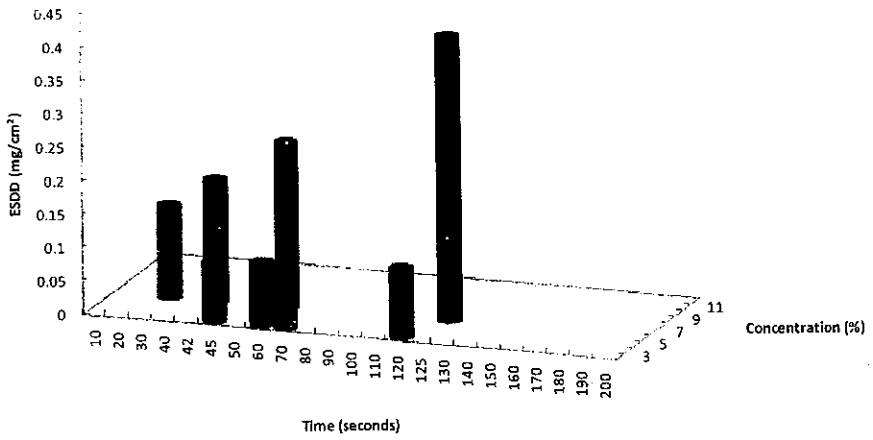

Figure 4.13 Analysis of ESDD level distribution

4.5.4 Developing the Multiple-Regression Model

Multiple-regression analysis was used primarily for the purpose of prediction of certain variable. The goal of multiple-regression analysis is for the development of a statistical model that can be used to predict the values of a dependent or response variable from the values of several explanatory or independent variable. The multiple linear regression model with *k* explanatory variable is expressed as follows.

$$Y_i = \beta_0 + \beta_1 X_{1i} + \beta_2 X_{2i} + \beta_3 X_{3i} + \ldots + \beta_k X_{ki} + \varepsilon_i \qquad (4.14)$$

Where.

β_0 = Y-intercept

β_1 = slope of Y with variable X_1 when variable $X_2, X_3, \ldots, X_k$ are held constant

β_2 = slope of Y with variable X_2 when variable $X_1, X_3, \ldots, X_k$ are held constant

β_3 = slope of Y with variable X_3 when variable $X_1, X_2, X_4, \ldots, X_k$ are held constant

.

.

.

β_k = slope of Y with variable X_k when variable $X_2, X_3, \ldots, X_{k-1}$ are held constant

ε_i = random error in Y for observation i

Therefore for data with two explanatory variables, the multiple linear regression models are expressed as follows.

$$Y_i = \beta_0 + \beta_1 X_{1i} + \beta_2 X_{2i} + \varepsilon_i \qquad (4.15)$$

where

β_0 = Y-intercept

β_1 = slope of Y with variable X_1 when variable X_2 is held constant

β_2 = slope of Y with variable X_2 when variable X_1 is held constant

ε_i = random error in Y for observation i

The slope β_1 represents the change in the mean of Y per unit change in X_1, tak
into account the effect of X_2. It is referred to as a net regression coefficient. Later on
sample regression coefficient (b_0, b_1, and b_2) are used as estimates of the populat
parameters (β_0, β_1, and β_2). Therefore the regression equation for a multiple lin
regression model with two explanatory variables can be expressed as follows.

$$\hat{Y}_i = b_0 + b_1 X_{1i} + b_2 X_{2i} \quad (4.$$

4.5.5 Building Empirical Models

To build the empirical model the data from Table 4.6 is expressed to
mathematical operation using matrix notation.

$$\mathbf{Y} = \mathbf{X}\beta + \varepsilon \quad (4.$$

The least square estimate of β is

$$\hat{\beta} = (\mathbf{X}'\mathbf{X})^{-1}\mathbf{X}'\mathbf{y} \quad (4.$$

By using the least square method, the values of the three sample regress
coefficients are obtained with PHStat add-in for Microsoft Excel. Figure 4.14 presents
partial output for the ESDD data from Microsoft Excel.

From it we obtained that the computed values of the regression coefficients are
follows:

b_0 = - 0.1112

b_1 = 0.0015

b_2 = 0.0422

Therefore, the multiple-regression equation can be expressed as

$$\hat{Y}_i = -0.1112 + 0.0015X_{1i} + 0.0422X_{2i} \quad (4$$

	A	B	C	D	E	F	G
1	Regression Analysis						
2							
3	*Regression Statistics*						
4	Multiple R	0.871868021					
5	R Square	0.759805139					
6	Adjusted R Square	0.679740185					
7	Standard Error	0.066359544					
8	Observations	9					
9							
10	ANOVA						
11		*df*	*SS*	*MS*	*F*	*Significance F*	
12	Regression	2	0.083578881	0.04178944	9.4898592	0.013857699	
13	Residual	6	0.026421535	0.00440359			
14	Total	8	0.110000416				
15							
16		*Coefficients*	*Standard Error*	*t Stat*	*P-value*	*Lower 95%*	*Upper 95%*
17	Intercept	-0.111926076	0.086569284	-1.68134714	0.14369115	-0.274815366	0.05096321
18	Times	0.001536949	0.000665772	2.30852243	0.06039097	-9.21369E-05	0.00318603
19	Concentration	0.042192718	0.012435035	3.39305179	0.01462053	0.011785261	0.07262018
20							

b_0 b_1 b_2

Figure 4.14 Regression analysis acquired from Microsoft Excel

4.5.6 Residual Analysis for the Empirical Model

A residual is the difference between the observation Y_i and the fitting $\hat{Y}_i$. The residual analysis is utilized to evaluate whether the empirical model is appropriated for the set of data. Table 4.7 presents the observation, fitted values, and residuals for the model.

The residual plots are presented in Figure 4.15 there appears to be very little or no pattern in the relationship between the residuals and either, the value of X_1 (times) or X_2 (concentrations). Then can be concluded that the multiple linear regression is appropriate for predicting the percentage of ESDD.

Table 4.7: Experimental, Fitted Value, and Residuals for ESDD data

Observation Number	Y_i	$\hat{Y}_i$	$e_i = Y_i - \hat{Y}_i$
1	0.047	-0.024	0.071
2	0.097	0.107	-0.01
3	0.0989	0.122	-0.023
4	0.0919	0.084	0.008
5	0.1065	0.199	-0.093
6	0.141	0.187	-0.046
7	0.25	0.233	0.017
8	0.186	0.206	-0.02
9	0.43	0.333	0.097

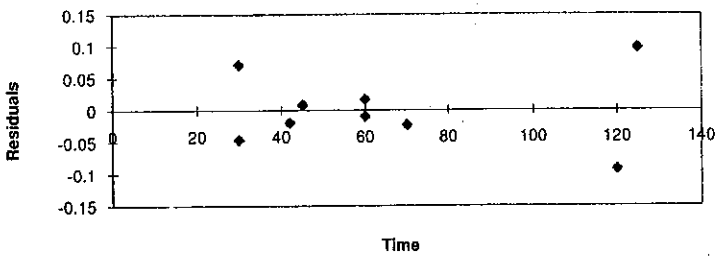

(a)

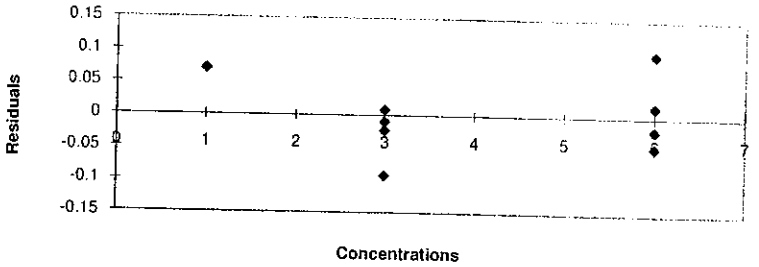

(b)

Figure 4.15 Residual plots for the ESDD model
(a) Residuals versus Time, (b) Residuals versus Concentrations

Finally based on the empirical model the desire ESDD can be predicted according to the time frame and the concentration level. Table 4.8 illustrates the prediction of ESDD according to the time frame and the concentration level. Figure 4.16 shows the graph. For example with 9% concentration level and 100 seconds time frame the prediction of ESDD is 0.493202 mg/cm^2.

Table 4.8: Prediction of ESDD level according to time frames and concentrations

Time	Concentrations									
	3	4	5	6	7	8	9	10	11	12
10	-0.026	0.031	0.089	0.146	0.203	0.260	0.318	0.375	0.432	0.489
20	-0.006	0.051	0.108	0.165	0.223	0.280	0.337	0.394	0.452	0.509
30	0.013	0.070	0.128	0.185	0.242	0.299	0.357	0.414	0.471	0.528
40	0.033	0.090	0.147	0.204	0.262	0.319	0.376	0.433	0.491	0.548
50	0.052	0.109	0.167	0.224	0.281	0.338	0.396	0.453	0.510	0.567
60	0.072	0.129	0.186	0.243	0.301	0.358	0.415	0.472	0.530	0.587
70	0.091	0.148	0.206	0.263	0.320	0.377	0.435	0.492	0.549	0.606
80	0.111	0.168	0.225	0.282	0.340	0.397	0.454	0.511	0.569	0.626
90	0.130	0.188	0.245	0.302	0.359	0.416	0.474	0.531	0.588	0.645
100	0.150	0.207	0.264	0.321	0.379	0.436	0.493	0.550	0.608	0.665
110	0.169	0.227	0.284	0.341	0.398	0.455	0.513	0.570	0.627	0.684
120	0.189	0.246	0.303	0.361	0.418	0.475	0.532	0.589	0.647	0.704
130	0.208	0.266	0.323	0.380	0.437	0.494	0.552	0.609	0.666	0.723
140	0.228	0.285	0.342	0.400	0.457	0.514	0.571	0.628	0.686	0.743
150	0.247	0.305	0.362	0.419	0.476	0.534	0.591	0.648	0.705	0.762
160	0.267	0.324	0.381	0.439	0.496	0.553	0.610	0.667	0.725	0.782
170	0.286	0.344	0.401	0.458	0.515	0.573	0.630	0.687	0.744	0.801
180	0.306	0.363	0.420	0.478	0.535	0.592	0.649	0.707	0.764	0.821
190	0.325	0.383	0.440	0.497	0.554	0.612	0.669	0.726	0.783	0.840
200	0.345	0.402	0.459	0.517	0.574	0.631	0.688	0.746	0.803	0.860

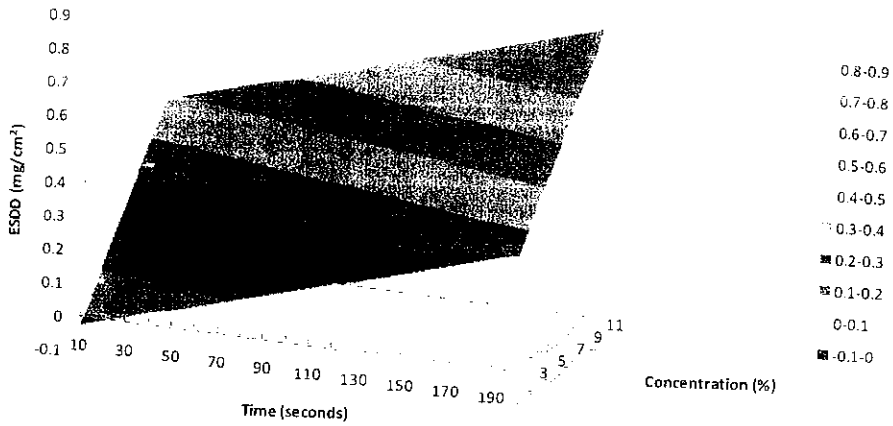

Figure 4.16 Visualization of ESDD level obtained from Table 4.8

CHAPTER 5
SUMMARIES OF CURRENT WORK

The following summaries can be drawn from the present work:

A mobile artificial contamination chamber has been designed and fabricated. The mobile artificial contamination chamber is provided with IEC standard nozzles for ceramic insulator with extended nozzles that could be used for the polymeric insulator contamination testing.

Leakage current measurement and flashover simulation are achievable with the used of the prototype that was designed and fabricated in-house. Not limited to, electronic instrumentation, video recording, data acquisition and GUI were also developed.

In line with that, a technique to segregate aged insulators was introduced that took account of the electrical defects. The segregation was made based on the ac and dc leakage current values, and tangent δ factor. This technique is effective for determining relative quality of aged glass insulators and the corona inception measurement provide more satisfactory result. However, improvements can still be considered.

Recycling of aged and used insulator is not heard of in the world of affluence and wasteful. But if the technique developed here as a result of contamination research, any type of string or post insulators which are no longer used in service can be recycled and used again for new or upgrade lines for instance in the distribution line. Also any insulator that is manufactured locally can now be locally tested especially the contamination test of insulator as proposed in the IEC standard.

The present artificial contamination chamber which was developed by the Institut Voltan dan Arus Tinggi (IVAT) insulation performance research group was a medium-scale chamber which could be used for an insulator with BIL and BSL of not more than 300 kV. For higher BIL and BSL insulator testing a large-scale chamber of larger dimensions will be required.

REFERENCES

[1] Khalifa, M. (1990). *High-Voltage Engineering*. USA: Marcel Dekker, Inc. New York.

[2] Zhicheng, Guan and Guchun, Cue (1994). *A Study On The Leakage Current Along The Surface of Polluted Insulator*. International Conference on Properties and Application of Dielectric Materials. Australia. 495-498.

[3] M. Abu Bakar Sidik, Hussein Ahmad, S. Shahnawaz Ahmed, M. Irfan Jambak, Z. Nawawi (2002). *Development of An Artificial Contamination Chamber for Insulator Performance Test*. Malaysia Science and Technology Congress (MSTC2002), Johor Bahru, Malaysia. September 19-21.

[4] Gdoutos, E.E., Pilakotas, K., Rodopoulus, C.A. (2000). *Failure Analysis of Industrial Composite Materials*. United State of America: The McGraw-Hill Companies, Ins.

[5] Karady, G.G., Rizk, M.M., Scheider, H.M. (1994). *Review of CIGRE and IEEE Research Into Pollution Performance of Non-ceramic Insulator Field and Ageing Effect and Laboratory Test Techniques*. CIGRE. 33-103.

[6] Vlatos, A.E., Sherif, E. (1990). *Natural Aging of EPDM Composite Insulator*. IEEE Transaction on Power Delivery. Vol. 5. No. 1. 406-414.

[7] Kindesberger, J., Kuhl, M., Barsch, R. (1995). *Evaluation of The Condition of Non-Ceramic Insulator After Long Term Operation Under Service Condition*. 9th ISH Graz, August 28 – September 1. paper no. 3193-1.

[8] CIGRE, WG 22.03, Insulator (1996). *Review of In Service Diagnosing Testing of Composite Insulator*. ELECTRA. No. 169. 104-120.

[9] Kuhl, M. (1995). *Report of Properties of SIR Composite Insulator After Long Term Exposure in Service*. IEEE/ KTH Stockholm Power Tech Conference, Stockholm, June 18-22. Paper SPT IS 12-4. 256-261.

[10] Bognas, A., et al. (1997). *Investigations on a 20 Years Old Composite Insulator*. 10th ISH Montreal. August 25-29.

[11] Looms, J.S.T. (1988). *Insulator for High Voltages*. Peter Peregrinus Ltd, London.

[12] Kuffel, E., Zaengl, W.S., Kuffel, J. (2000). *High Voltage Engineering Fundamental*. 2nd.ed. Great Britain: Butterworth-Heiemann.

[13] Tu Yanming (2000). *Approaches to Aging of Composite Insulators*. Proceeding of The 6th International Conference on Properties and Application of Dielectric Materials. Xi'an Jiaotong University, Xi'an, China. pp. 371-374.

[14] Pasaribu, Pardomuan (1982). *Pemilihan Isolator Hantaran Udara Tegangan Tinggi pada Daerah Terpolusi dengan Metode Statistik*. ITB.

[15] Kind, D., Karner, H. (1985). *High Voltage Insulation Technology*. Friedr, Vieweg & Sohn, Braunschweig.

[16] Mackevich, J., Shah, M., (1997). *Polymer Outdoor Insulating Material Part 1: Comparison of Porcelain and Polymer Electrical Insulation*. IEEE Electrical Insulation Magazine.

[17] Steven Brewer (1994). *Polymer Solutions to Contaminated Environments*. The Ohio Brass Company, EU1379-H.

[18] James F. Hall (1993). *History and Bibliography of Polymeric Insulators for Outdoor Applications*. IEEE Transaction on Power Delivery, Vol. 8, No. 1, pp. 376-385.

[19] Dietz, H., and co-workers (1986). *Latest Development and Experience with Composite Long Rod Insultors*. CIGRE Session. paper 15-09

[20] Gorur, R.S.; Karady, G.G.; Jagota, A.; Shah, M.; Yates, A.M (1992). *Ageing in Silicone Rubber Used for Outdoor insulation*. IEEE Transaction on Power Delivery, Vol.7, p. 525-538.

[21] Takeshi Goto, Yoshikatsu Hori, Tokui Yonemura, Masahiro Suetsugu (2000). *Artificial Contamination Tests of Silicone Rubber Cylindrical Models*. Proceeding of The 6th International Conference on Properties and Application of Dielectric Materials. Xi'an Jiaotong University, Xi'an, China. pp. 272-275.

[22] Liang Xidong, Wang Shaowu, Huang Lengceng, Shen Qinghe, Cheng Xueqi (1999). *Artificial Pollution Test and Pollution Performance of Composite Insulators*. Conference of High Voltage Engineering Symposium, No. 467, pp. 337-340.

[23] Schneider, H. M., Hall, J. F., Karady, G. G., and Rendowden, J. (1989). *Non-ceramic Insulators for Transmission Lines*. IEEE Transaction on Power Delivery, Vol.4, pp.2214-2220.

[24] Ryan, H.M. (1994). *High Voltage Engineering and Testing*. England: Peter Peregrinus Ltd.

[25] Chang, J., and Gorur, R. S. (1989). *Surface Hydrophobicity of Polymeric Materials Used for Outdoor Insulation*. Sixth International Symposium on HV Engineering, New Orleans, USA, Paper No. 30.05.X

[26] George G. Karady (1999). *Flashover Mechanism of Non-Ceramic Insulators*. IEEE Transaction on Dielectrics and Electrical Insulation, Vol.6, No.5, pp.718-723.

[27] Sherif, E.M., Vlastos, A. E. (1987). *Influence of Ageing on the Electrical Properties of Composite Insulators*. 5th ISH Braunschweig. Paper 51.01.

[28] Kulkani,R., et.al (1982). *Sea Salt in Coastal Air and its Deposition on Porcelain Insulators.* Journal Applied Meteorology. Vol. 21. pp. 350-355.

[29] Alame, N., Shihab. S. (1992). *A Model for Calculating the Field Distribution of Polluted Post Insulators During Flashovers.* Electrical Insulation and Dielectric Phenomena.

[30] Butler. K. L., Khan. S., Russell. B. D. (1999). *Analysis of Incipient Behavior of Multiple Distribution Insulators.* Transmission and Distribution Conference, IEEE , Volume: 2 , pp. 675 -680 vol.2.

[31] Burnham, J. T., Busch, D. W., Renowden, J. D. (1993). *FPL's Christmas 1991 Transmission Outages.* IEEE Transaction on Power Delivery, Vol. 8, No. 4, pp. 1874-1881.XX

[32] Y. Taniguchi, N. Arai, Y. Imano (1979). *Natural Contamination Test of Insulators at Noto Testing Station Near Japan Sea.* IEEE Transaction on Power Apparatus and System, Vol. PAS-98, No. 1, pp. 239-245.

[33] Ahmad S. Ahmad (1999). *Study on High Voltage Insulator Performance Under Adverse Contaminated Conditions.* MEE Thesis, Universiti Teknologi Malaysia.

[34] Nam Ho Choi, Sang Ok Han, and Kang Sik Park (2001). *Distribution Characteristics of Salt Contaminants.* Proceedings of 2001 International Symposium on Electrical Insulating Materials, pp.270 –273.

[35] Gutman, I. (1999). *Field Testing of Composite Insulators at Natal Test Stations in South Africa.* High Voltage Engineering Symposium, No. 467, pp.50-53.

[36] Sangkasaad, S., Staub, B., Marangsree, B., Pattanadech, N. (2000). *Investigation on Electrical Performance of Semiconducting Glazed Insulators Under Natural Pollution in Thailand.* Proceedings. PowerCon 2000, International Conference on Power System Technology, Vol. 3, pp. 1229-1232.

[37] Sirait, K. T., Salama, Suwarno, (1999). *Surface Hydrophobicity of Silicone Rubber Under Natural Tropical Conditions.* High Voltage Engineering Symposium. pp. 4.38.S19-4.41.S19.

[38] CIGRE WG 33-04. *Polluted Insulator Guide.* 1996.

[39] CIGRE WG.04 (1979). *The measurement of site pollution severity and its application to insulator dimensioning for A.C. systems.* Electra, No. 64, pp. 101-116.

[40] Ricardo, W. S., Basignoli, R., Gomes, E. Jr. (1991). *Influence of the Non-uniform of Pollution Distribution on The Electrical Behaviour of Insulators.* Proceeding of the 3rd International Conference on Properties and Application of Dielectric Materials, pp. 342-345.

[41] IEC 60- 1 (1989). *High Voltage Test Techniques.*

[42] IEC 507 (1991). *Artificial Pollution Tests on HV Insulators to be Used on AC Systems.*

[43] Gyula Besztercey and George G. Karady (1998). *A new Contamination Method for Clean Fog Test of Composite Insulator.* IEEE International Symposium on Electrical Insulation. Arlington. Virginia. USA. pp. 365-368.

[44] Md. Abdul Salam, Hussein Ahmad, Zulkifly Saadom. Razali Budin, T. Tamsir, Z. Buntat, M.A.M. Piah (2000). *Effect of Equivalent Salt Deposit Density on Flashover voltage of Contaminated Insulator Energized by HVDC.* Proceeding of the 6th International Conference on Properties and Application of Dielectric Materials, Xi'an, China, pp. 821-824.

[45] Cui Jiangliu, Su Zhiyi, Yi Hui (1999). *Application and Prospect of Silicone Rubber Composite Insulator in China.* High Voltage Engineering Symposium. pp. 4.5.S17-4.8.S17.

[46] Cherney, E.A., et.al. (1983). *The Clean Fog Test for Contaminated Insulator.* IEEE Transactions on Power Apparatus and Systems. Vol. PAS-107, No. 3, pp.604-613.

[47] De Tourreil, C.H., Lambeth P.J. (1990). *Aging of Composite Insulator: Simulation by Electrical Test.* IEEE Transaction on Power Delivery, Vol. 5, No. 3. pp. 1558-1567.

[48] De La O, A., Gorur, R. S., Chang, J., (1994). *AC Clean Fog Tests on Non-Ceramic Insulating Materials and a Comparison with Porcelain.* IEEE Transaction on Power Delivery. Vol. 9. No. 4. pp. 2000-2008

[49] Eklund, A., Hartings, R. (1994). *The Dust Cycle Method: A new pollution test method for ceramic and non-ceramic insulator.*" SEE Workshop. Paris.

[50] George G. Karady, Vincent Rayapa, A., Mukund Muralidhar, Don L. Ruff (1996). *A New Method for Pre-contamination and Testing of Non-ceramic Insulators.* IEEE International Symposium on Electrical Insulation. Montreal. Quebed. Canada. pp. 263-266.

[51] Gyula Besztercey and George G. Karady (2000). *An Artificial Contamination Method for Composite Insulators.* IEEE Transaction on Power Delivery, Vol. 15. No. 2. pp. 732-737.

[52] Stephne A. Sebo, Tiebin Zhao (1999). *Utilization of Fog Chambers for Non-ceramic Outdoors Insulator Evaluation.* IEEE Transaction on Dielectrics and Electrical Insulation. Vol. 6. No.5. pp. 676-687.

[53] Devendranath, D.. Mohan Rao, N.S., Channakeshava, Rajkumar, A. D. (2000). *Aging Studies On RTV Coated Insulator In Salt-Fog Pollution.* Power Engineering Society Winter Meeting. Vol. 4. pp. 2822-2829.

[54] Stephen A. Sebo, Edgar P. Casale, Jose R. Cedeno, Wibawa Tjokrodiponto, Sheikh A. Akbar (1996). *Review of Features of Fog Chamber at The Ohio State University for Polymeric Insulator Evaluation.* Conference on Electrical Insulation and Dielectric Phenomena. San Fransisco. pp. 443-446.

[55] Edgar P. Casale, Stephen A. Sebo (1996). *Polymeric Insulator For Chamber Project: Data Acquisition System Development.* Conference on Electrical Insulation and Dielectric Phenomena, San Fransisco. pp. 447-450.

[56] K. Isaka, Y. Yokoi. K. Naito, R. Matsuoka, S. Ito, K. Sakanishi, O. Fuji (1990). *Development of Real-time System for Simultaneous Observation of Visual Discharges and Leakage Current on Contaminated dc Insulators.* IEEE Transaction on Electrical Insulation. Vol. 25. No. 6. pp. 1153-1160.

[57] Wibawa T., Stephen A. Sebo. John D. Sakich. Tiebin Zhao (1997a). *Simultaneous Electrical and Visual Measurement of Leakage Current Along Polymer Insulators in Artificial Pollution Tests.* Proceeding of the 5th International Conference on Properties and Application of Dielectric Materials. Seoul. Korea. pp. 738-741.

[58] Wibawa T., Stephen A. Sebo, John D. Sakich, Tiebin Zhao (1997b). *Leakage Current Magnitude and Waveshapes Along Polymer Insulators.* Conference on Electrical Insulation and Dielectric Phenomena. Minneapolis. pp. 390-393.

[59] Tiebin Zhao, John Sakich (1996). *Salt Fog Test on Non-ceramic Insulators and Fog Chamber Data Acquisition System.* Conference on Electrical Insulation and Dielectric Phenomena. San Fransisco. pp. 377-380.

[60] Gorur,R. (1999). *Report from Task Force Activities on Measurments of Surface Resistance on Non-ceramic insulator.* IEEE PES Winter Meeting, New York, USA.

[61] Topalis, F. V., Gonos, I. F., Stathopulos, I. A. (2001). *Dielectric Behaviour of Polluted Porcelain Insulators.* IEEE Proceeding Generation Transmission and Distribution, Vol.148, No.4. pp. 269-274

[62] Suwarno (1999). *Pengurangan Arus Bocor/Rugi-rugi Daya Pada Isolator Keramik dengan Lapisan Senyawa Silikon.* Seminar Nasional & Workshop Teknik Tegangan Tinggi II, Universitas Gajah Mada, Yogyakarta. pp. B1-1.1 – B1-1.6.

[63] Fernando, M.A.R.M., Gubanski, S.M. (1999). *Leakage Current Pattern on Contaminated Polymeric Surface.* IEEE Transaction on Dielectric and Electrical Insulation. Vol. 6. No. 5. pp. 688-694.

[64] Fernando, M.A.R.M., Gubanski, S.M. (1996). *Leakage Current Patterns on Artificially Polluted Composite Insulators.* Conference on Electrical Insulation and Dielectric Phenomena. San Fransisco. pp. 394-397.

[65] Isaias R. V., Jose Luis F. C., (1999). *Criteria for the Diagnostic of Polluted Ceramic Insulators Based on the Leakage Current Monitoring Technique.* Conference on Electrical Insulation and Dielectric Phenomena. pp. 715-718.

[66] Bologna, F. F., Britten, A. C., Watridge, G., Stevens, D. J., Grigorakis, G. (1999). *Leakage Currents on Lightly Polluted on 275 kV Glass Disc Insulator Strings in Conditions of Light Wetting.* Africon. Vol. 2. pp. 739-742.

[67] H. Matsuo, T. Fujishima, T. Yamashita, K. Hatase (1999). *Relation between Leakage Impedance and Equivalent Salt Deposit Density on an Insulator under a Saltwater Spray.* IEEE Transaction on Dielectric and Electrical Insulation. Vol. 6. No. 1. pp. 117-121.

[68] Masashi Sato, Yuuji Mishima, Akihiro Nakajima, Masao Sugai (1997). *Leakage Current on Outdoor Insulators under Rapid Pollution Conditions.* Proceeding of the 5th International Conference on Properties and Application of Dielectric Materials. Seoul. Korea. pp. 762-765.

[69] Devendranath, D., Channakeshave, Rajkumar, A. D. (2002). *Leakage Current and Charge in RTV Coated Insulators Under Pollution Conditions.* IEEE Transaction on Dielectric and Electrical Insulation. Vol. 9. No. 2. pp. 294-299.

[70] George G. Karady, Felix Amarh (1999). *Signature Analysis for Leakage Current Wave Forms of Polluted Insulators.* IEEE Transmission and Distribution Conference. Vol. 2. pp. 806-811.

[71] George G. Karady. Felix Amarh (2000). *Extreme Value Analysis of Leakage Current Envelope of Polluted Insulator.* Power Engineering Society Summer Meeting, 2000. IEEE , Vol. 4. pp. 2531 -2535.

[72] M. Sato, A. Nakajima, T. Komukai, T. Oyamada (1998). *Spectral Analysis of Leakage Current on Contaminated Insulators by Auto Regressive Method.* Conference on Electrical Insulation and Dielectric Phenomena, Vol. 1. pp. 64-66.

[73] Fierro-Chavez, J. L., Ramirez-Vazquez, I., Montoya-Tena, G. (1996). *Online Leakage Current Monitoring of 400 kV Insulator Strings in Polluted Areas.* IEEE Proceeding Generation, Transmission and Distribution. Vol. 143. No. 6. pp. 560-564.

[74] Felix Amarth, George G. Karady, Raji Sundararajan (2001). *Level Crossing Analysis of Leakage Current Envelope of Polluted Insulators.* IEEE Power Engineering Riview. pp. 46-49.

[75] Lozno-Sousa, C., Diaz-Acosta, R., Ramos-Niembro, G. (1990). *Patterns of Pollution on Insulators: Clustering by Seasonal Variation and Exposure Period.* IEEE Transaction on Power Delivery, Volume 5, No. 1, pp. 324-329.

[76] Rizk, F.A.M. (1981). *Mathematical Models for Pollution Flashover.* Electra Vol. 78, pp. 71-103.

[77] Mercure, H.P. (1989). *Insulator Pollution Performance at High Altitude: major trends.* IEEE Transaction on Power Delivery, Vol.4, pp.1461-1468.

[78] Farouk A, Rizk, M., Rezazada, A. Q. (1996). *Modelling of Altitude Effects on AC Flashover of Polluted High Voltage Insulator.* IEEE/PES Winter Meeting, Paper 96 WM 104-0 PWRD.

[79] L. Shu, M. Farzaneh, Y. Li, and C. Sun (2001). *AC Flashover performance of polluted insulators covered with artificial ice at low atmospheric pressure.* Conference on Electrical Insulation and Dielectric Phenomena." pp. 609-612.

[80] Izzularab, M.A., Shwehdi, M.H., Farag, A.S., Belhadj, C.A. (1998). *Flashover Due To Lightning of Composite Insulators Used On Distribution Lines.* IEEE International Symposium on Electrical Insulation, Arlington, Virginia, USA. pp. 395-398.

[81] Gonos, I.F., Topalis, F.V., Stathopolos, I.A. (2002). *Genetic Algorithm Approach To The Modelling of Polluted Insulators.* IEEE Proceeding on Generator, Transmission and Distribution, Vol. 149, No. 3, pp.373-376.

[82] S. Gopal, M.E., and Prof. Y.N. Raom, Dr-Ing (1984). *Flashover Phenomena of Pulluted Insulators.* IEE Proceedings, Vol. 131, Pt. C, No. 4, pp.140-143.

[83] R. Sundararajan and R. W. Nowlin (1996).*Effect of altitude on the Flashover Voltage of Contaminated Insulators.* Proceeding of CEIP, San Francisco, pp. 433-436.

[84] Ghosh, P.S., Chakravorti, S. (1995). *Estimation of Time-to-flashover Characteristic of Contaminated Electrolytic Surface using a Neural Network.* IEEE Transactions on Dielectrics and Electrical Insulation, Vol. 2, No.6, pp. 1064-1074.

[85] Jermendy, I., and Fogarasi, I. (1999). *Detection of Insulator Ageing.* International Conference on Electric Power Engineering, PowerTech Budapest, pp.128.

[86] Spellman, C. A., Young, H. M., Haddad, A., Rowlands, A. R., Waters, R. T. (1999). *Survey of Polymeric Insulator Ageing Factors.* High Voltage Engineering Symposium. pp.160-163.

[87] Zhicheng, Guan and Guchun, Cue (1994). *A Study On The Leakage Current Along The Surface of Polluted Insulator.* International Conference on Properties and Application of Dielectric Materials. Australia. 495-498.

[88] Liang Xidong, Chen Xupeng, Xue Jiaqi (1994). *Effective Contaminant Deposit Density—A New Concept of the Pollution Level of Composite Insulators.* Proceeding of the 4th International Conference on Properties and Applications of Dielectric Materials." Brisbane Australia. pp. 523-526.

[89] Muhammad Abu Bakar Sidik, (2009). *Karakteristik Arus Bocor Isolator Keramik Tegangan Tinggi pada Sistem Penyaluran Energi Listrik di Indonesia.*Jurnal Rekayasa Sriwijaya No. 1, Vol. 18, March.

[90] George Omura (1992). *Matering AutoCAD Release 12.* Sybec Inc.

[91] Handi Chandra (2000). *Menggambar 3D dengan AutoCAD 2000.* Jakarta: PT. Elex Meida Komputindo.

[92] Handi Chandra (2000). *Fasilitas Baru AutoCAD 2000.* Jakarta: PT. Elex Media Komputindo.

[93] Gallagher, T.J., Permain, A.J. (1983). *High Voltage Measurement, Testing and Design.* Jonh Wiley & Sons, Great Britain.

[94] David M. Levine, Patricia P. Ramsey, Robert K. Smidt. (2001). *Applied Statistics for Engineers an Scientist.* USA.: Prentice-Hall. Inc. 567-615.

[95] Douglas C. Montgomery, George C. Runger, Norma F. Hubelu. (2001). *Engineering Statistic.* 2nd. Ed. USA.: John Wiley & Sons, Inc. 293-350

[96] Michael C. Fleming, Joseph G. Nellis (2000). *Principles of Applied Statistic.* 2nd. Ed. United Kingdom.: Thomson Learning. 269-311

[97] Ahmad S. Ahmad, Hussein Ahmad, Md. Abdul Salam, Ahmad Saad. (2000a). *Regression Technique for Prediction of Salt Contamination Severity on High Voltage Insulators.* Annual Report Conference on Electrical Insulation and Dielectric Phenomena. , Vol. 1 , pp.218 -221.

[98] Gary W. Johnson (1994). *LabVIEW Graphical Programing.* USA: McGraw-Hill, Inc.

[99] National Instrument (1998). *LabView User Manual.* National Instrument Cooperation, USA.

[100] National Semiconductor.(2001). *LM355 Temperature Sensor Data Sheet.* Available as PDF from http://www.national.com/pf/LM/LM35.html#Datasheet.

[101] Thermometrics (2001). *HU10 Humidity Sensor Data Sheet.* Available as PDF from http://www.thermometrics.com/html/docs/numindex.htm.

[102] Cenwick Electronic, Ltd. (2001). *Trimmers Multiturn BOURNS type 3299*. Available as PDF from http://www.anqliac.com.

[103] Messwandler-Bau GMBH Bamberg. *High Voltage Construction Kit*. Western Germany.

[104] Pico Technology, Ltd., a. *ADC-11 User Manual*. United Kingdom.

[105] Pico Technology, Ltd., b. *ADC-200 User Manual*. United Kingdom.

[106] M.A.R. Manjula Fernando, *Performance of Non-ceramic Insulators in Tropical Environments*, PhD Thesis, Department of Electrical Power Engineering, Chalmers University of Technology, Goteborg, Sweden, 1999.

[107] Andreas Dernfalk, *Diagnostic Methods for Composite Insulators with Biological Growth*, PhD Thesis, Department of Electrical Power Engineering, Chalmers University of Technology, Goteborg, Sweden, 2004.

[108] Lan Gao *Characteristics of Streamer Discharges in Air and along Insulating Surfaces* Comprehensive Summaries of Uppsala Dissertations, Uppsala University, Sweden, 2000.

APPENDIX

COMPLETE TECHNICAL DRAWING OF THE ARTIFICIAL CONTAMINATION CHAMBER

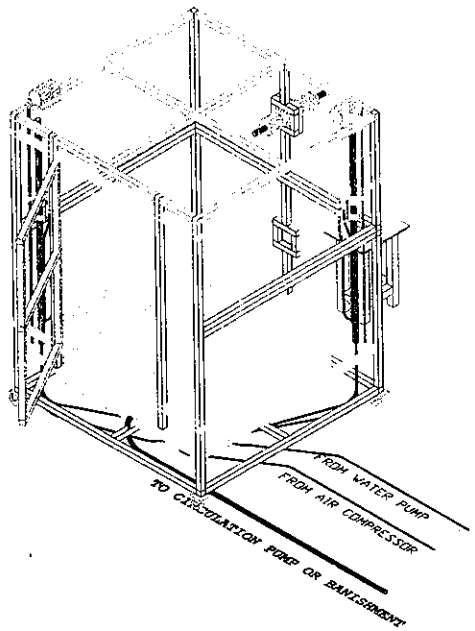

No.	Description	Qty.	Material	Remark

UNIVERSITI TEKNOLOGI MALAYSIA
FACULTY OF ELECTRICAL ENGINEERING

DESIGN	M. ABU BAKAR S
DRAWN	M. ABU BAKAR S
CHECKED	

DIMENSIONS IN mm

UNSPECFIED TOLERANCES
LINIER +/- :
ANGULAR +/- :

SCALE | A4 | FINE | MEDIUM ● | ROUGH

COMPLETE DESIGN
MOBILE ARTIFICIAL CONTAMINATION CHAMBER

Drw. No. CD. 01.00 | No. sheet

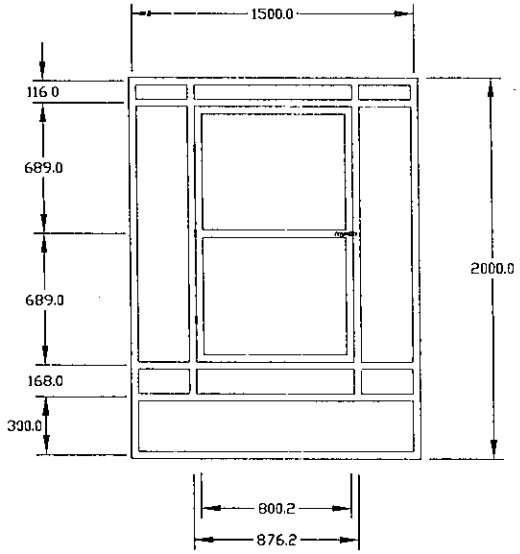

Front View

No.	Description	Qty.	Material	Remark

Material : Steel Square Hollow Beam

UNIVERSITI TEKNOLOGI MALAYSIA
FACULTY OF ELECTRICAL ENGINEERING

DESIGN	M. ABU BAKAR S
DRAWN	M. ABU BAKAR S
CHECKED	

DIMENSIONS IN mm

UNSPECFIED TOLERANCES
LINIER +/- :
ANGULAR +/- :

SCALE | A4 | FINE | MEDIUM ● | ROUGH

DESIGN OF CHAMBER STRUCTURE
MOBILE ARTIFICIAL CONTAMINATION CHAMBER

Drw. No. CS. 01.00 | No. sheet

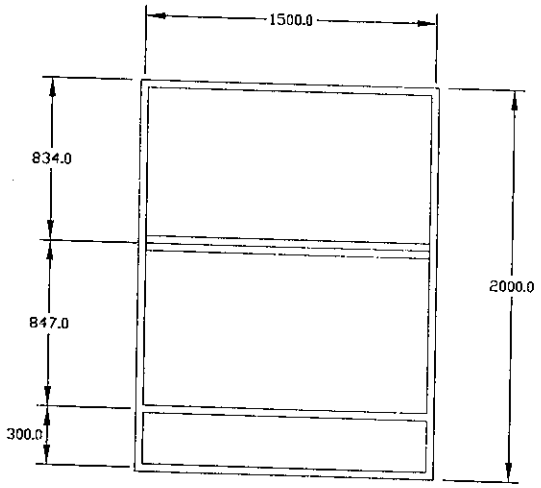

Side View

UNIVERSITI TEKNOLOGI MALAYSIA FACULTY OF ELECTRICAL ENGINEERING	DESIGN	M. ABU BAKAR S	DIMENSIONS IN mm	No. / Description / Qty. / Material / Remark Material : Steel Square Hollow Beam	
	DRAWN	M. ABU BAKAR S		DESIGN OF CHAMBER STRUCTURE MOBILE ARTIFICIAL CONTAMINATION CHAMBER	
SCALE A4	CHECKED		UNSPECFIED TOLERANCES LINIER +/- : ANGULAR +/- :	Drw. No. CS. 02.00	No. sheet
FINE / MEDIUM / ROUGH					

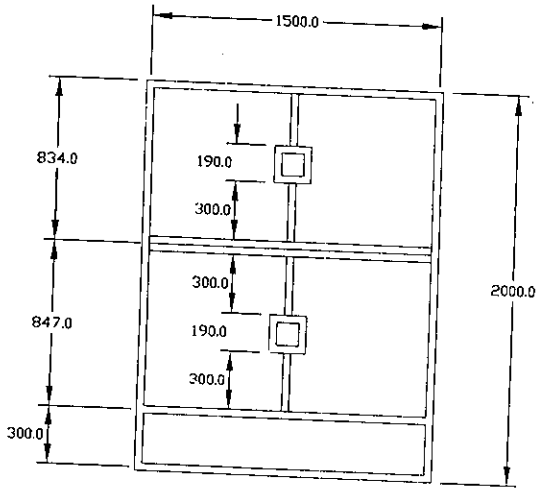

Back View

UNIVERSITI TEKNOLOGI MALAYSIA FACULTY OF ELECTRICAL ENGINEERING	DESIGN	M. ABU BAKAR S	DIMENSIONS IN mm	No. / Description / Qty. / Material / Remark Material : Steel Square Hollow Beam	
	DRAWN	M. ABU BAKAR S		DESIGN OF CHAMBER STRUCTURE MOBILE ARTIFICIAL CONTAMINATION CHAMBER	
SCALE A4	CHECKED		UNSPECFIED TOLERANCES LINIER +/- : ANGULAR +/- :	Drw. No. CS. 03.00	No. sheet
FINE / MEDIUM / ROUGH					

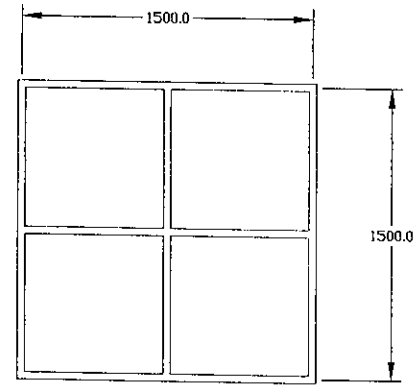

Top View / Bottom View

No.	Description	Qty.	Material	Remark
Material :	Steel Square Hollow Beam			

UNIVERSITI TEKNOLOGI MALAYSIA
FACULTY OF ELECTRICAL ENGINEERING

DESIGN	M. ABU BAKAR S
DRAWN	M. ABU BAKAR S
CHECKED	

DIMENSIONS IN mm

UNSPECFIED TOLERANCES
LINIER +/- :
ANGULAR +/- :

SCALE | A4 | FINE | MEDIUM | ROUGH

DESIGN OF CHAMBER STRUCTURE
MOBILE ARTIFICIAL CONTAMINATION CHAMBER

Drw. No. CS. 04.00

No. sheet

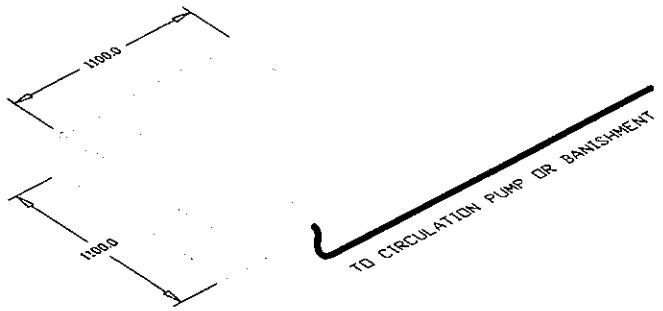

No.	Description	Qty.	Material	Remark
3	Pipe	-	PVC	-
2	Inside cover	-	Polycarbonate	-
1	Structure	-	Steel	-

UNIVERSITI TEKNOLOGI MALAYSIA
FACULTY OF ELECTRICAL ENGINEERING

DESIGN	M. ABU BAKAR S
DRAWN	M. ABU BAKAR S
CHECKED	

DIMENSIONS IN mm

UNSPECFIED TOLERANCES
LINIER +/- :
ANGULAR +/- :

SCALE | A4 | FINE | MEDIUM | ROUGH

DESIGN OF DRAINING RESERVOIR
MOBILE ARTIFICIAL CONTAMINATION CHAMBER

Drw. No. DR. 01.00

No. sheet

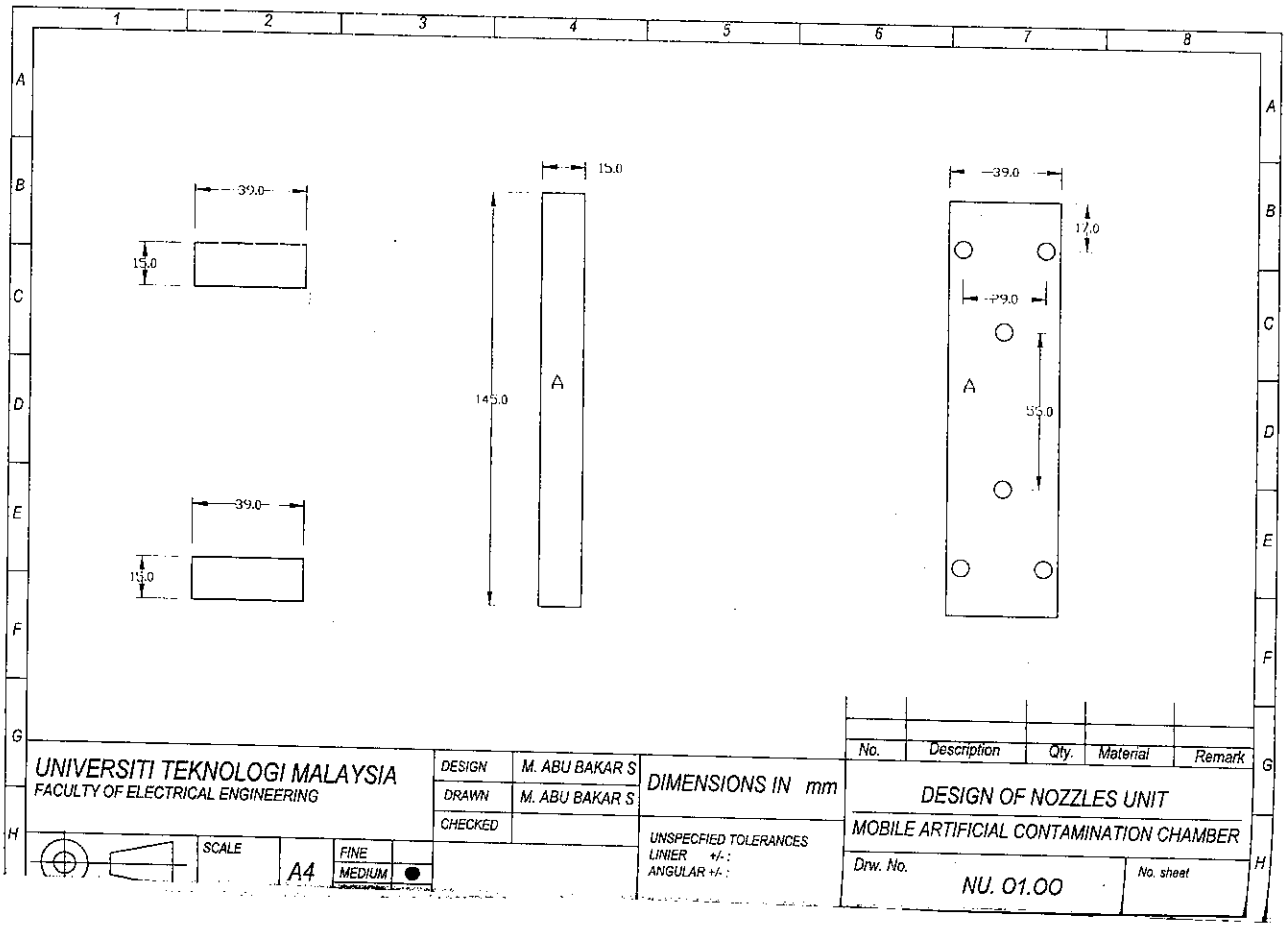

UNIVERSITI TEKNOLOGI MALAYSIA FACULTY OF ELECTRICAL ENGINEERING	DESIGN	M. ABU BAKAR S	DIMENSIONS IN mm
	DRAWN	M. ABU BAKAR S	
	CHECKED		UNSPECFIED TOLERANCES LINIER +/- : ANGULAR +/- :
SCALE A4 FINE MEDIUM			

No.	Description	Qty.	Material	Remark

DESIGN OF NOZZLES UNIT

MOBILE ARTIFICIAL CONTAMINATION CHAMBER

Drw. No. NU. 01.00 | No. sheet

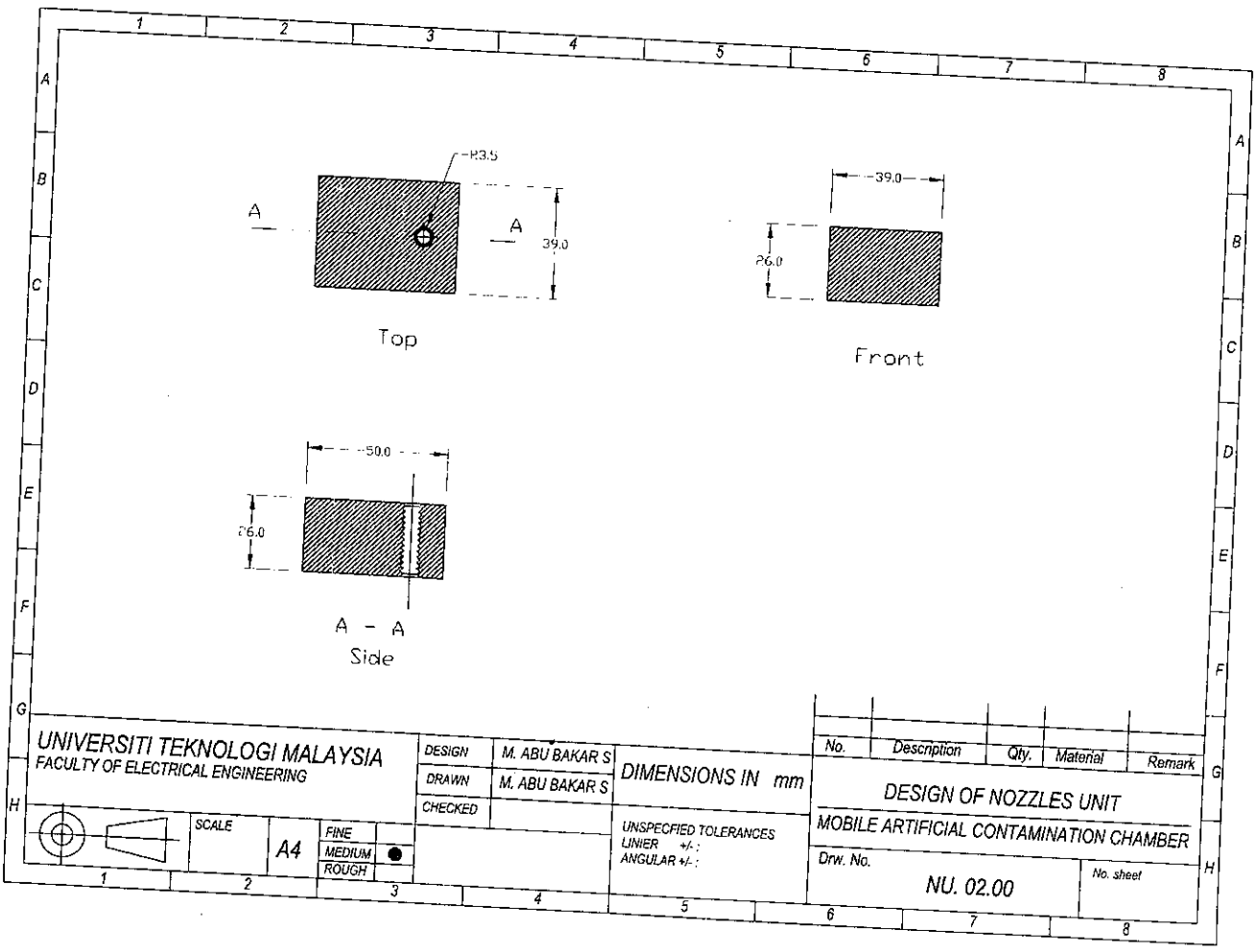

UNIVERSITI TEKNOLOGI MALAYSIA FACULTY OF ELECTRICAL ENGINEERING	DESIGN	M. ABU BAKAR S	DIMENSIONS IN mm
	DRAWN	M. ABU BAKAR S	
	CHECKED		UNSPECFIED TOLERANCES LINIER +/- : ANGULAR +/- :
SCALE A4 FINE MEDIUM ROUGH			

No.	Description	Qty.	Material	Remark

DESIGN OF NOZZLES UNIT

MOBILE ARTIFICIAL CONTAMINATION CHAMBER

Drw. No. NU. 02.00 | No. sheet

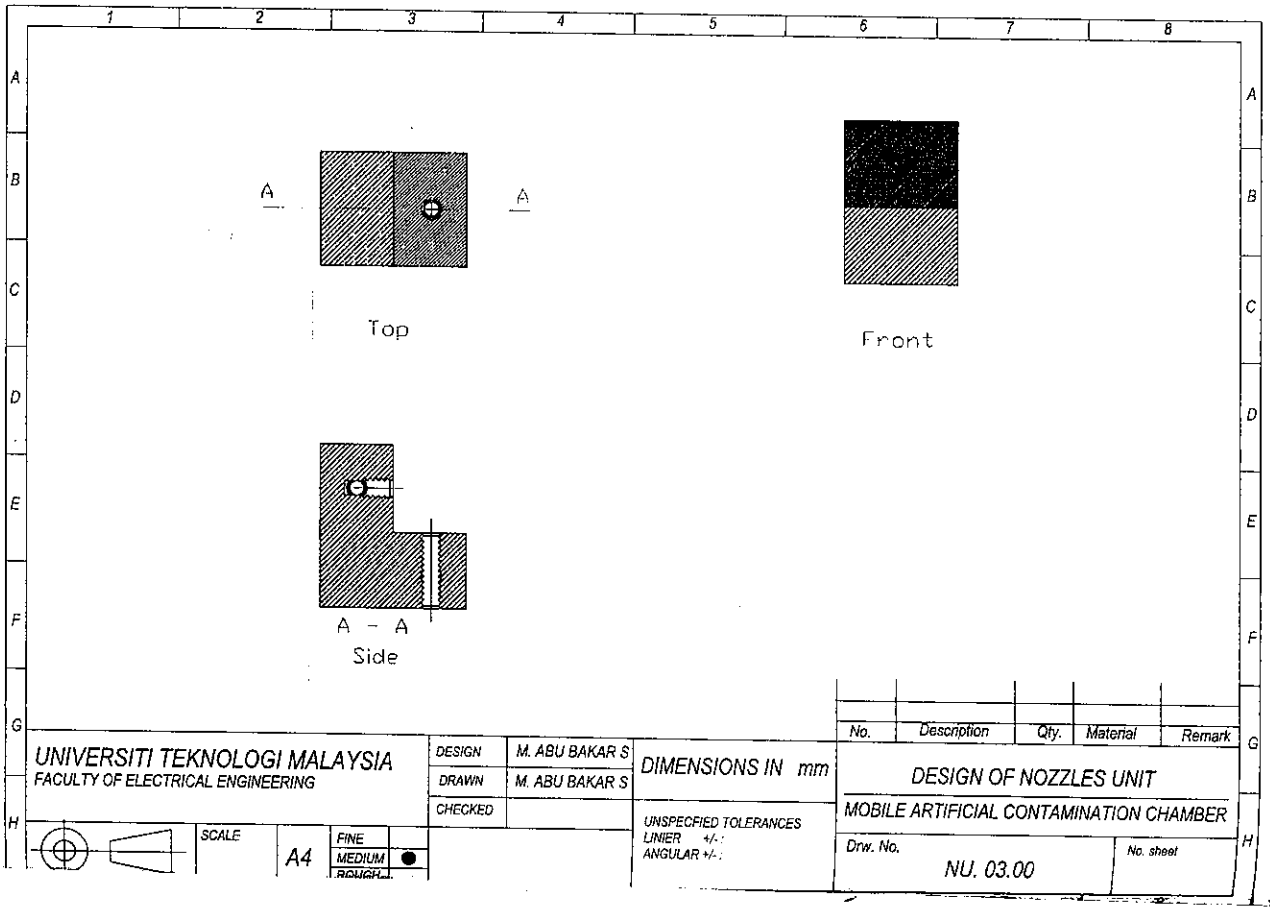

No.	Description	Qty.	Material	Remark

UNIVERSITI TEKNOLOGI MALAYSIA
FACULTY OF ELECTRICAL ENGINEERING

DESIGN	M. ABU BAKAR S	DIMENSIONS IN mm
DRAWN	M. ABU BAKAR S	
CHECKED		UNSPECFIED TOLERANCES LINIER +/- : ANGULAR +/- :

SCALE | A4 | FINE | MEDIUM | ROUGH

DESIGN OF NOZZLES UNIT
MOBILE ARTIFICIAL CONTAMINATION CHAMBER

Drw. No. NU. 03.00 | No. sheet

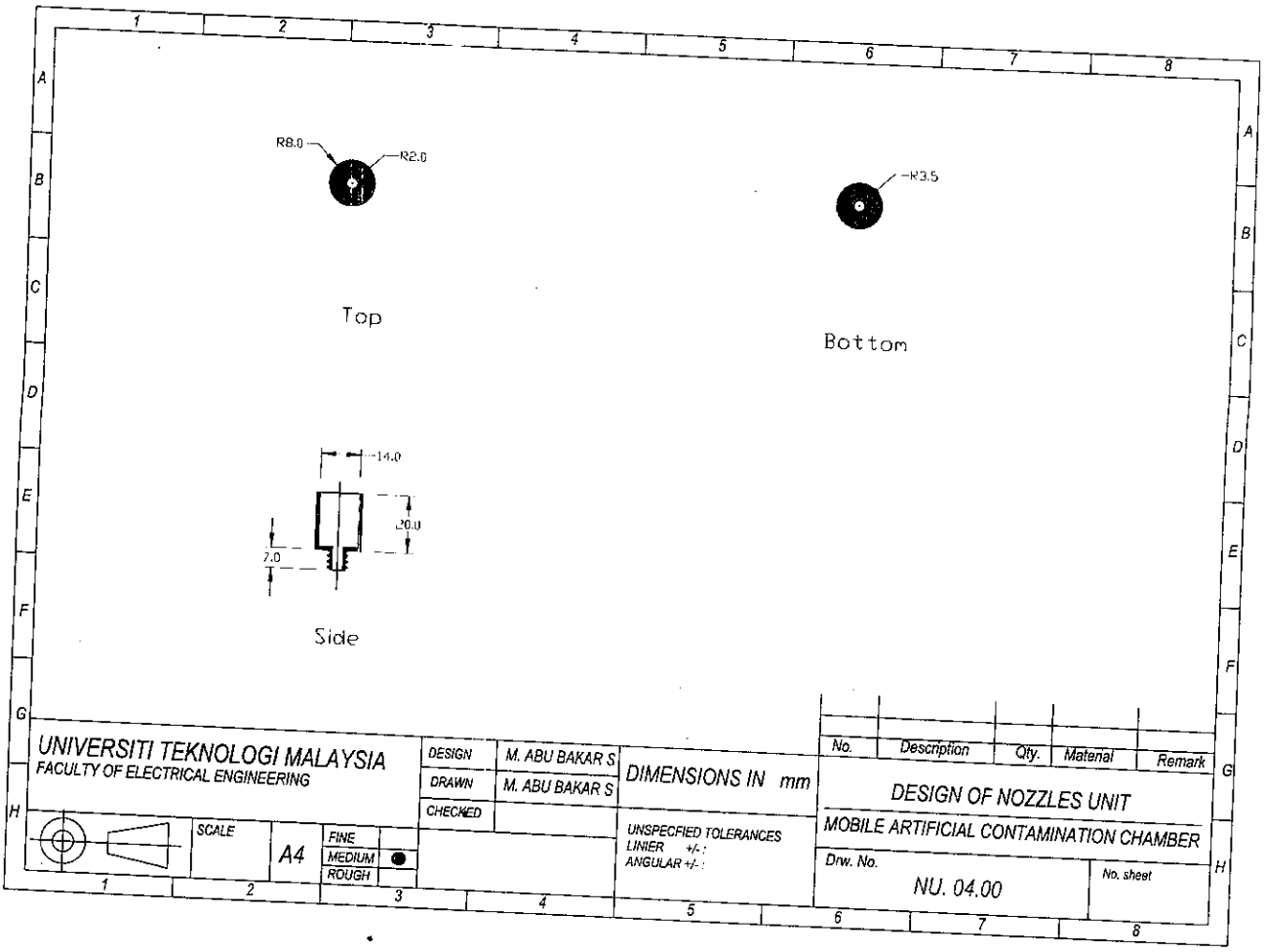

No.	Description	Qty.	Material	Remark

UNIVERSITI TEKNOLOGI MALAYSIA
FACULTY OF ELECTRICAL ENGINEERING

DESIGN	M. ABU BAKAR S	DIMENSIONS IN mm
DRAWN	M. ABU BAKAR S	
CHECKED		UNSPECFIED TOLERANCES LINIER +/- : ANGULAR +/- :

SCALE | A4 | FINE | MEDIUM | ROUGH

DESIGN OF NOZZLES UNIT
MOBILE ARTIFICIAL CONTAMINATION CHAMBER

Drw. No. NU. 04.00 | No. sheet

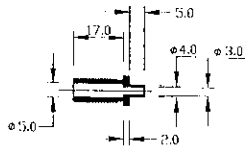

No.	Description	Qty.	Material	Remark

UNIVERSITI TEKNOLOGI MALAYSIA
FACULTY OF ELECTRICAL ENGINEERING

DESIGN	M. ABU BAKAR S
DRAWN	M. ABU BAKAR S
CHECKED	

DIMENSIONS IN mm

UNSPECFIED TOLERANCES
LINIER +/- :
ANGULAR +/- :

SCALE | A4 | FINE | MEDIUM ● | ROUGH

DESIGN OF NOZZLES UNIT
MOBILE ARTIFICIAL CONTAMINATION CHAMBER

Drw. No. NU. 05.00

No. sheet

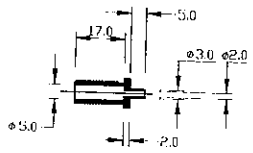

No.	Description	Qty.	Material	Remark

UNIVERSITI TEKNOLOGI MALAYSIA
FACULTY OF ELECTRICAL ENGINEERING

DESIGN	M. ABU BAKAR S
DRAWN	M. ABU BAKAR S
CHECKED	

DIMENSIONS IN mm

UNSPECFIED TOLERANCES
LINIER +/- :
ANGULAR +/- :

SCALE | A4 | FINE | MEDIUM ● | ROUGH

DESIGN OF NOZZLES UNIT
MOBILE ARTIFICIAL CONTAMINATION CHAMBER

Drw. No. NU. 06.00

No. sheet

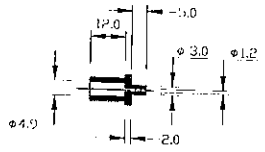

UNIVERSITI TEKNOLOGI MALAYSIA FACULTY OF ELECTRICAL ENGINEERING	DESIGN	M. ABU BAKAR S	DIMENSIONS IN mm	DESIGN OF NOZZLES UNIT
	DRAWN	M. ABU BAKAR S		MOBILE ARTIFICIAL CONTAMINATION CHAMBER
SCALE A4	CHECKED		UNSPECFIED TOLERANCES LINIER +/- : ANGULAR +/- :	Drw. No. NU. 07.00
FINE / MEDIUM / ROUGH				No. sheet

No.	Description	Qty.	Material	Remark

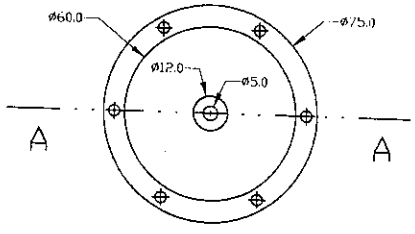

Bottom

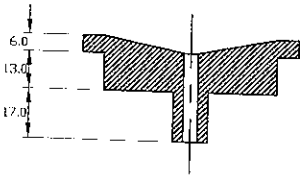

A - A

Side

UNIVERSITI TEKNOLOGI MALAYSIA FACULTY OF ELECTRICAL ENGINEERING	DESIGN	M. ABU BAKAR S	DIMENSIONS IN mm	DESIGN OF NOZZLES UNIT
	DRAWN	M. ABU BAKAR S		MOBILE ARTIFICIAL CONTAMINATION CHAMBER
SCALE A4	CHECKED		UNSPECFIED TOLERANCES LINIER +/- : ANGULAR +/- :	Drw. No. NU. 08.01
FINE / MEDIUM / ROUGH				No. sheet

No.	Description	Qty.	Material	Remark

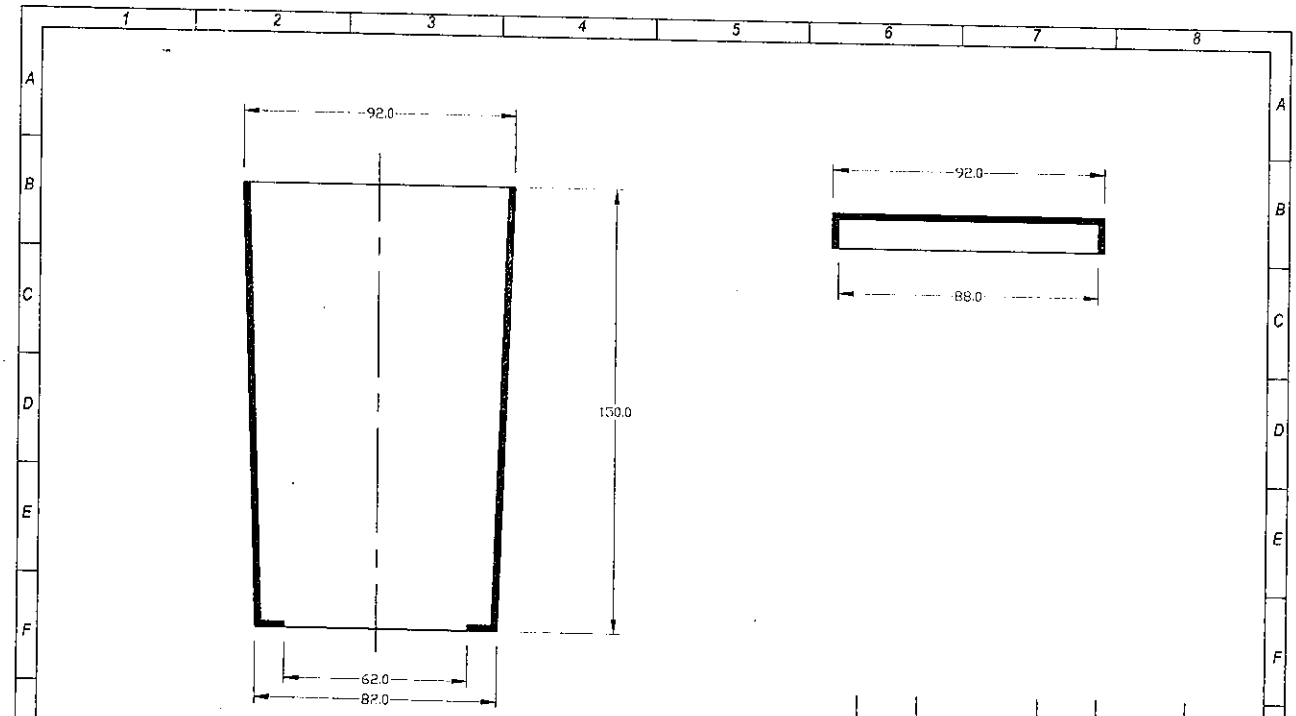

No.	Description	Qty.	Material	Remark	

UNIVERSITI TEKNOLOGI MALAYSIA
FACULTY OF ELECTRICAL ENGINEERING

DESIGN	M. ABU BAKAR S
DRAWN	M. ABU BAKAR S
CHECKED	

DIMENSIONS IN mm

UNSPECFIED TOLERANCES
LINIER +/- :
ANGULAR +/- :

SCALE | A4 | FINE | MEDIUM ● | ROUGH

DESIGN OF NOZZLES UNIT
MOBILE ARTIFICIAL CONTAMINATION CHAMBER

Drw. No. NU. O8.02

No. sheet

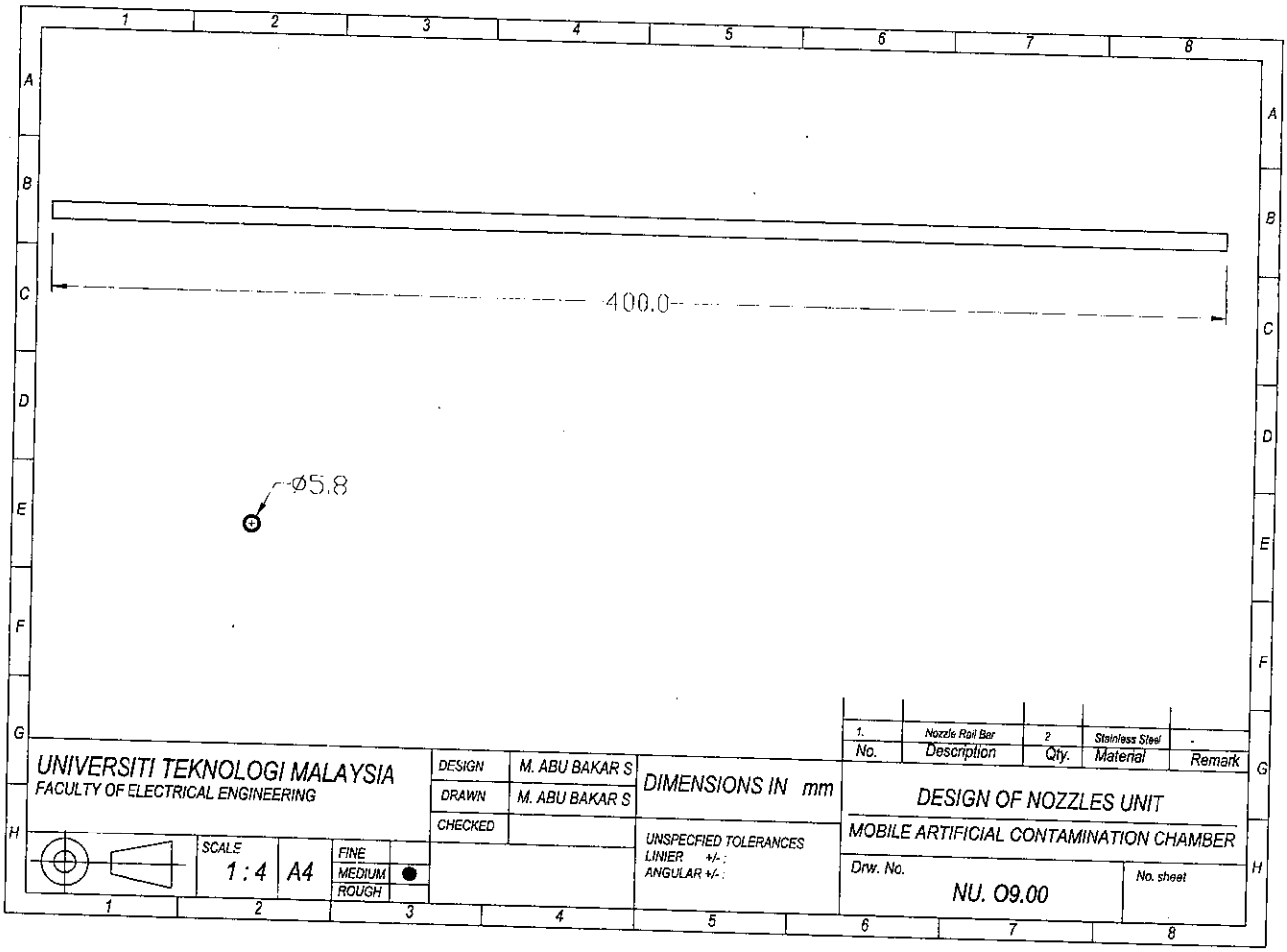

No.	Description	Qty.	Material	Remark
1.	Nozzle Rail Bar	2	Stainless Steel	-

UNIVERSITI TEKNOLOGI MALAYSIA
FACULTY OF ELECTRICAL ENGINEERING

DESIGN	M. ABU BAKAR S
DRAWN	M. ABU BAKAR S
CHECKED	

DIMENSIONS IN mm

UNSPECFIED TOLERANCES
LINIER +/- :
ANGULAR +/- :

SCALE 1 : 4 | A4 | FINE | MEDIUM ● | ROUGH

DESIGN OF NOZZLES UNIT
MOBILE ARTIFICIAL CONTAMINATION CHAMBER

Drw. No. NU. O9.00

No. sheet

Traditional glass and porcelain cap-and-pin transmission line insulators are slowly being replaced by new insulating materials which have better electrical and mechanical properties such as silicon rubber and polymeric. The non-ceramic materials are currently gaining popularity in transmission line applications. For any new type of insulator to be used on transmission line, it has to be tested so that it complies with the requirements of International Electrotechnical Commission Standard on insulators. This book provides comprehensive information concerning the design and development of Artificial Contamination Chamber which encompasses the aspects of electronic instrumentation, video recording, artificial contamination generation system, high voltage source data acquisition system and virtual instrument development. The chamber has all the basic features to conduct type-tests on insulators of ceramic and non-ceramic types.

Muhammad Abu Bakar Sidik, Hussein Ahmad
Muhammad Abu Bakar Sidik, PhD: Staff of Department of Electrical Engineering, Faculty of Engineering, Sriwijaya University and Senior Lecturer at Institute of High Voltage and High Current, Universiti Teknologi Malaysia.
Hussein Ahmad, PhD: Professor and Director of Institute of High Voltage and High Current, Universiti Teknologi Malaysia.

978-3-639-34968-9